

Forschungszentrum Karlsruhe
Technik und Umwelt

Wissenschaftliche Berichte
FZKA 5953

Integral Data Tests of the FENDL-1, EFF-2, EFF-3 and JENDL-FF Fusion Nuclear Data Libraries

Y. Wu, U. Fischer

**Institut für Neutronenphysik und Reaktortechnik
Projekt Kernfusion**

Februar 1998

Forschungszentrum Karlsruhe

Technik und Umwelt
Wissenschaftliche Berichte
FZKA 5953

**Integral Data Tests of the FENDL-1, EFF-2, EFF-3 and JENDL-FF
Fusion Nuclear Data Libraries**

Yican WU*, Ulrich FISCHER

**Institut für Neutronenphysik und Reaktortechnik
Projekt Kernfusion**

*Permanent address: Institute of Plasma Physics, Academia Sinica, P.O. Box 1126,
Hefei, Anhui, 230031, P.R. China

Forschungszentrum Karlsruhe GmbH, Karlsruhe

1998

Als Manuskript gedruckt
Für diesen Bericht behalten wir uns alle Rechte vor
Forschungszentrum Karlsruhe GmbH
Postfach 3640, 76021 Karlsruhe
Mitglied der Hermann von Helmholtz-Gemeinschaft
Deutscher Forschungszentren (HGF)
ISSN 0947-8620

Abstract

In the framework of the EFF (European Fusion File) - project of the European Fusion Technology Programme comprehensive benchmark analyses have been performed for selected nuclear data evaluations from EFF-2, EFF-3, JENDL-FF (JAERI Fusion File) and FENDL-1 (Fusion Evaluated Nuclear Data Library). A variety of existing integral 14 MeV benchmark experiments has been analysed for that purpose by means of coupled neutron-photon transport calculations with the Monte Carlo code MCNP4A, the discrete ordinates code ONEDANT and the nodal transport code NGSN/1D. The analysed experiments cover a wide range of fusion-relevant materials including iron, beryllium, aluminium, silicon, molybdenum, cobalt, chromium, copper, titanium, manganese, zirconium, niobium, tungsten and vanadium. The report provides a comprehensive documentation of the performed analyses including detailed numerical data test results in graphical and tabulated form.

Integrale Datentests der Fusionskerndatenbibliotheken FENDL-1, EFF-2, EFF-3 und JENDL-FF

Zusammenfassung

Im Rahmen des EFF (European Fusion Files) - Projektes des Europäischen Fusionstechnologieprogrammes wurden umfassende Benchmarkanalysen für ausgewählte Datenauswertungen der Kernfusionsdatenbibliotheken EFF-2, EFF-3, JENDL-FF (JAERI Fusion File) und FENDL-1 (Fusion Evaluated Nuclear Data Library) durchgeführt. Zu diesem Zweck wurde eine Vielzahl von integralen 14-MeV-Neutronenexperimenten auf der Basis von gekoppelten Neutronen-Photonen-Transportrechnungen mit dem Monte-Carlo-Programm MCNP4A, dem S_n -Code ONEDANT und dem nodalen Transportprogramm NGSN/1D analysiert. Es wurden folgende fusionsrelevante Materialien berücksichtigt: Eisen, Beryllium, Aluminium, Silizium, Molybdän, Kobalt, Chrom, Kupfer, Titan, Mangan, Zirkon, Niob, Wolfram und Vanadium. Der Bericht gibt eine zusammenfassende Darstellung der durchgeführten Analysen und enthält detaillierte numerische Ergebnisse der Datentestrechnungen in graphischer und tabellarischer Form.

Contents

1. Introduction	5
2. Calculational Codes and Data Libraries	7
3. Simulation of Anisotropic D-T Neutron Source	9
3.1 Angular Distribution of Source Neutrons	9
3.2 Energy-Angular Distribution of Source Neutrons	12
4. Calculation of Integral Benchmark Experiments	13
4.1 Technical University of Dresden (TUD) Iron Slab Experiment	13
4.2 Institute of Physics and Power Energy (IPPE) Iron Spherical Shell Experiment	20
4.3 FNS Iron Slab Time-of-Flight Experiment	33
4.4 FNS Iron In-system Experiment	39
4.5 FNS Beryllium Slab Time-of-Flight Experiment	48
4.6 KANT Beryllium Spherical Shell Experiment	54
4.7 OKTAVIAN Beryllium Spherical Shell Experiment	54
4.8 OKTAVIAN Sphere Pile Experiments	57
4.9 IPPE Vanadium Spherical Shell Experiment	72
5. Discussion of Results	75
5.1 Iron	75
5.2 Beryllium	78
5.3 Aluminum	78
5.4 Silicon	78
5.5 Molybdenum	79
5.6 Cobalt	79
5.7 Chromium	79
5.8 Copper	79
5.9 Titanium	80
5.10 Manganese	80
5.11 Zirconium	80
5.12 Niobium	80
5.13 Tungsten	80
5.14 Vanadium	81
6. Summary	82
7. Acknowledgement	84
8. References	85

1. Introduction

Nuclear design calculations for fusion reactors rely on the use of available neutron transport codes and nuclear cross-section data. While the available codes are well established and validated, this is not true for the cross-section data. For that reason, nuclear data libraries are still under development for fusion applications. Within this framework, integral data tests are being performed as part of the quality assurance procedure for the evaluated nuclear data. A series of fusion neutronics benchmark experiments has been conducted over the past decade to provide a suitable experimental data base comprising the majority of materials relevant for fusion applications.

The objective of this report is to analyze and qualify the EFF-2 & -3 (European Fusion Files) working libraries for fusion applications as compared to FENDL-1 (Fusion Evaluated Nuclear Data Library) and JENDL-FF (Japanese Evaluated Nuclear Data Library - Fusion Files) and to elaborate recommendations for further data improvements.

FENDL-1, EFF and JENDL-FF are evaluated nuclear data files developed for fusion technology applications in the framework of international and national projects. The Fusion Evaluated Nuclear Data Library FENDL-1 e. g. was selected in an international effort initiated and co-ordinated by the IAEA Nuclear Data Section from the nuclear data files ENDF/B-VI (USA), BROND-2 (Russian Federation) and JENDL-3 (Japan). Working libraries derived from FENDL-1 are in use for design calculations in the current Engineering Design Activity (EDA) phase of the ITER (International Thermonuclear Experimental Reactor) project. The EFF-2, -3 and JENDL-FF fusion nuclear data libraries were developed more recently by the European Union and JAERI, respectively, in the framework of their fusion technology programmes. While EFF-2 is frozen, EFF-3 is currently under development.

Within the EFF-project of the European Fusion Technology Programme, comprehensive benchmark analyses have been performed for selected new data evaluations from the EFF-2 and EFF-3 libraries including comparisons with JENDL-FF and FENDL-1 data. The analyses formed also part of the selection procedure for the forthcoming FENDL-2 data file. A large variety of existing integral 14 MeV benchmark experiments have been analyzed for that purpose by means of coupled neutron-photon transport calculations with the Monte Carlo code MCNP4A, the discrete ordinates code ONEDANT and the nodal transport code NGSN/1D. The analysed experiments cover a wide range of fusion-relevant materials. In particular, 14 MeV neutron transmission experiments on rectangular iron and beryllium slabs, and on spherical iron, beryllium, aluminum, silicon, molybdenum, cobalt, chromium, copper, titanium, manganese, zirconium, niobium, tungsten and vanadium shells with measurements of neutron leakage spectra were analyzed. The experiments had been performed previously at the Fusion Neutron Source Laboratory (FNS, JAERI), the Institute of Power Physics (IPPE) Obninsk, the Technical University of Dresden (TUD), the University of Osaka (OKTAVIAN facility) and the Research Centre Karlsruhe (FZK). Where available, measured photon leakage spectra data and neutron reaction rate data are included in the analysis.

The benchmark analyses comprise MCNP-calculations using detailed three-dimensional models of the experimental configurations and taking into account the proper energy-angle distribution of the (D,T) source neutrons, comparisons to one-dimensional calculations and comparisons to multi-group (VITAMIN-J) based deterministic transport calculations. In

addition, comparisons are included of processed and measured cross-section data where appropriate and needed.

The neutron flux or leakage spectra, photon flux spectra, reaction rates and the associated C/E (ratio of calculational to experimental) values are presented both in graphical and tabulated form. The findings and comprehensive conclusions are given.

2. Computational Tools and Data

2.1 Transport Codes

MCNP4A^[1] is the current version of the Monte Carlo N-Particle Transport Code System (Dec., 1993) developed by Los Alamos National Laboratory. It treats an arbitrary three-dimensional configuration of materials. Pointwise continuous energy cross-section data are used. For neutrons, all reactions in a particular cross-section evaluation are accounted for. Both free gas and S (α , β) thermal treatments may be used. For photons, the code takes into account incoherent and coherent scattering with and without electron binding effects, the possibility of fluorescent emission following photoelectric absorption, and absorption in pair production with local emission of annihilation radiation

ONEDANT^[2] is part of a modular computer programme package designed to solve the time-independent, multi-group discrete ordinates form of the Boltzmann equation in several different geometries. The discrete ordinates approximation (commonly referred to as the S_N method) and the finite difference approximation are used for the discretization of the angular and the spatial variable, respectively. The scattering transfer probability is represented by a finite Legendre polynomial series expansion.

NDSN/1D^[3] is a one-dimensional discrete ordinates nodal transport code developed at ASIPP, Hefei. The multigroup discrete ordinates form of the Boltzmann equation is solved in one-dimensional plane, spherical and cylindrical geometries by the nodal Green's Function method using the Legendre polynomial series expansion for the spatial dependence and the discrete ordinates (S_N) approximation for the angular dependence. The scattering transfer probability is processed by using the same method as that in ONEDANT. The nodal method provides very accurate numerical results on a coarse spatial mesh grid. In the framework of this work, we further improved and tested the code and applied it to the fusion benchmark problems. The following functions have been integrated to the programme: calculation of the vacuum node, negative flux correction, central zero-current correction in curvilinear geometries and input of multi-group data of various formats. A detailed description of model and code will be separately given.

2.2 Data Libraries

The **FENDL-1** general purpose evaluation data file, designated as FENDL/E-1.0, had been compiled from the BROND-2, ENDF/B-VI and JENDL-3 data files^[4]. It includes neutron interaction and photon production cross-section data. The second version of the general purpose file of the European Fusion File, **EFF-2**, had been developed in the framework of EFF-project of the European Fusion Technology Programme by several European research laboratories and universities. The data file contains neutron nuclear data for 13 newly evaluated materials and data evaluations for 43 other materials selected from recently released libraries (JEF-2, ENDF/B-VI and JENDL-3)^[5]. While EFF-2 is frozen, the next version **EFF-3** is being developed. The current working library of EFF-3 currently contains only ⁵⁶Fe and Vanadium data.

The FENDL-1, EFF-2.4 (and EFF-3) were processed into working libraries for MCNP (ACE-format) and multigroup data in the Vitamin-J 175 neutron and 42 photon group

structure, respectively, by R. E. MacFarlane at LANL (denoted as FENDL/MC-1.0 and FENDL/MG-1.0)^[6]. The EFF2.4 and EFF-3 data were processed by different European laboratories (ENEA Bologna, ENEA Frascati, ECN Petten) into ACE and multi-group data libraries^[7]. The TRANSX^[8] - code has been used to convert the MATXS-format data into transport tables for use with ONEDANT and NGSN.

The **JENDL-FF**^[9] ACE data library has been provided by JAERI for inclusion in the benchmark analyses for the selection of the FENDL-2 data evaluations.

3. Simulation of Anisotropic D-T Neutron Source Distribution

The angular and energy distribution of the neutrons emitted in the $t(d,n)^4\text{He}$ - reaction in the TiT target depends slightly on the energy of the incident deuteron and the emission angle as referred to the direction of the D-ion beam. An approximative source model will be described in the following based on the D-T reaction kinematics and taking into account the slowing-down of the D-ions in the Ti- target. Computational results for some of the experiments using that model are presented in Section 4.

3.1 Angular Distribution of Source Neutrons

The probability P of a deuteron undergoing a reaction while traveling a distance, dx , in a target material containing N_t tritium atoms/cm³ is given by

$$P = N_t \sigma dx \quad (1)$$

where σ is the cross-section of the $T(D, n)\alpha$ reaction, and is usually given in barn. As σ is a rapidly varying function of energy, it is convenient to use the relation

$$\sigma dx = \sigma dE / (dE/dx) \quad (2)$$

where (dE/dx) is the rate of energy loss of the deuteron in the target material. Combining the two equations above, one gets

$$P = N_t \sigma dE / (dE/dx) \quad (3)$$

In the following, a thick TiT target is assumed, i.e. the TiT layer thickness is large compared to the penetration depth of the accelerated deuterons. Since the probability of a deuteron undergoing a $T(D,n)\alpha$ reaction is very small (it is, for instance, approximately 10^{-6} for a deuteron of 200 keV) during its slowing down time in the target material, essentially each deuteron has a finite probability of reacting throughout the range of energy values from 0 to the accelerating potential, E . Thus, one may write for the total probability of a deuteron reacting in the target material

$$P = N_t \int_0^E \sigma dE / (dE/dx) \quad (4)$$

The above equation also represents the total probability for creating a neutron or an α particle. Thus, the probability for creating a neutron at an emission angle of θ in terms of the differential cross section for neutron emission in the laboratory system of coordinates can be written as

$$P_n(\Omega, \theta) = N_t \int_0^E \sigma(\Omega, \theta) dE / (dE/dx) \quad (5)$$

A brief discussion of $\sigma(\Omega, \theta)$, N_t and dE/dx is given based on the following assumptions:

- The reaction products are isotropically distributed in the centre-of-mass (CM) system.
- A pure D_1^+ - beam is incident upon the target, that is, no other deuteron ions (D_2^+ , D_3^+) are assumed in the beam.
- There is a uniform loading of tritium atoms up to a depth equal to the range of the incident deuterons.
- There is no scattering of incident deuterons, that is, no energy loss of deuterons before reaching an area in which the target is uniformly loaded with tritium.
- The deuteron beam is focused with a high degree of precision or the target geometry approaches a point source.
- Any other neutron creating competition reaction is neglected, e. g. the $D(D,n)^3\text{He}$ where the incident D probably reacts with the loaded D in the target and in the drift tube and becomes a secondary particle.

Generally, it is estimated that the total cumulative error from the above assumptions should be less than approximately 10%^[10].

(1) $\sigma(\Omega, \theta)$, differential cross section in the lab system of coordinates

It has been shown that the reaction products of $T(D,n)\alpha$ are isotropically distributed in the CM system for deuteron energies below 300 keV^[11,12]. Experimental data for the differential cross section, $\sigma(\Omega, \text{CM})$, are available in the literature^[13,14,15]. There is fairly good agreement between the various published data. The values given in Table 3.1 were taken from Ref.[10, 16]. The transformation from the centre-of-mass to the laboratory system can be formulated as follows^[12]:

$$\sigma(\Omega, \theta) = \sigma(\Omega, \text{CM}) (d\Omega_{\text{CM}}/d\Omega)_n, \quad (6)$$

$$(d\Omega_{\text{CM}}/d\Omega)_n = \frac{\gamma(\cos \theta) + \sqrt{\frac{1}{\gamma^2} - \sin^2 \theta}}{\sqrt{\frac{1}{\gamma^2} - \sin^2 \theta}}, \quad (7)$$

$$\gamma = \frac{1}{\sqrt{\frac{m_\alpha(m_D + m_T)}{m_n \cdot m_D} \left(\frac{m_T}{m_D + m_T} + \frac{Q}{E_D} \right)}}, \quad (8)$$

where

m_α = mass of α -particle

m_n = mass of neutron

m_T = mass of Tritium

m_D = mass of deuteron

E_D = incident energy of deuteron

$$Q = 17.6 \text{ MeV}$$

For an isotropic distribution of the reaction products in the mass system we have:

$$\sigma(\Omega, CM) = \sigma/4\pi$$

Therefore, the angular distribution of the probability for creating a neutron at a emission angle θ can be calculated according to:

$$P_n(\Omega, \theta) = N_t \int_0^E \sigma/4\pi (d\Omega_{CM}/d\Omega)_n dE / (dE/dx) \quad (9)$$

Table 3.1 Experimental data used for the calculation of the source neutron distribution

E (keV)	$\sigma/4\pi$ (b/steradian)	$(dE/dx)_{Ti}$ (keV/mg/cm ²)	$(dE/dx)_T$ (keV/mg/cm ²)
10	1.5×10^{-4}	82	640
15	1.2×10^{-3}	100	720
20	4.3×10^{-3}	115	784
25	1.20×10^{-2}	129	838
30	2.20	141	894
35	3.60	153	936
40	5.70	163	980
45	8.1	173	1016
50	1.10×10^{-1}	183	1044
60	1.73	200	1114
70	2.43	214	1172
80	3.10	226	1216
90	3.60	236	1250
100	3.95	245	1270
110	4.00	251	1284
120	3.95	257	1284
130	3.75	262	1278
140	3.50	266	1268
150	3.20	270	1256
160	2.90	273	1240
170	2.65	276	1224
180	2.50	277	1204
190	2.30	279	1186
200	2.10	280	1166

- Note: The data above 200 keV up to 500keV have been taken from the MCNP source routine developed by M. Pillon, ENEA Frascati, for the FNG experiment.

(2) dE/dx , rate of energy loss and N_t , tritium atoms per cm³

There are no experimental data available for the energy loss of deuterons in TiT, Ti, or T alone, but there are some evaluated data available, by several authors, of dE/dx for D in T and D in Ti which are in very good agreement. The values from [10,16] are given in Table 3.1.

The best approximation to represent the energy loss of D in TiT_N is to assume that Bragg's law is valid

$$(dE/dx)_{TiT_N} = 48/(48+3N)(dE/dx)_{Ti} + 3N/(48+3N)(dE/dx)_T \quad (10)$$

where the maximum value of N is 1.8 as obtained by the standard absorption technique. In general, however, $N = 1.5$ is a good average value. The maximum theoretical value is 2 because of the bivalent nature of Titanium.

3.2 Energy-Angular Distribution of Source Neutrons

On the basis of the two-body reaction model, the expression for $E_n(E_D, \theta_n)$ in the case of the $T(D, n)\alpha$ reaction reads as follows:

$$E_n(E_D, \theta_n) = 0.08E_D \cos(2\theta_n) + 0.8(0.6E_D + 17.6) + 0.8 \cos(\theta_n) \sqrt{0.4E_D(0.6E_D + 17.6)} \sqrt{1 - \frac{E_D \sin^2 \theta_n}{10(0.6E_D + 17.6)}} \quad (11)$$

where $E_n(E_D, \theta_n)$ is the energy of the emitted neutrons,

E_D is the energy of the incident deuterons,

θ_n is the angle of the emitted neutrons with respect to the direction of the incident deuteron beam.

As discussed above, each deuteron has a finite probability of reacting throughout the energy range from 0 up to the accelerating potential E . Therefore, the energy distribution for the emitted neutrons at a fixed emission angle θ_n may be represented as follows:

$$E_n = E_n(E_D, \theta_n), \quad 0 \leq E_D \leq E \quad (12)$$

and the probability for emission of a neutron at energy E_n can be calculated by inserting the associated deuteron energy E_D and the neutron emission angle θ_n into the following equation

$$P_n(\Omega, \theta_n, E_n) = N_t \sigma(\Omega, CM) (d\Omega_{CM}/d\Omega)_n (dE/dx) \quad (13)$$

Note that $\sigma(\Omega, CM)$, $(d\Omega_{CM}/d\Omega)_n$ and (dE/dx) are functions of the deuteron energy E_D related to energy E_n of the emitted neutron.

4. Calculation of Integral Benchmark Experiments

4.1 Technical University of Dresden (TUD) Iron Slab Experiment

Iron slab assemblies with and without a gap were irradiated with 14 MeV Deuterium-Tritium neutrons at the Technical University of Dresden, Germany. Neutrons were produced with a 125 keV pulsed deuteron beam impinging on a T-Ti target. The neutron source and the detectors are point-like. The iron slab has a front area of 100x100 cm and a thickness of 30 cm. The distance between the source and the detector is 349 cm, and amounts to 19 cm between the source and the assembly. For the benchmark analyses presented here, only the experimental configuration without gap was considered. For that case, the total fluences has been calculated at the position of the point detector.

The effective iron density is 7.85 g/cm³. The chemical composition of the irradiated iron is given in Table 4.1.1.

Table 4.1.1 Chemical Composition of Iron Sample

Element	Fe	Ni	Si	Mn	Cr	S, Ti
Fraction (weight %)	97.5	0.1	1.5	0.5	0.2	0.1

In the experiment, the spectral neutron fluence, the spectral photon fluence and the neutron time-of-arrival fluence were measured.

A detailed description of the experiment can be found in Ref.[17].

The MCNP model includes the collimator, the floor, the wall, the air, the assembly rack, the target backing, the cooling and the target holder so that the calculated fluences can be directly compared to the measured ones.

Fig. 4.1.1 shows the angular distribution of the neutron source in the target as given by the d-t kinematics model and taking into account the slowing-down of the D-ions as described in Section 3. The neutron source energy spectrum depends on the neutron emission angle with respect to the d-beam direction. Fig. 4.1.2 shows the neutron source energy spectra in the directions of the central axis and the edge of the iron slab.

The neutron and photon flux spectra are calculated with MCNP4A and FENDL-1, EFF-2, EFF-3 and JENDL-FF (elemental evaluations) data, respectively, using both a simplified geometrical model (iron slab and isotropic neutron source only) and a complete geometrical model which takes into account the effect of the room-return radiation and the anisotropic angular distribution of source neutrons. In Fig. 4.1.3 ~ Fig. 4.1.4 are shown the calculated and measured flux spectra per unit energy (/MeV) or per lethargy (/u) normalized to one source neutron (/sn) for the complete geometry. The C (Calculational) /E (Experimental) ratios of integral neutron and photon spectra are listed in Table 4.1.2 ~ Table 4.1.5.

The effect of iron impurities on the neutron spectrum has also been calculated and is shown in Fig. 4.1.5 and Table 4.1.4.

Table 4.1.2 C/E-data for integrated neutron spectra in the TUD iron slab experiment (MCNP with full 3D model without gap, anisotropic neutron source)

Particle Type	Energy Range(MeV)	Measured Fluence(1/cm ² /s)	Experimental error (%)	C/E of Integral Neutron Flux			
				EFF-3	EFF-2	FENDL-1	JENDL-FF
Neutron	0.03~1.0	3.23×10 ⁻⁷	11	.93	.91	.89	.96
	1.0~5.0	4.84×10 ⁻⁸	2	.93	.91	.88	.86
	5.0~10.0	3.64×10 ⁻⁹	2	.70	.85	.90	.83
	10.0~20.0	1.58×10 ⁻⁸	2	.88	.92	.83	.79
	>0.03	3.91×10 ⁻⁷	9	.93	.91	.89	.94

Table 4.1.3 C/E of TUD-Iron-Experiment Integral Neutron Spectra (MCNP, ideal geometry without gap, isotropic neutron source)

Energy Range (MeV)	Experimental Fluence (1/cm ² /sn)	C/E of Integral Neutron Flux			
		EFF-3	EFF-2	FENDL-1	JENDL-FF
0.03~1.0	.250E-06	.810	.790	.776	.823
1.0~5.0	.358E-07	.833	.816	.784	.768
5.0~10.0	.287E-08	.576	.751	.756	.626
10.0~20.0	.150E-07	.860	.824	.762	.768
>0.03	.303E-06	.813	.794	.776	.812

Table 4.1.4 Effect of impurities on the integrated neutron spectra in the TUD iron slab experiment (MCNP, ideal geometry without gap, isotropic neutron source, FENDL-1)

Energy Range (MeV)	Measured Fluence (1/cm ² /sn)	C/E of Integral Neutron Flux (FENDL-1)	
		Natural Fe	Nat.Fe+Impurities
0.03~1.0	.250E-06	.776	.775
1.0~5.0	.358E-07	.784	.779
5.0~10.0	.287E-08	.756	.758
10.0~20.0	.150E-07	.762	.769
>0.03	.303E-06	.776	.775

Table 4.1.5 C/E data for integrated photon spectra in the TUD iron slab experiment (MCNP with full 3D model without gap, anisotropic neutron source)

Energy Range (MeV)	Measured Fluence (1/cm ² /sn)	C/E of Integral Photon Flux			
		EFF-3	EFF-2	FENDL-1	JENDL-FF
0.40~1.0	.107E-07	1.17	.87	.82	.79
1.0~8.08	.115E-07	1.19	.76	.69	.67
>0.40	.222E-07 (±1.5%)*	1.18	.81	.75	.73

the number in parenthesis is the estimated relative error

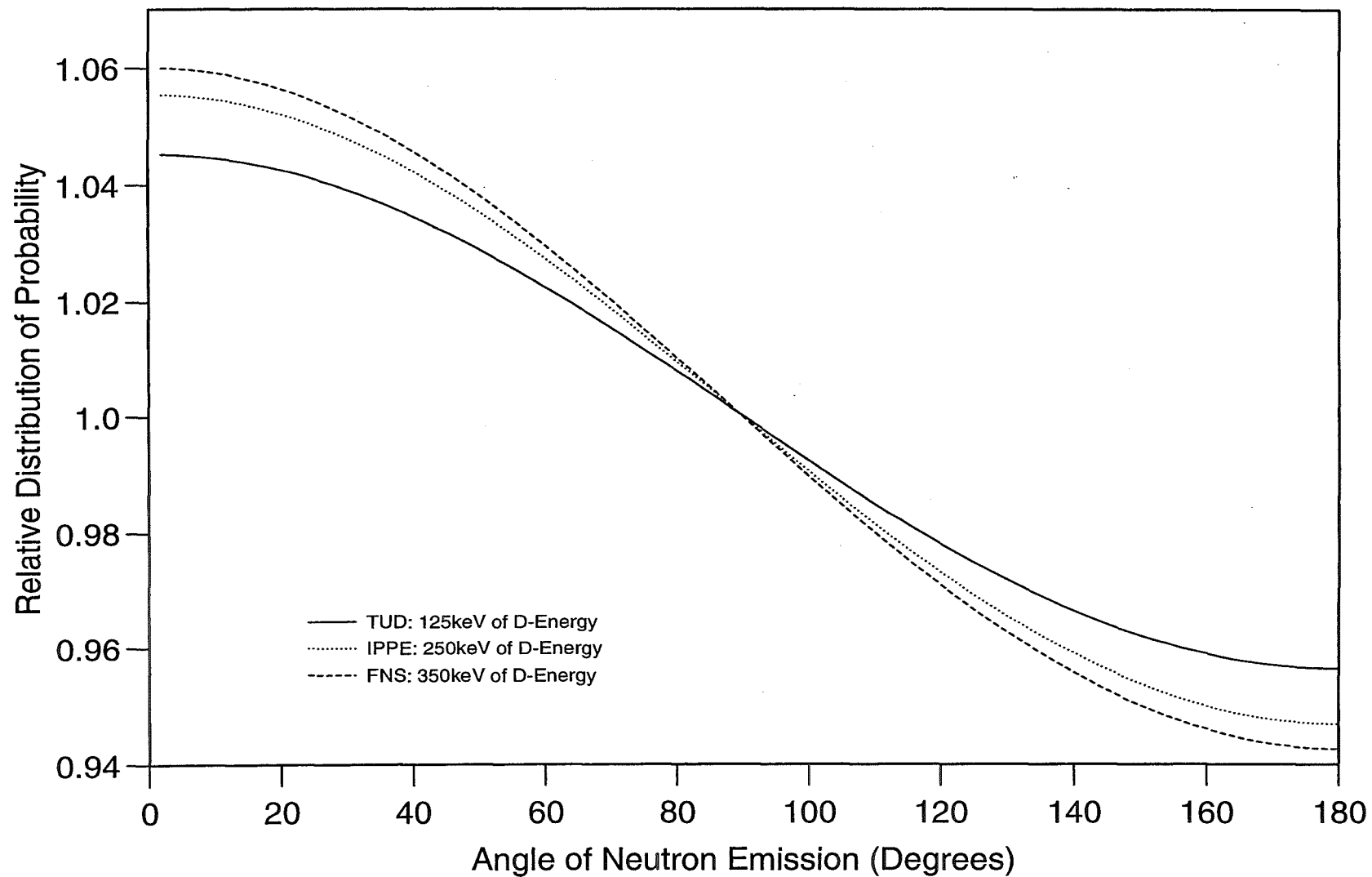


Fig.4.1.1 Relative Angular Distribution of D-T Neutron Source

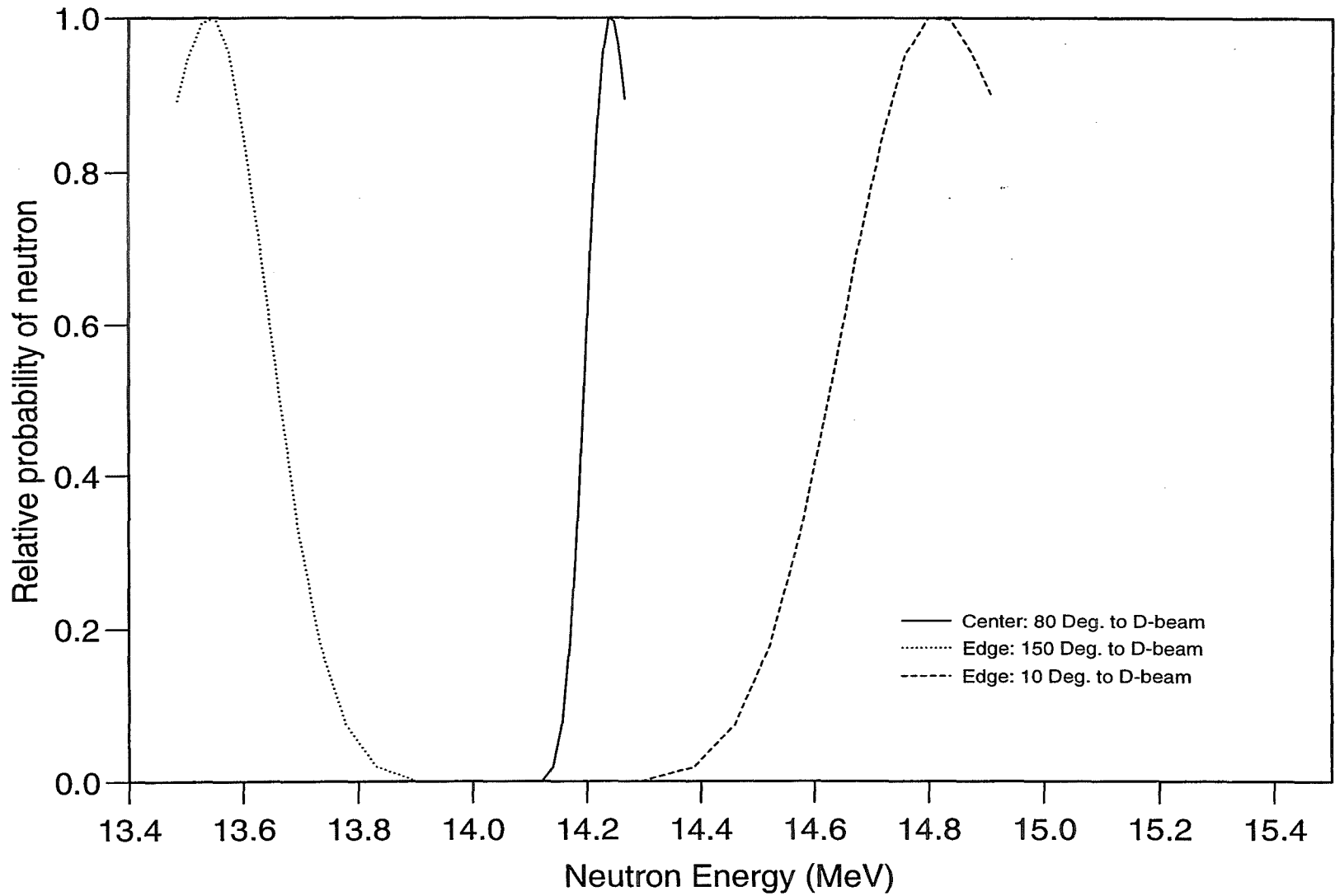


Fig.4.1.2 Energy and Angular Distribution of TUD D-T Neutron Source

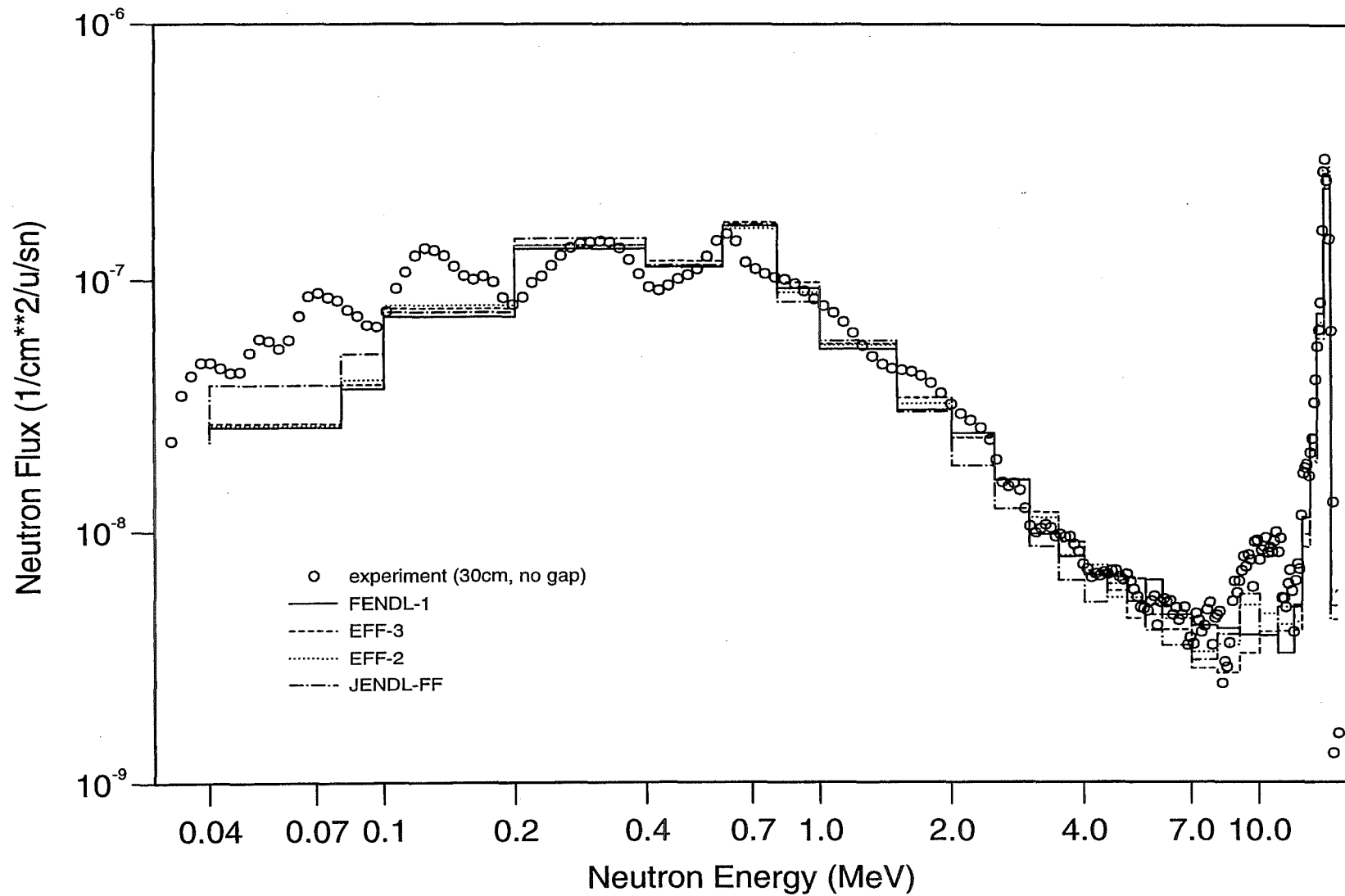


Fig.4.1.3 TUD Iron Slab Experiment Neutron Spectra

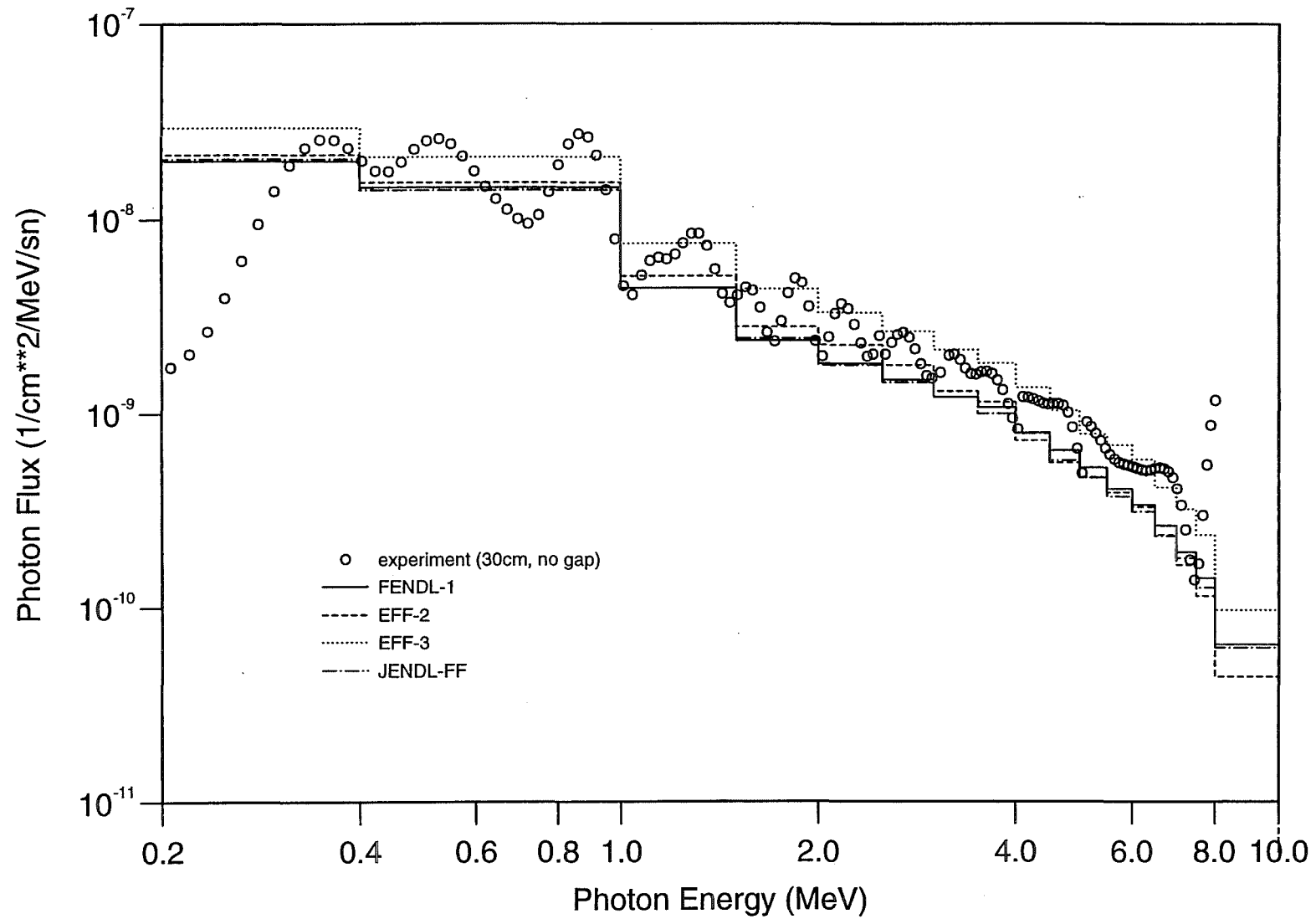


Fig.4.1.4 TUD Iron Slab Experiment Photon Spectra

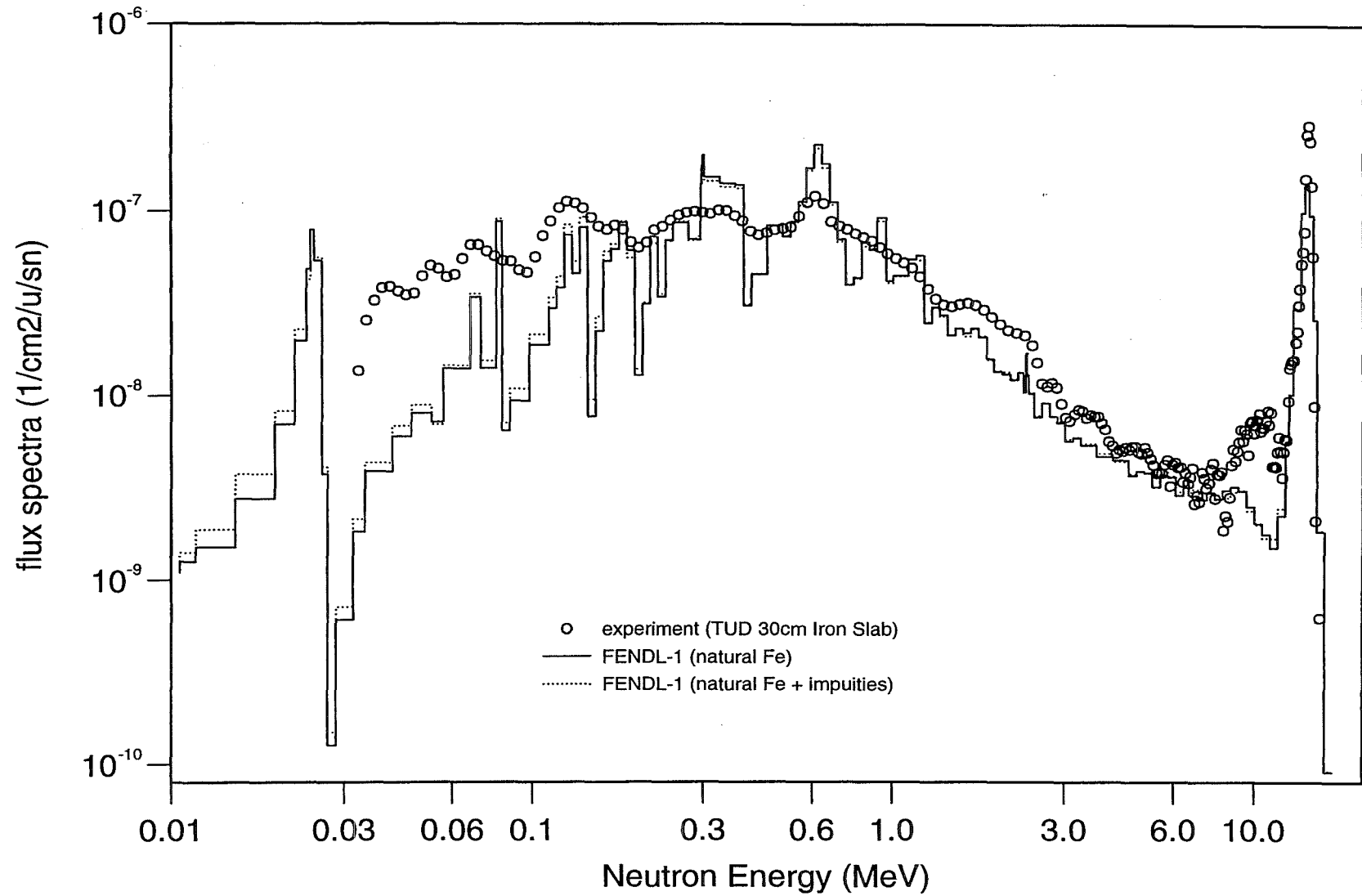


Fig.4.1.5 Effect of Impurities on Neutron Spectrum

4.2 Institute of Physics and Power Energy (IPPE) Iron Spherical Shell Experiment

Iron spherical shells with various thicknesses of 2.5, 7.5, 12, 18.1 and 28 cm were irradiated by 14 MeV D-T neutrons at the Institute of Physics and Power Energy, Russian Federation. The source neutrons were generated by a 250 keV deuteron beam impinging on a Titanium-Tritium solid target at the center of the sphere.

The neutron leakage spectra from the outer surfaces of five shells were measured by the Time-of-Flight (TOF) method. A detailed description of experiment can be found in Ref.[18].

The effect of the background radiation (“room-return”, etc.) has been taken into account in the measured data by a correction derived from the measured background counting rates when using a shadow bar.

Table 4.2.1 C/E data for integrated neutron leakage spectra in the IPPE iron shell experiment (MCNP, 3-D geometry, anisotropic neutron source distribution)

Shell Thickness (cm)	Energy Range (MeV)	Experimental Leakage (1/sn)	C/E of Integral Leakage			
			EFF-3	EFF-2	FENDL-1	JENDL-FF
2.5 (0.5 MFP*)	0.05~1.0	.994E-01 (±5%) ^{&}	0.96	0.89	0.93	1.09
	1.0~5.0	.140E+00 (±4%)	1.05	1.06	0.99	1.01
	5.0~10.0	.318E-01 (±5%)	0.76	0.91	0.98	0.84
	10.0~20.0	.740E+00 (±7%)	1.05	1.05	1.05	1.05
	>0.05	.101E+01 (±5%)	1.03	1.03	1.03	1.04
7.5 (1.6 MFP)	0.05~1.0	.317E+00 (±5%)	1.15	1.00	1.02	1.02
	1.0~5.0	.252E+00 (±4%)	1.12	1.13	1.08	1.08
	5.0~10.0	.345E-01 (±6%)	0.93	1.14	1.24	1.06
	10.0~20.0	.432E+00 (±7%)	1.01	1.01	1.01	0.99
	>0.05	.104E+01 (±5%)	1.04	1.04	1.04	1.06
10.0 (2.2 MFP)	0.05~1.0	.387E+00 (±5%)	0.99	0.96	0.98	1.09
	1.0~5.0	.271E+00 (±4%)	1.09	1.09	1.05	1.05
	5.0~10.0	.332E-01 (±6%)	0.94	1.16	1.26	1.07
	10.0~20.0	.352E+00 (±7%)	0.93	0.92	0.92	0.91
	>0.05	.104E+01 (±5%)	0.99	0.99	0.99	1.02
18.1 (3.9 MFP)	0.05~1.0	.649E+00 (±5%)	1.07	1.05	1.06	1.12
	1.0~5.0	.211E+00 (±4%)	1.14	1.14	1.11	1.08
	5.0~10.0	.168E-01 (±6%)	1.02	1.27	1.39	1.17
	10.0~20.0	.110E+00 (±7%)	1.08	1.07	1.06	1.05
	>0.05	.986E+00 (±5%)	1.08	1.07	1.08	1.10
28.0 (6.1 MFP)	0.05~1.0	.786E+00 (±5%)	1.09	1.07	1.08	1.09
	1.0~5.0	.115E+00 (±4%)	1.06	1.06	1.04	0.99
	5.0~10.0	.627E-02 (±6%)	0.98	1.20	1.27	1.09
	10.0~20.0	.343E-01 (±7%)	0.98	0.98	0.94	0.93
	>0.05	.941E+00 (±5%)	1.08	1.07	1.07	1.07

& The numbers in parentheses represents estimated relative uncertainty.

* MFP represents Mean Free Path of neutron in the materials.

Table 4.2.2 Comparison of 1 and 3D-calculations with MC- and MG-data for the IPPE iron shell experiment (isotropic neutron source, FENDL-1 data)

Shell Thickness (cm)	Energy Range (MeV)	Experimental Leakage (1/sn)	C/E of Integral Leakage			
			MCNP (3D)	MCNP (1D)	ONEDANT(1D)	NGSN (1D)
2.5	0.05~1.0	.9938E-01	.9206	1.0828	1.1776	1.1507
	1.0~5.0	.1400E+00	.9654	1.1116	1.1116	1.0857
	5.0~10.0	.3176E-01	.9495	1.0505	1.0392	1.0150
	10.0~20.	.7397E+00	.9963	1.0009	.9884	.9945
	>0.05	.1011E+01	.9831	1.0259	1.0257	1.0231
7.5	0.05~1.0	.3172E+00	1.0187	1.0886	1.1166	/
	1.0~5.0	.2518E+00	1.0521	1.0997	1.0680	
	5.0~10.0	.3453E-01	1.2048	1.2332	1.2213	
	10.0~20.	.4317E+00	.9492	.9526	.9378	
	>0.05	.1035E+01	1.0041	1.0394	1.0337	
10.0	0.05~1.0	.3869E+00	.9743	1.1197	1.1414	/
	1.0~5.0	.2714E+00	1.0200	1.1139	1.0724	
	5.0~10.0	.3318E-01	1.2224	1.2766	1.2623	
	10.0~20.	.3523E+00	.8725	.8761	.8614	
	>0.05	.1044E+01	.9597	1.0409	1.0328	
18.1	0.05~1.0	.6487E+00	1.0625	1.1016	1.0945	/
	1.0~5.0	.2106E+00	1.0836	1.1037	1.0024	
	5.0~10.0	.1677E-01	1.3306	1.3522	1.3323	
	10.0~20.	.1102E+00	.9936	.9940	.9748	
	>0.05	.9863E+00	1.0639	1.0943	1.0655	
28.0	0.05~1.0	.7858E+00	1.0848	1.1110	1.0118	1.0080
	1.0~5.0	.1150E+00	1.0057	1.0254	.8372	.8451
	5.0~10.0	.6274E-02	1.2251	1.2527	1.2381	1.2773
	10.0~20.	.3426E-01	.8783	.8847	.8649	.8994
	>0.05	.9413E+00	1.0686	1.0933	.9866	.9859

Calculations have been performed both for 1-D and 3-D geometrical models. The 3-D model takes into account the hole of D-beam tube in the spherical shells. For the 1-D calculation, the transport codes MCNP4A, ONEDANT, NGSN have been used, comprising Monte Carlo calculations with continuous-energy cross-section data (MC-data) and multigroup (MG) data in the Vitamin-J, 175-group-structure for EFF-2 and FENDL-1. The source neutron spectrum includes two parts: direct high energy source neutrons (98% of total source neutrons) and low energy neutrons being scattering by the target materials (2% of the total). The high energy component was calculated on the basis of the above derived model for the anisotropic emission of source neutrons (see Fig.4.1.1) in the T-Ti target while the low energy component was assumed to be isotropic. For that component the measured source neutron energy spectra was used. Fig.4.2.1 shows the source neutron energy spectra at 0, 60, 90 and 180° with respect to the D-beam.

The comparison of the calculated results with anisotropic neutron source and experimental data is shown in Fig. 4.2.2 ~ Fig. 4.2.6 and Table 4.2.1. The comparison of results obtained with 1-D and 3-D calculations, continuous-energy and multigroup data are shown in Fig.4.2.7

~ 4.2.10 and Table 4.2.2 ~ 4.2.3 for FENDL-1 and EFF-2 data, respectively. In the calculation with MG-data an isotropic neutron source distribution with uniform energy distribution in the source energy group (13.36 ~ 14.89 MeV) is included along with the low energy component described above in order to make visible the anisotropy effect.

Table 4.2.3 Comparison of 1 and 3D-calculations with MC- and MG-data for the IPPE iron shell experiment (isotropic neutron source, EFF-2 data)

Shell Thickness (cm)	Energy Range (MeV)	Experimental Leakage (1/sn)	C/E of Integral Leakage			
			MCNP (3D)	MCNP (1D)	ONEDANT(1D)	NGSN (1D)
2.5	0.05~1.0	.994E-01	.8887	1.025	1.113	1.086
	1.0~5.0	.140E+00	1.031	1.170	1.170	1.141
	5.0~10.0	.318E-01	.8931	.9724	.9563	.9318
	10.0~20.	.740E+00	.9939	.9963	.9846	.9886
	>0.05	.101E+01	.984	1.022	1.022	1.018
28.0	0.05~1.0	.786E+00	1.068	1.098	.9855	.9835
	1.0~5.0	.115E+00	1.020	1.038	.8464	.8509
	5.0~10.0	.627E-02	1.166	1.182	1.116	1.127
	10.0~20.	.343E-01	.8908	.9039	.8682	.8814
	>0.05	.941E+00	1.056	1.084	.9651	.9645

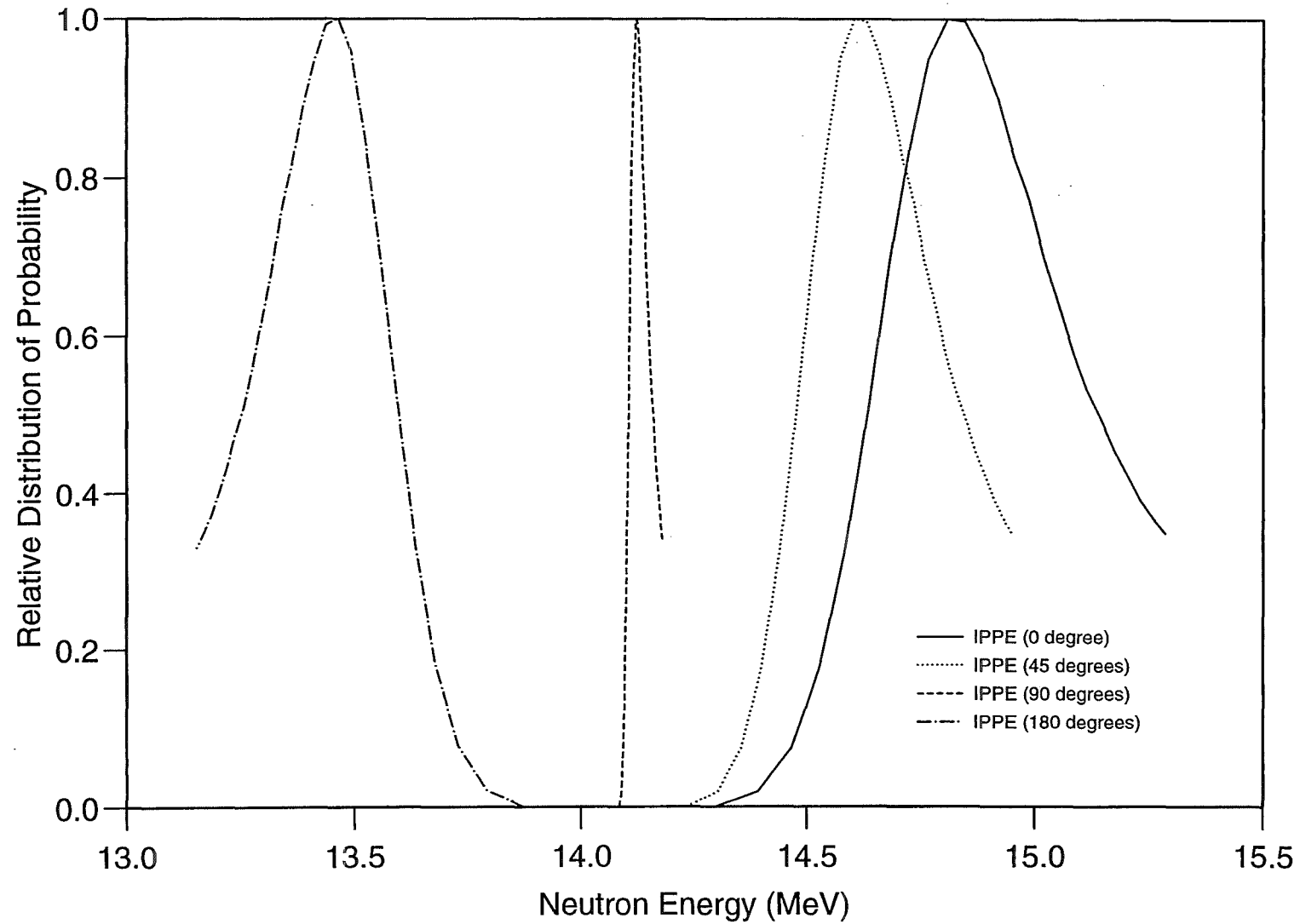


Fig.4.2.1 Energy and Angular Distribution of IPPE D-T neutron Source

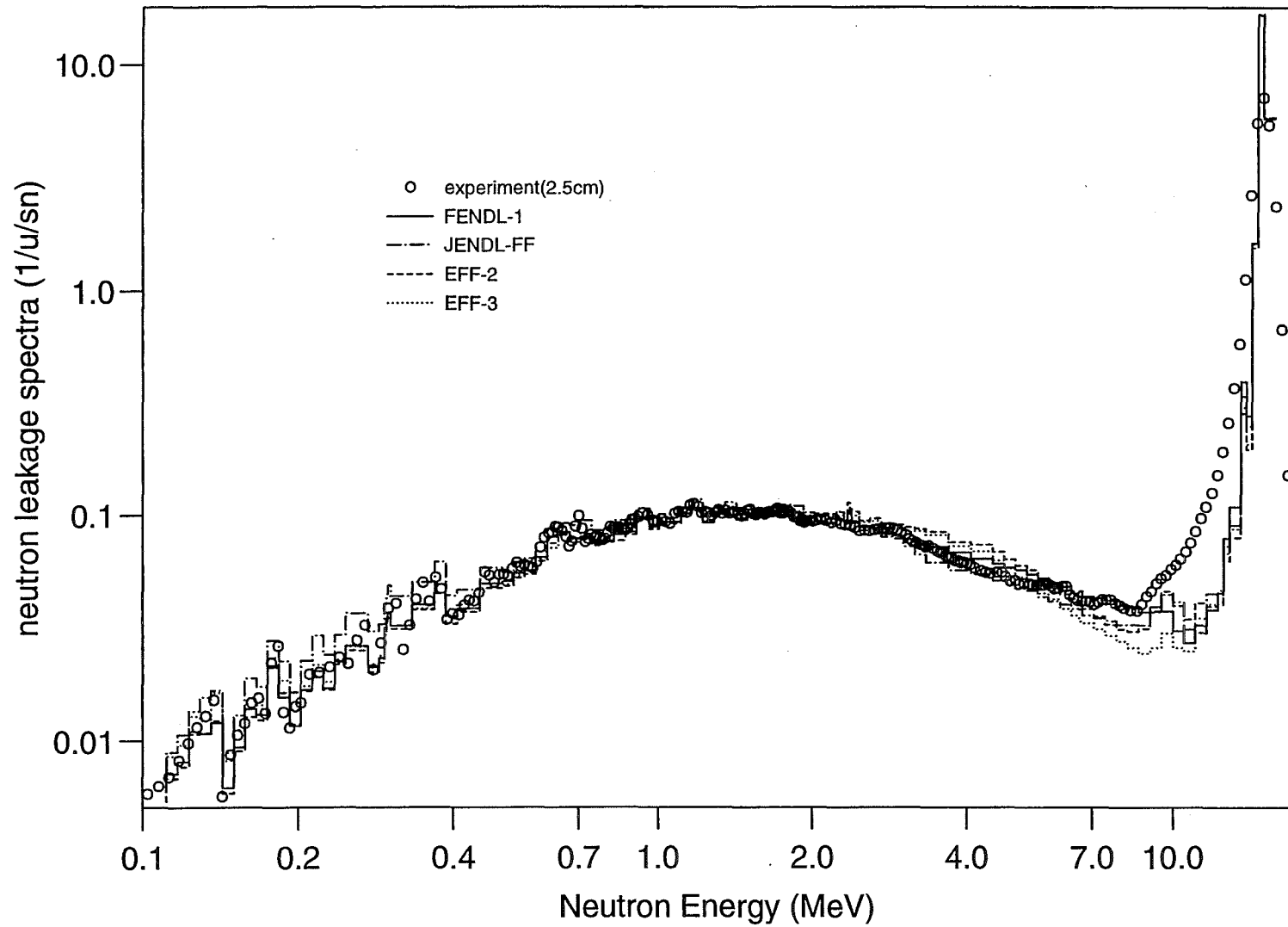


Fig.4.2.2 IPPE Iron Shell Experiment Neutron Spectra (2.5cm)

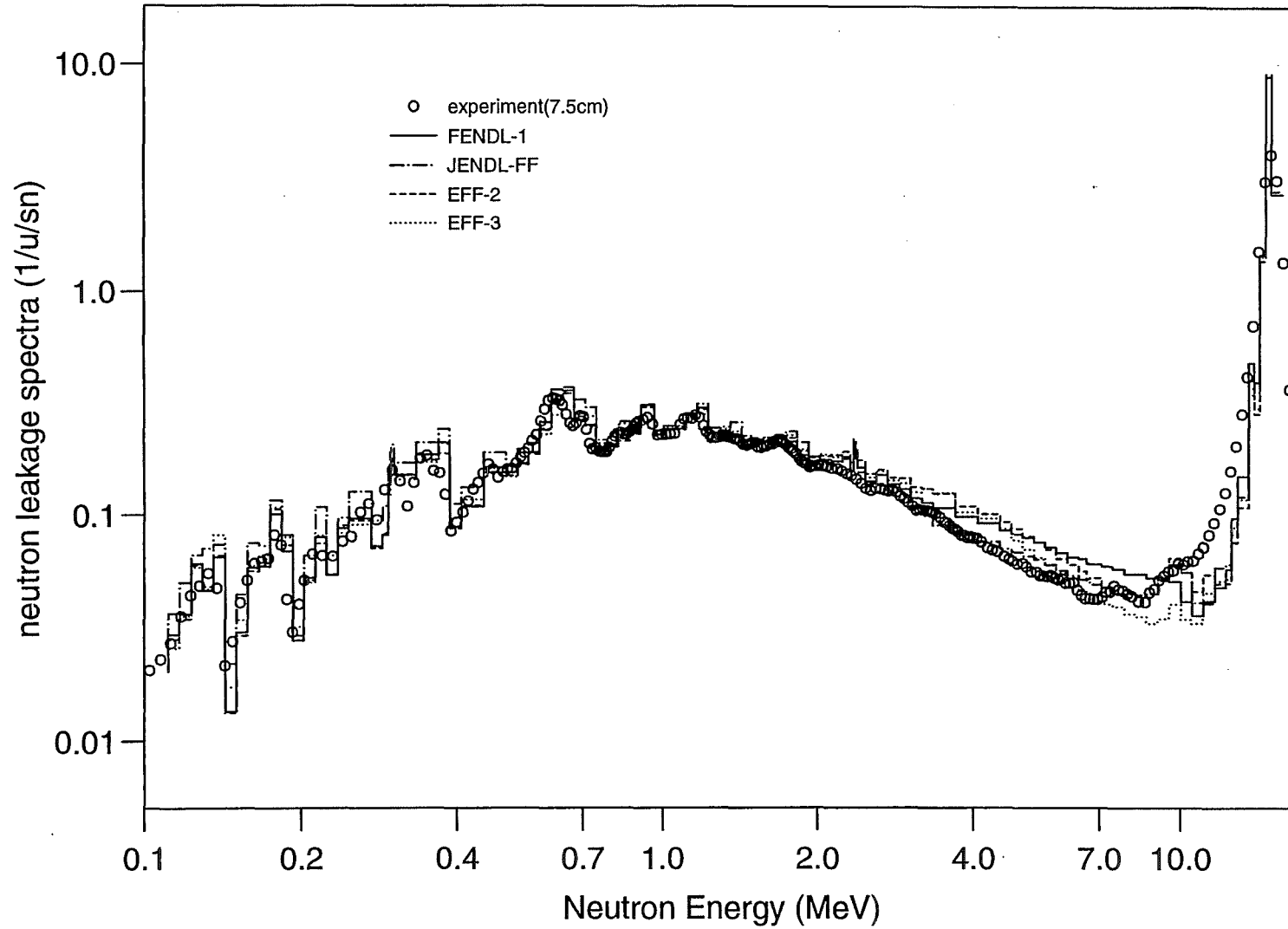


Fig.4.2.3 IPPE Iron Shell Experiment Neutron Spectra (7.5cm)

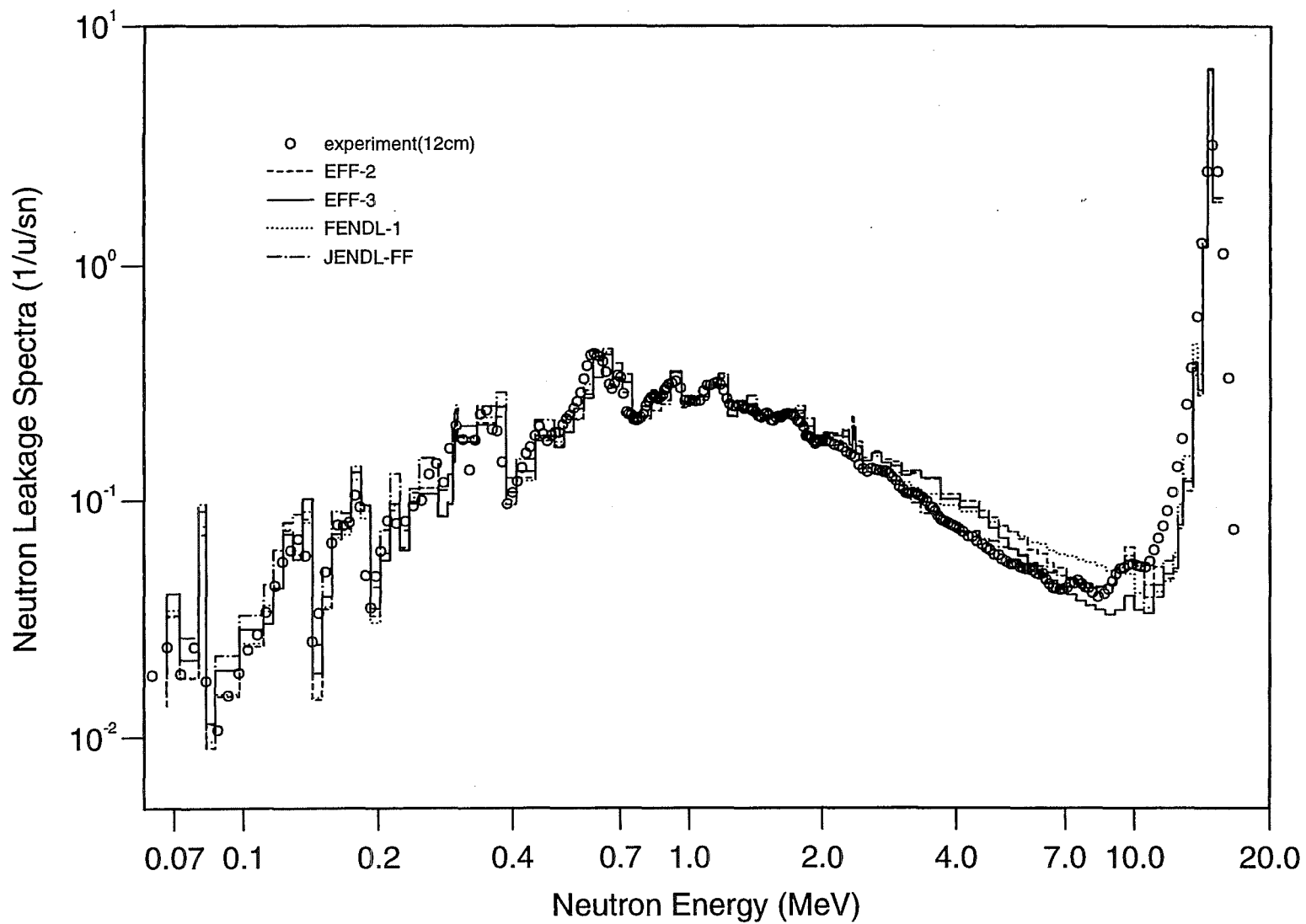


Fig.4.2.4 IPPE Iron Shell Experiment Neutron Spectra (12cm)

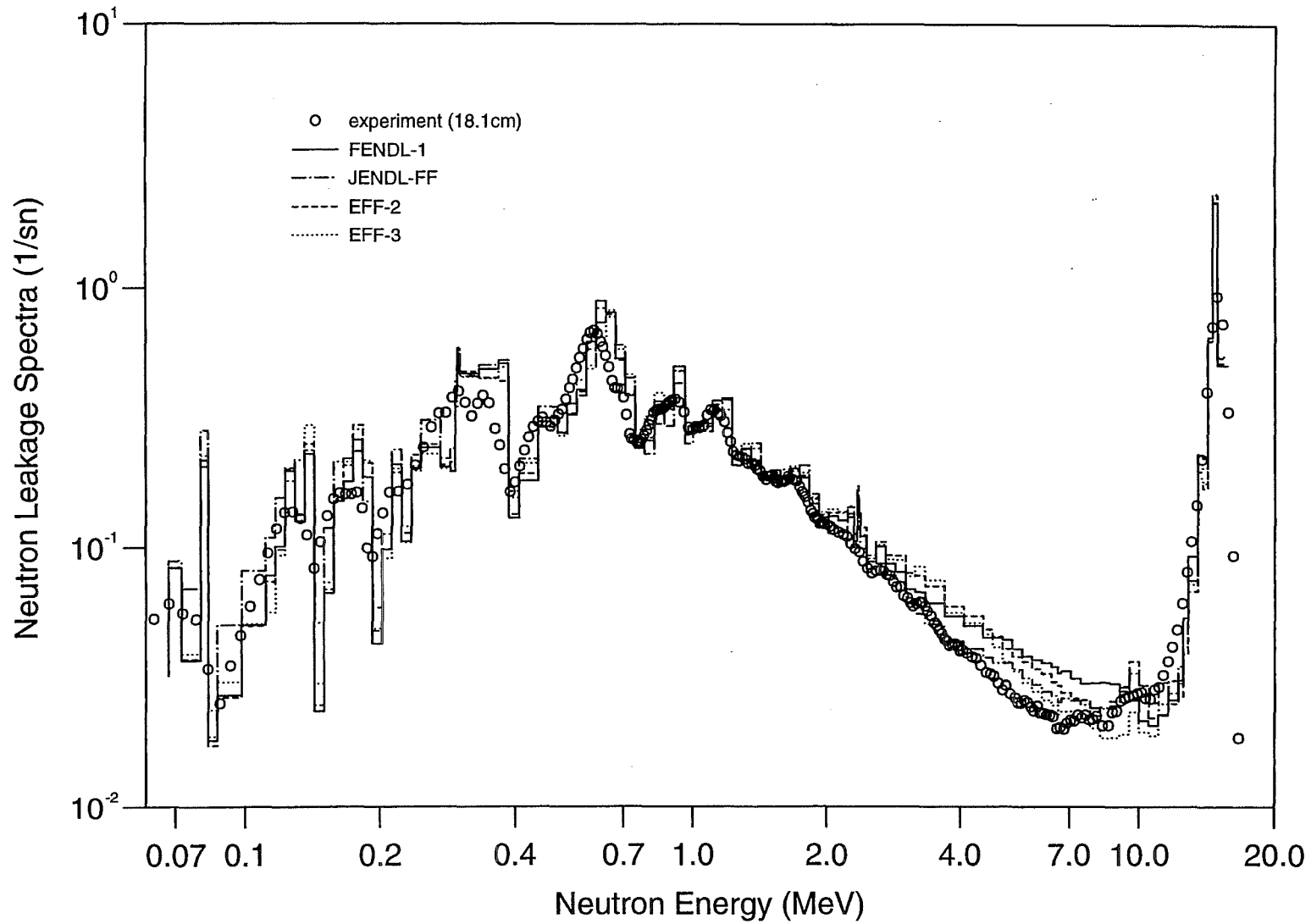


Fig.4.2.5 IPPE Iron Shell Experiment Neutron Spectra (18cm)

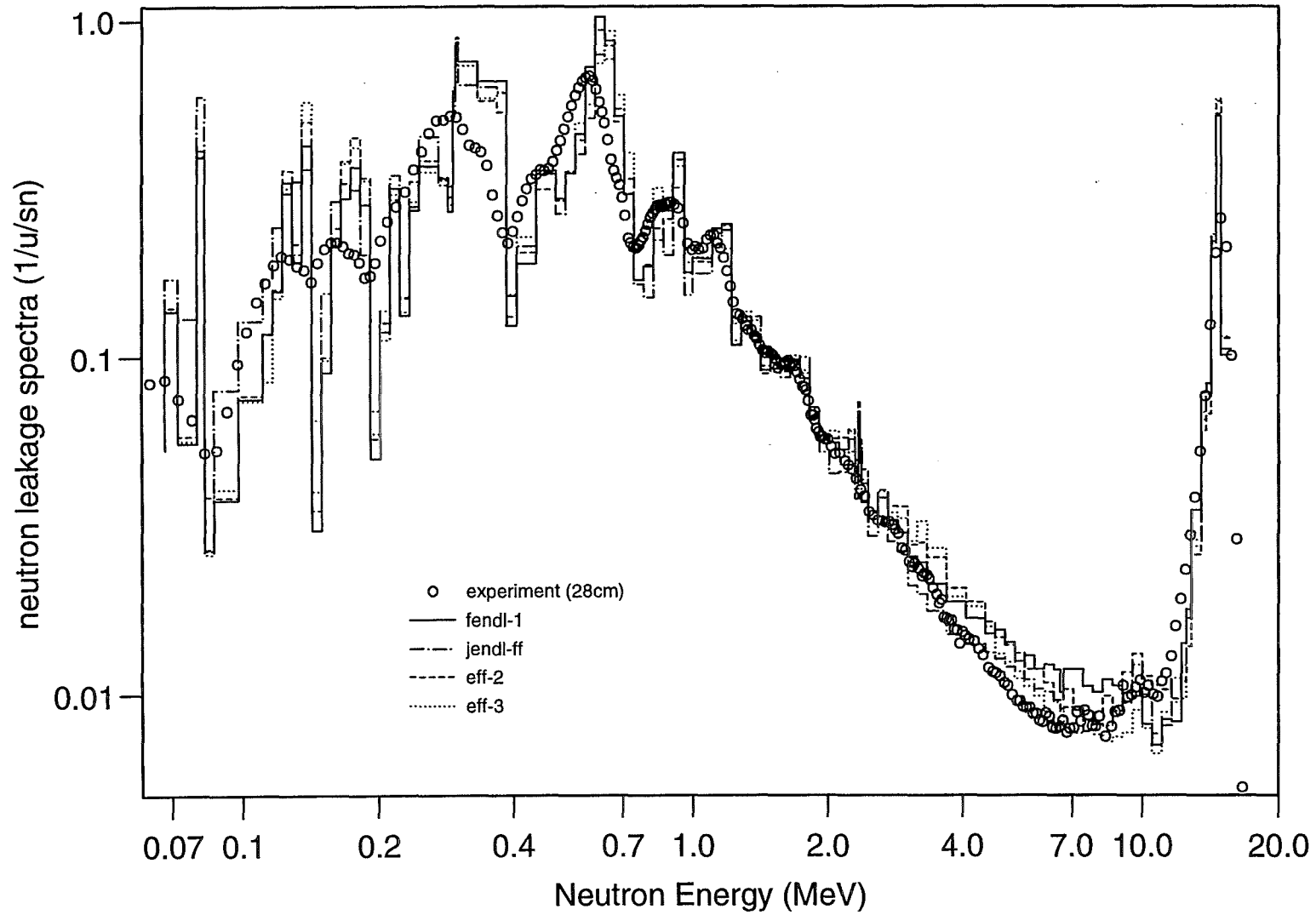


Fig.4.2.6 IPPE Iron Shell Experiment Neutron Spectra (28cm)

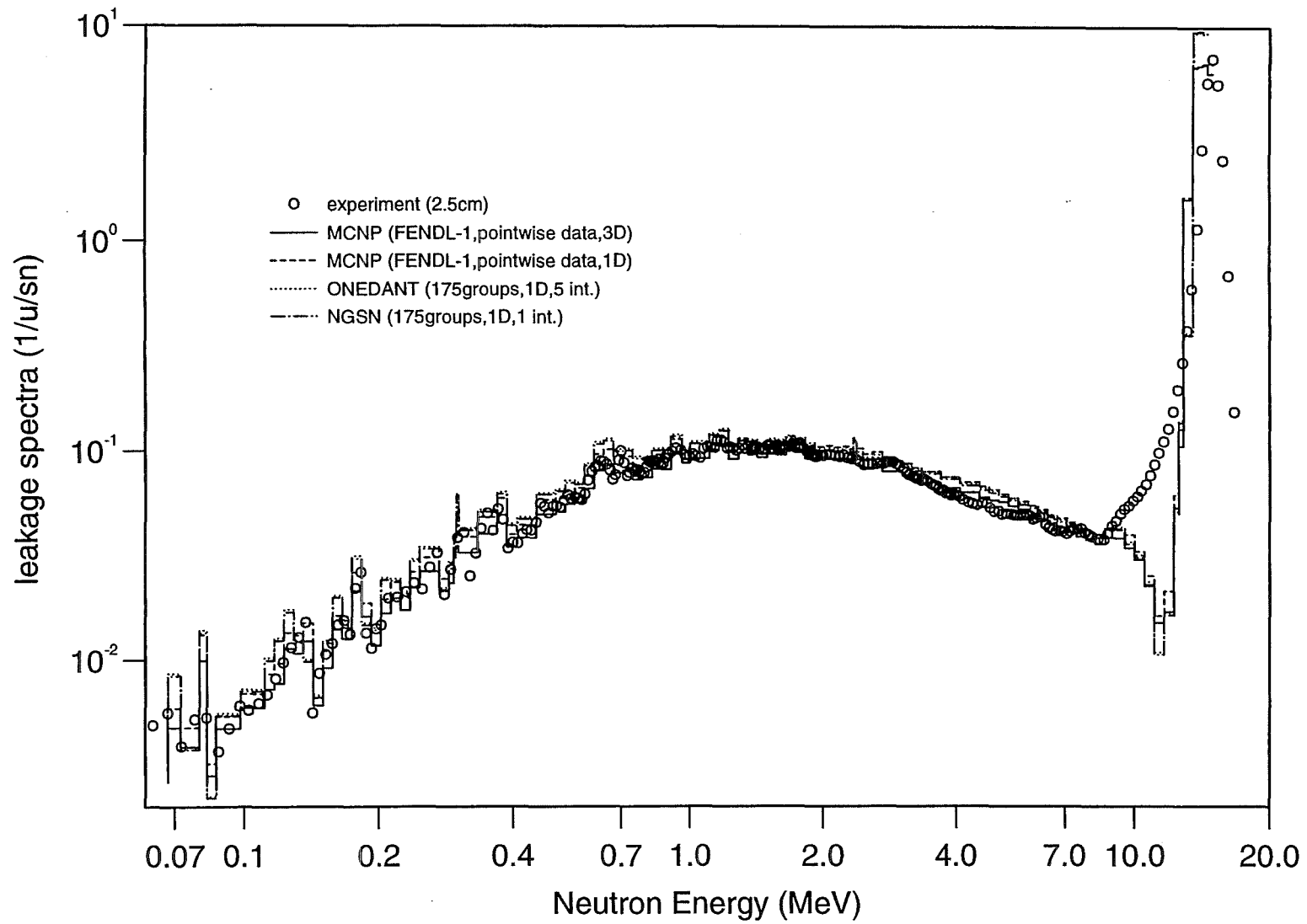


Fig.4.2.7 Comparison of MC- and MG- data, 1D- and 3D- Geometry

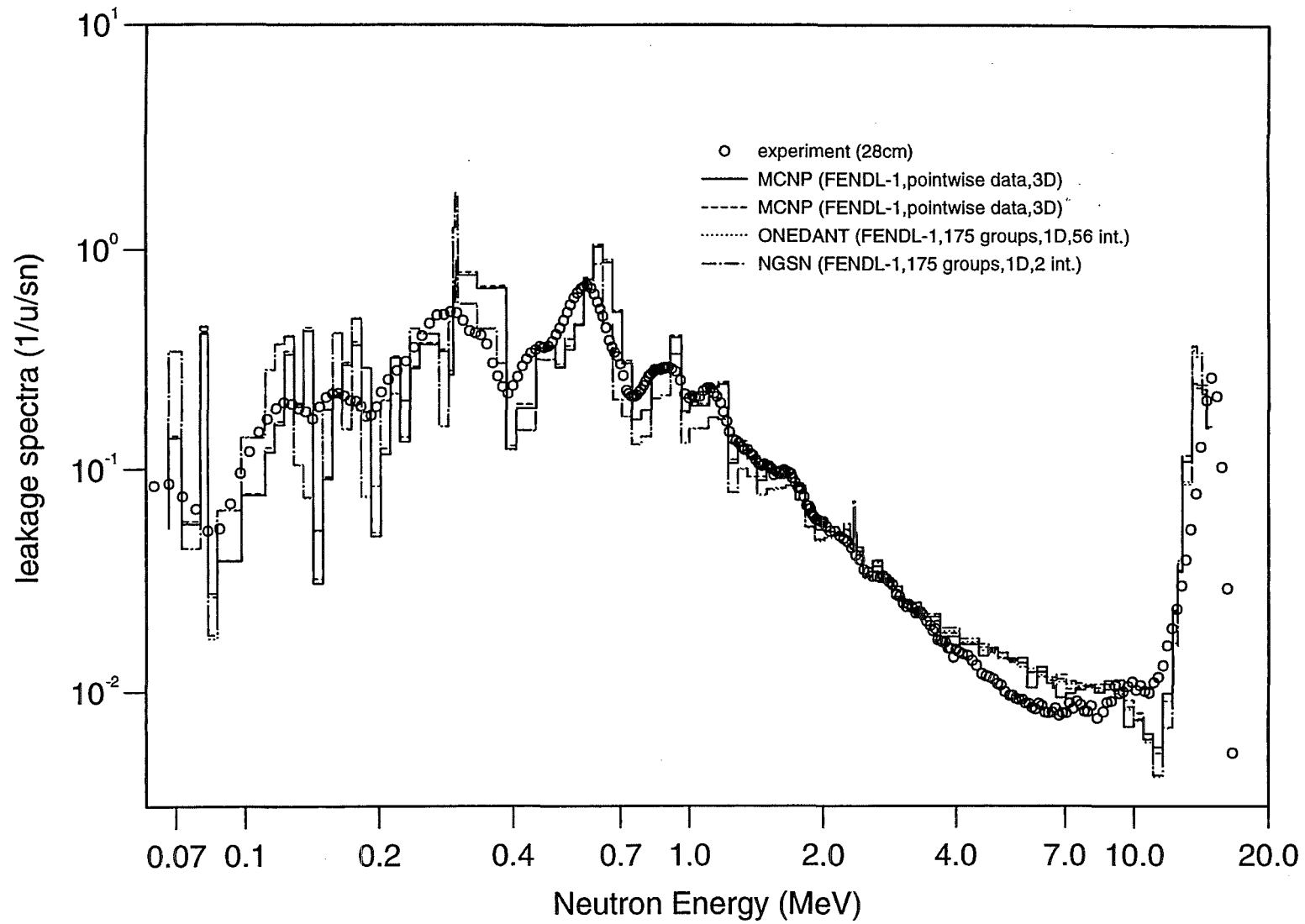


Fig.4.2.8 Comparison of MC- and MG- Data, 1D- and 3D- Geometry

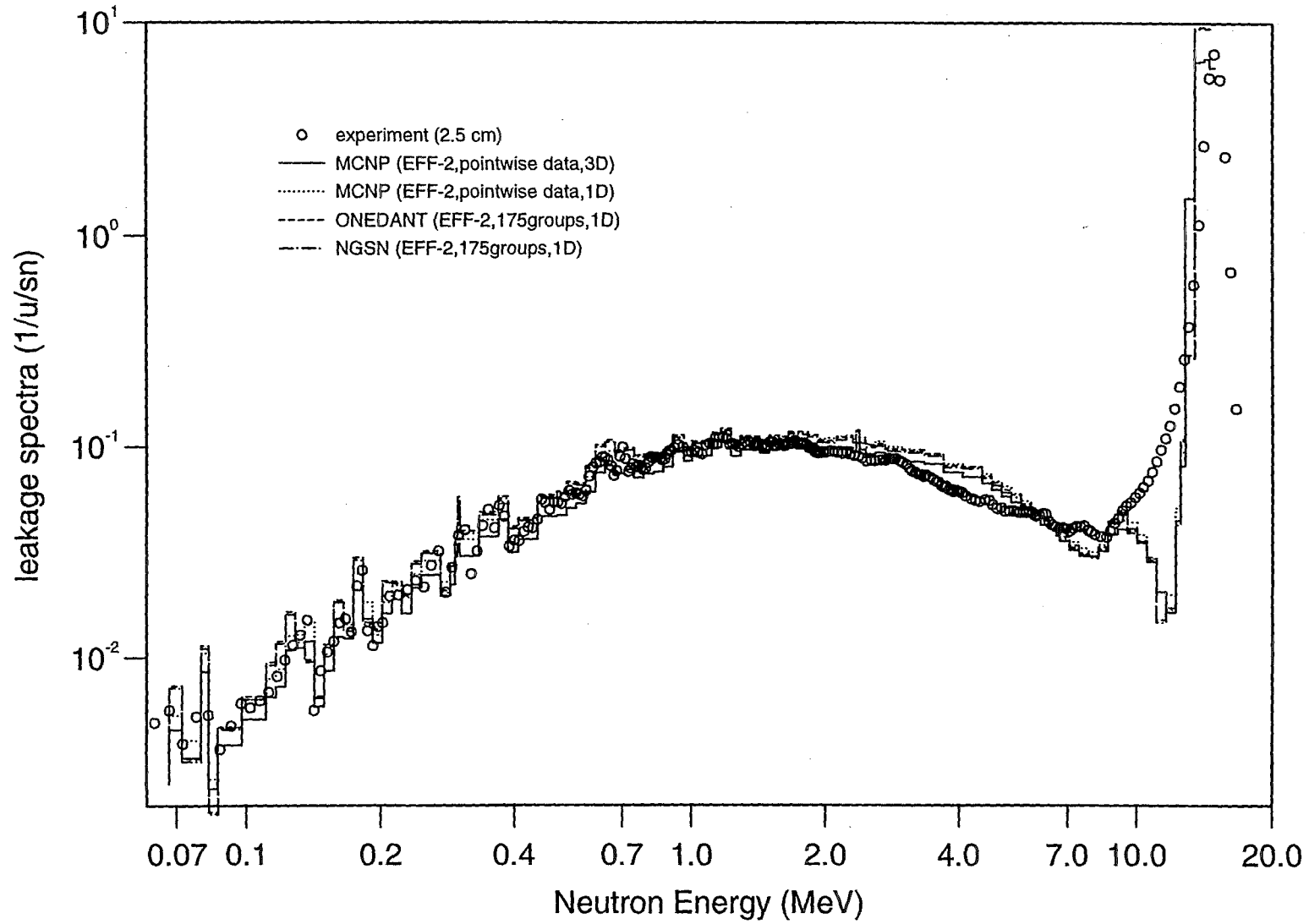


Fig.4.2.9 Comparison of MC- and MG- data, 1D- and 3D- Geometry

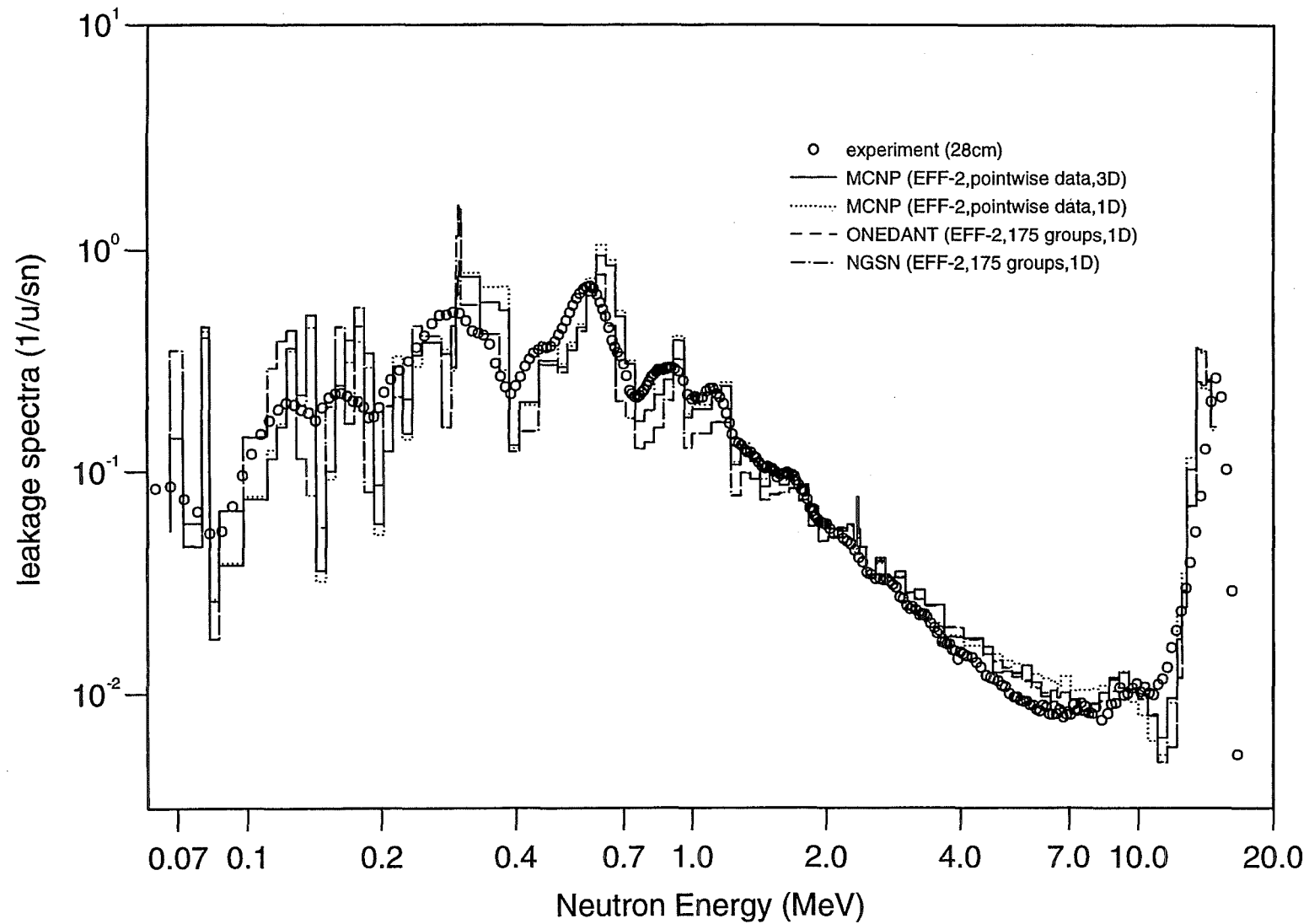


Fig.4.2.10 Comparison of MC- and MG- Data, 1D- and 3D- Geometry

4.3 FNS (JAERI) Iron Slab TOF Experiment

Angular neutron flux spectra leaking from iron slabs were measured as a function of slab thickness for D-T source neutrons at the Fusion Neutronics Source (FNS) facility, JAERI, by applying the TOF (Time-of-Flight) method.

The iron slab was made of combinations of 5 and 10 cm thick \times 100 cm (diameter) cylindrical plates. The slab was placed at a distance of 20 cm from the T-target (350 keV D-ion energy). Slab thicknesses of 5, 20, 40 and 60 cm were chosen. The chemical composition of the plate was 98.75% iron with small amounts of impurities. The density was 7.78 g/cm³.

A 5.08 cm-diameter \times 5.08 cm-long NE-213 liquid scintillator was used for the neutron detection with the TOF-method. The neutron flight path was about 7 m, and the measuring angles were at 0, 12.2, 24.9, 41.8 and 66.8 degrees with respect to the deuteron beam.

The experimental uncertainty consists of a systematic error and a statistical error as listed in Table 4.3.1. The systematic error had been estimated as follows:

- Detector Efficiency
 - En > 200 keV < 2%
 - 80 < En < 200 keV 5~10%
 - 50 < En < 80 keV 10~20%
- Solid Angle << 1%
- Effective measured area < 2%

A detailed description of the experiment can be found in Ref. [19,29,30].

In the calculation, the anisotropy of the D-T neutron source was taken into account on the basis of the model described in Section 3.

In this work, only the 20 cm thick iron plate is considered.

Angular neutron flux spectra were calculated at 0, 12.2, 24.9, 41.8 and 66.8 degrees with respect to the deuteron beam direction and are compared with the measured results in Fig. 4.3.1 ~ 5. The C/E values for energy-integrated angular fluxes are shown in Table 4.3.1.

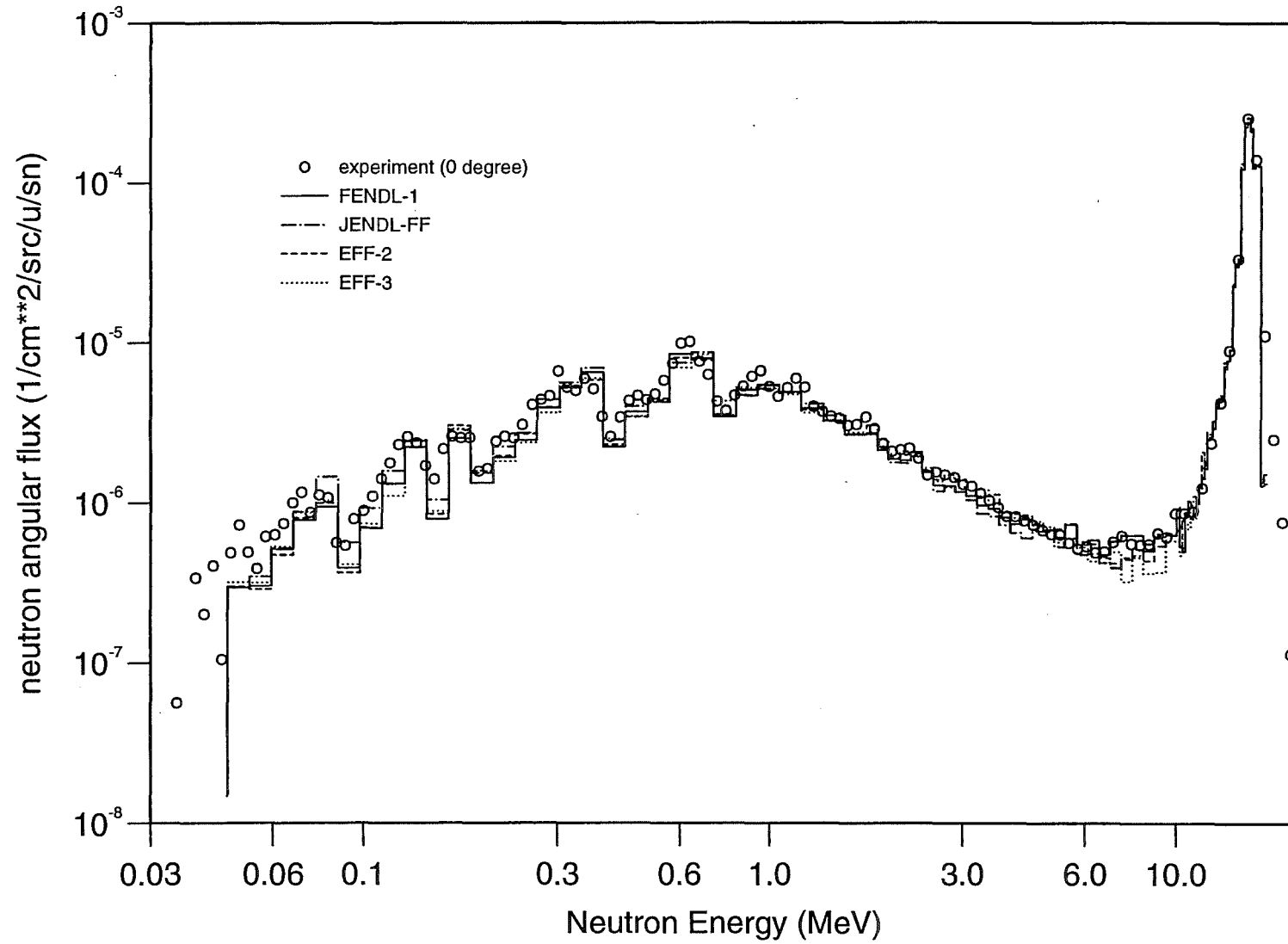


Fig.4.3.1 FNS(TOF) Iron Slab Experiment Neutron Spectra (0 deg.)

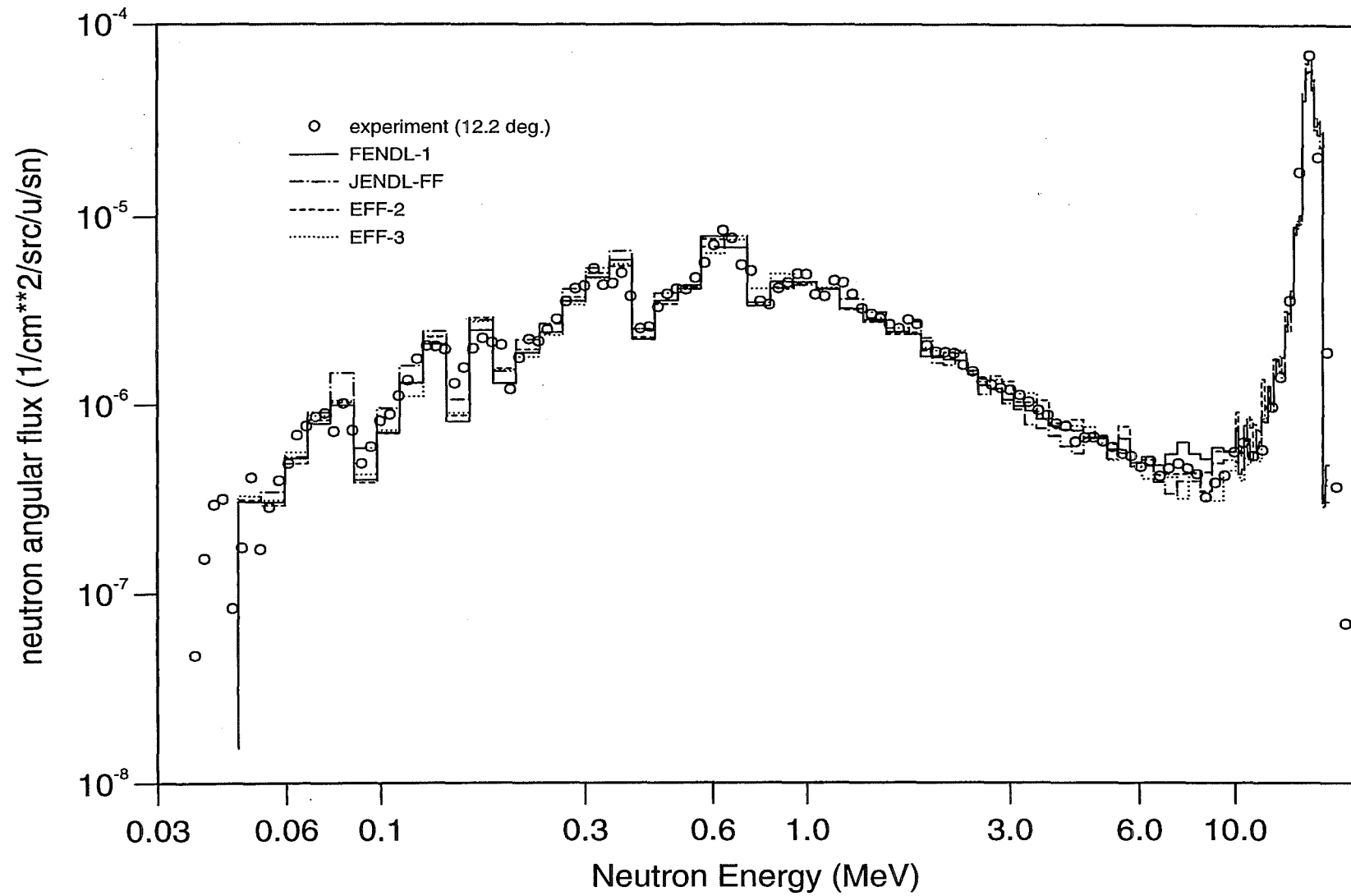


Fig.4.3.2 FNS(TOF) Iron Slab Experiment Neutron Spectra (12.2 deg.)

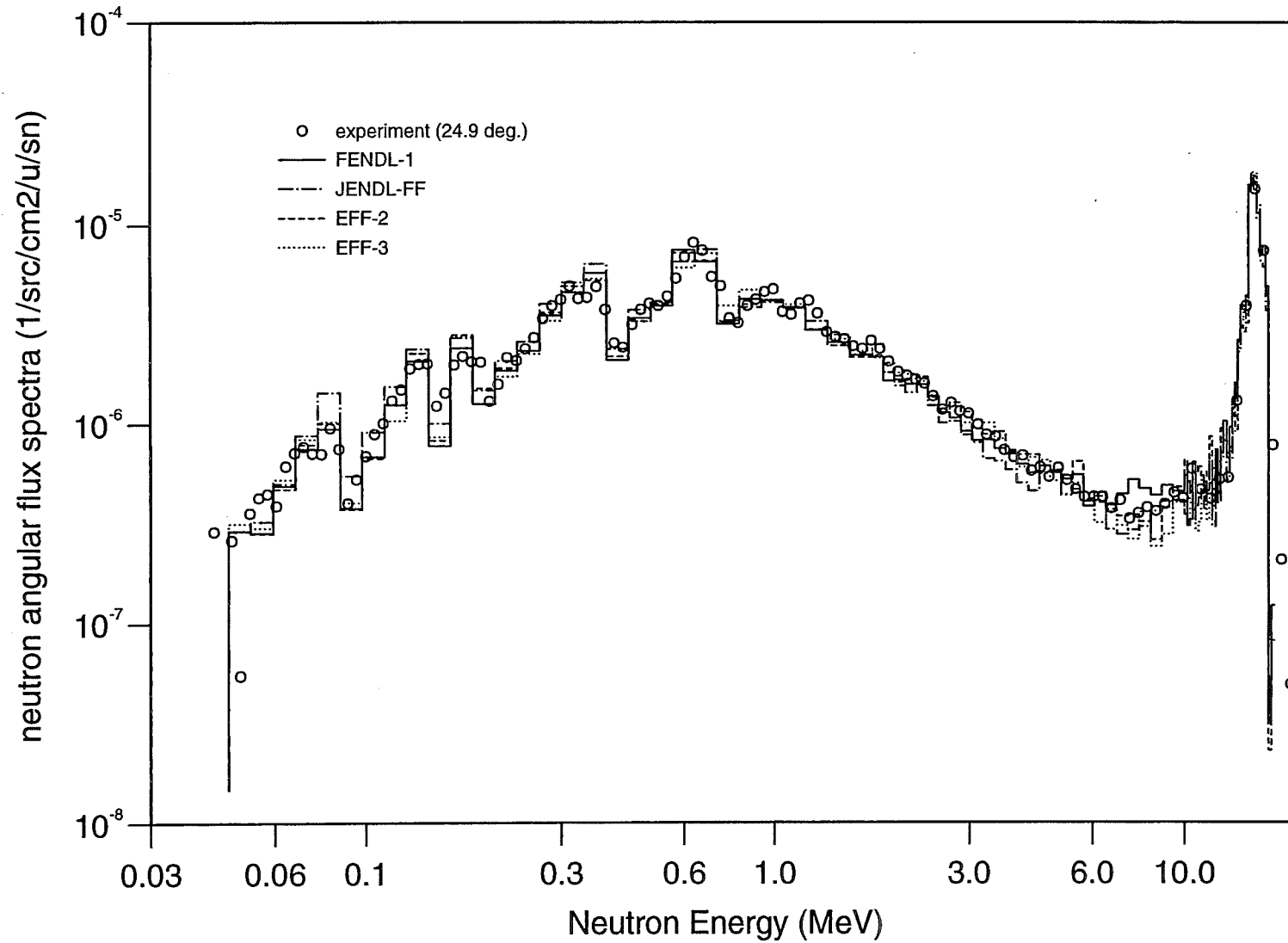


Fig.4.3.3 FNS(TOF) Iron Slab Experiment Neutron Spectra (24.9 deg.)

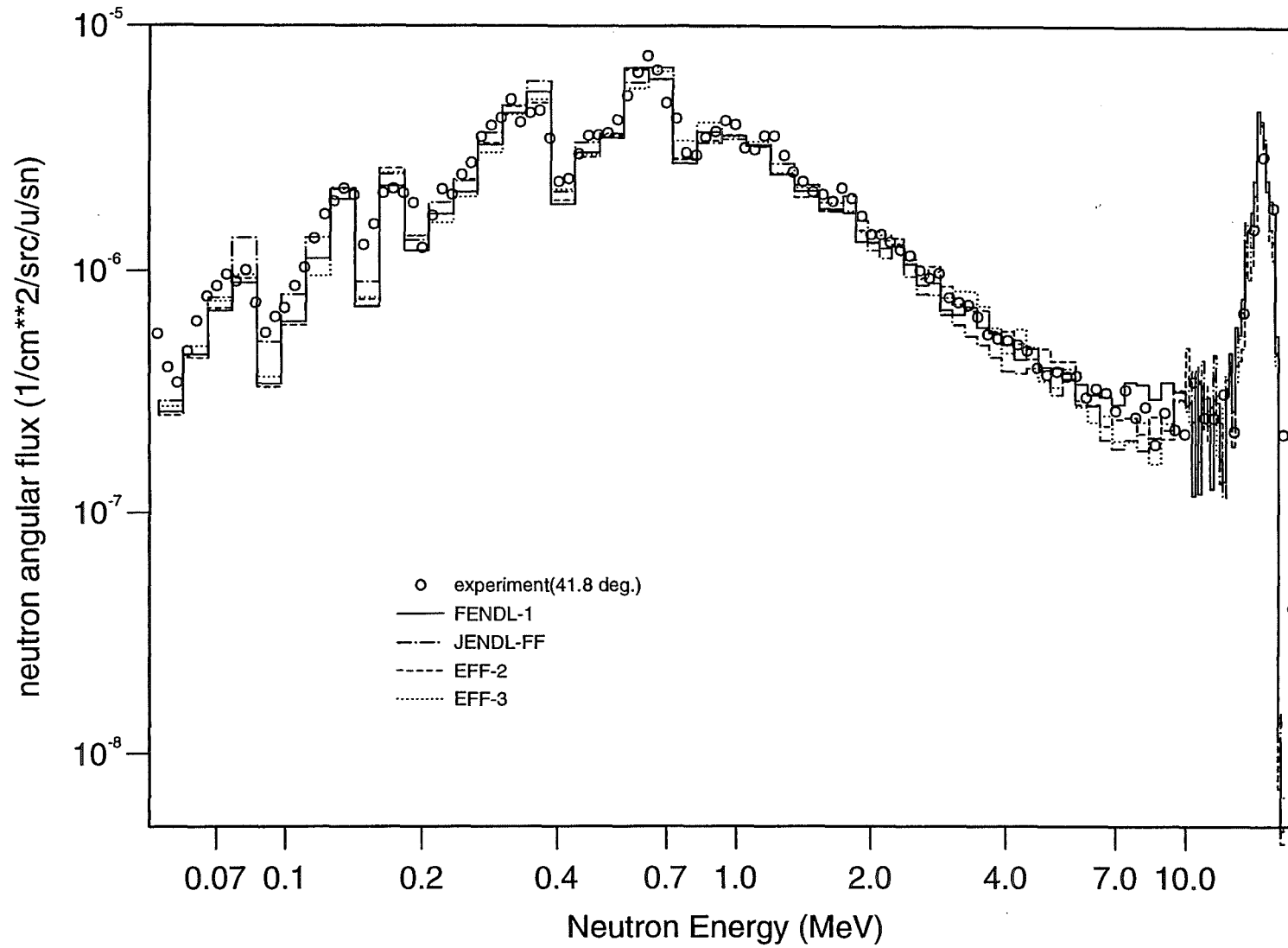


Fig.4.3.4 FNS(TOF) Iron Slab Experiment Neutron Spectra (41.8 deg.)

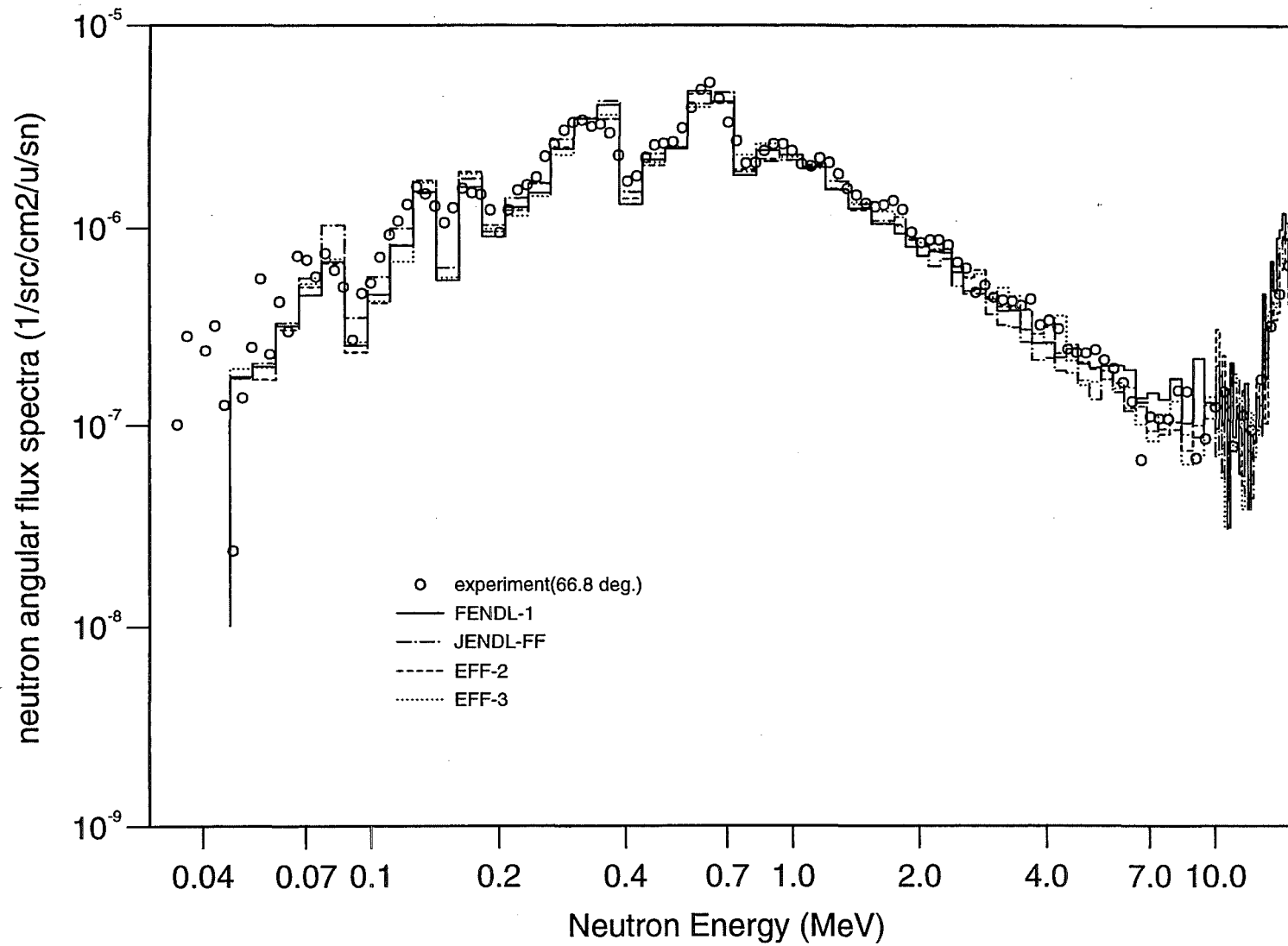


Fig.4.3.5 FNS(TOF) Iron Slab Experiment Neutron Spectra (66.8 deg.)

Table 4.3.1 C/E data for integrated neutron flux spectra in the FNS iron slab experiment

Angle (degree)	Energy Range (MeV)	Experimental Angular Flux (1/src/cm ² /sn)	Experimental Statistic Error (%)	C/E of Neutron Flux			
				FENDL-1	EFF-3	EFF-2	JENDL-FF
0	0.03~1.0	.103-4*	2.5	.867	.878	.870	.918
	1.0~5.0	.381-5	~2.7	1.04	1.03	1.06	1.04
	5.0~10.0	.416-6	9.0	1.13	.885	1.05	.947
	10.0~20.0	.231-4	0.6	.907	.951	.948	.930
	>0.03	.376-4	1.5	.912	.939	.939	.938
12.2	0.03~1.0	.850-5	2.7	.973	1.00	.991	1.05
	1.0~5.0	.324-5	2.7	1.05	1.09	1.08	1.07
	5.0~10.0	.331-6	8.8	1.31	.999	1.22	1.07
	10.0~20.0	.587-5	1.2	.919	1.00	.988	.882
	>0.03	.179-4	2.3	.976	1.02	1.01	1.00
24.9	0.03~1.0	.804-5	1.6	.989	1.02	1.01	1.07
	1.0~5.0	.298-5	2.5	1.04	1.08	1.07	1.05
	5.0~10.0	.291-6	8.3	1.24	.960	1.15	.994
	10.0~20.0	.157-5	2.4	1.06	1.08	1.05	.961
	>0.03	.129-4	2.1	1.02	1.04	1.03	1.05
41.8	0.03~1.0	.774-5	2.6	.932	.952	.949	.997
	1.0~5.0	.244-5	3.2	1.04	1.08	1.07	1.03
	5.0~10.0	.202-6	12.9	1.23	.977	1.16	.982
	10.0~20.0	.429-6	6.1	1.16	1.01	.990	1.04
	>0.03	.108-4	3.1	.972	.983	.982	1.00
66.8	0.03~1.0	.559-5	3.7	.926	.934	.935	.972
	1.0~5.0	.151-5	4.7	1.01	1.05	1.04	.987
	5.0~10.0	.967-7	29.9	1.31	.949	1.11	.940
	10.0~20.0	.135-6	18.9	1.10	.923	.883	.951
	>0.03	.733-5	4.5	.952	.959	.957	.974

Note: .103-4 represents 0.103×10^{-4}

4.4 FNS(JAERI) Iron In-system Experiment

The Slowing-Down-Time (SDT) method was adopted as an innovative technique for in-situ measurements of the low energy neutron spectrum at the FNS facility of JAERI. In this experiment, an iron assembly was used with 1000 mm diameter and 950 mm thickness. The iron contained 0.834wt% manganese, 0.185wt% carbon and 0.148wt% sulfur as impurities. The front surface of the assembly was placed at a distance of 200 mm from the Ti-T target. There were six experimental holes (measuring positions) of 21x21 square millimeters at positions of 110, 210, 310, 410, 610, 810 mm from the front surface of the assembly.

Table 4.4.1 C/E-data for integrated neutron flux spectra in the FNS iron in-system experiment

Position (mm)	Energy Range (MeV)	Experimental Flux (1/cm ² /sn)	Experimental Error (%)	C/E of Neutron Flux			
				FENDL-1	EFF-3	EFF-2	JENDL-FF
110	10 ⁻⁶ ~10 ⁻⁵	.58-6*	6.6	0.93	<i>1.12</i>	<i>1.15</i>	0.95
	10 ⁻⁵ ~10 ⁻⁴	.15-5	7.8	0.93	<i>1.13</i>	<i>1.13</i>	0.90
	10 ⁻⁴ ~10 ⁻³	.24-5	12.5	1.03	<i>1.19</i>	<i>1.19</i>	<i>1.07</i>
	10 ⁻³ ~10 ⁻²	.32-5	36.2	<i>1.64</i>	<i>1.81</i>	<i>1.95</i>	<i>1.95</i>
	10 ⁻² ~10 ⁻¹	.29-4	14.7	0.85	0.93	0.89	0.94
	10 ⁻¹ ~10 ⁰	.16-3	3.4	0.91	0.94	0.96	1.04
	Total*	.19-3	6.2	0.90	0.94	0.96	1.01
210	10 ⁻⁶ ~10 ⁻⁵	.78-6	5.7	0.96	<i>1.11</i>	<i>1.18</i>	1.02
	10 ⁻⁵ ~10 ⁻⁴	.19-5	6.9	0.98	<i>1.12</i>	<i>1.15</i>	1.02
	10 ⁻⁴ ~10 ⁻³	.28-5	11.4	1.05	<i>1.19</i>	<i>1.26</i>	<i>1.15</i>
	10 ⁻³ ~10 ⁻²	.51-5	19.0	1.04	<i>1.13</i>	<i>1.24</i>	<i>1.28</i>
	10 ⁻² ~10 ⁻¹	.25-4	10.1	0.90	0.94	0.93	1.06
	10 ⁻¹ ~10 ⁰	.96-4	3.4	0.95	1.00	1.00	1.03
	Total	.13-3	5.5	0.93	0.99	0.99	1.03
310	10 ⁻⁶ ~10 ⁻⁵	.73-6	6.1	1.00	<i>1.14</i>	<i>1.17</i>	<i>1.13</i>
	10 ⁻⁵ ~10 ⁻⁴	.17-5	7.3	1.01	<i>1.15</i>	<i>1.22</i>	<i>1.12</i>
	10 ⁻⁴ ~10 ⁻³	.24-5	11.8	<i>1.09</i>	<i>1.20</i>	<i>1.26</i>	<i>1.26</i>
	10 ⁻³ ~10 ⁻²	.46-5	16.9	0.99	<i>1.03</i>	<i>1.11</i>	<i>1.23</i>
	10 ⁻² ~10 ⁻¹	.19-4	7.5	0.91	0.95	0.98	1.10
	10 ⁻¹ ~10 ⁰	.54-4	3.2	0.95	1.01	1.00	1.00
	Total	.82-4	5.3	0.94	1.00	1.01	1.04
410	10 ⁻⁶ ~10 ⁻⁵	.65-7	5.9	0.97	<i>1.07</i>	<i>1.19</i>	<i>1.10</i>
	10 ⁻⁵ ~10 ⁻⁴	.15-5	7.0	0.98	<i>1.10</i>	<i>1.11</i>	<i>1.06</i>
	10 ⁻⁴ ~10 ⁻³	.21-5	11.5	1.02	<i>1.11</i>	<i>1.19</i>	<i>1.17</i>
	10 ⁻³ ~10 ⁻²	.30-5	18.9	<i>1.23</i>	<i>1.24</i>	<i>1.32</i>	<i>1.51</i>
	10 ⁻² ~10 ⁻¹	.13-4	7.7	0.94	0.96	1.01	1.12
	10 ⁻¹ ~10 ⁰	.30-4	2.6	0.97	1.02	1.00	0.98
	Total	.50-4	5.5	0.97	1.02	1.03	1.05
610	10 ⁻⁶ ~10 ⁻⁵	.38-6	5.9	0.95	<i>1.01</i>	<i>1.11</i>	<i>1.07</i>
	10 ⁻⁵ ~10 ⁻⁴	.85-6	7.1	1.00	<i>1.05</i>	<i>1.12</i>	<i>1.07</i>
	10 ⁻⁴ ~10 ⁻³	.12-5	11.4	0.99	<i>1.05</i>	<i>1.15</i>	<i>1.10</i>
	10 ⁻³ ~10 ⁻²	.18-5	16.4	<i>1.11</i>	<i>1.13</i>	<i>1.21</i>	<i>1.34</i>
	10 ⁻² ~10 ⁻¹	.64-5	6.1	0.91	0.93	0.95	1.02
	10 ⁻¹ ~10 ⁰	.93-5	2.4	0.93	0.99	0.95	0.91
	Total	.20-3	5.7	0.95	0.99	1.00	1.00
810	10 ⁻⁶ ~10 ⁻⁵	.15-6	6.2	0.95	1.01	<i>1.07</i>	<i>1.05</i>
	10 ⁻⁵ ~10 ⁻⁴	.34-6	7.4	0.96	1.01	<i>1.09</i>	<i>1.04</i>
	10 ⁻⁴ ~10 ⁻³	.48-6	11.8	0.97	1.02	<i>1.10</i>	<i>1.09</i>
	10 ⁻³ ~10 ⁻²	.81-6	14.4	0.97	0.95	1.00	<i>1.13</i>
	10 ⁻² ~10 ⁻¹	.25-5	5.6	0.87	0.89	0.91	0.95
	10 ⁻¹ ~10 ⁰	.28-5	2.6	0.92	0.93	0.88	0.83
	Total	.71-5	5.9	0.91	0.93	0.93	0.94

Note: Hereafter, “.58-6” represents 0.58×10^{-6} ; “Total” is referred to the total energy range considered.

The neutron spectrum above 1 MeV was measured with a small NE213 spectrometer and various reaction rates applying the foil activation technique, the neutron spectra between 3 keV and 1 MeV by using a pair of PRCs (Proton Recoil Gas Proportional Counters) and the neutron spectrum between 0.3 eV and 10 keV by the SDT method. The different reaction rates were also measured at different positions.

The estimated overall experimental errors in the energy ranges below 1 keV and between 1 and 10 keV were 5-9% and 8-13%, respectively [20].

A detailed description of experiment can be found in Ref.[20,21].

In the calculation, the same anisotropic neutron source as that in the FNS-Iron-Slab-Experiment was adopted on the basis of the model described in Section 3.

The neutron spectra at the positions of 110, 210, 310, 410, 610, and 810 mm have been calculated by using MCNP and the continuous energy cross-section data of FENDL-1, EFF-2, EFF-3 and JENDL-FF and are presented in Fig 4.4.1~4.4.6 (for < 1 MeV). The C/E values for the integrated flux spectra are given in Table 4.4.1. The C/E comparison for the reaction rates Fe(n, p), Al(n, α), Zr (n,2n) and Au(n, γ) are presented in Table 4.4.2 at the positions of 0, 100, 200, 300, 400, 500, 700 mm.

Table 4.1.2 C/E data for reaction rates measured in the FNS iron in-system experiment &

Position (mm)	Reaction Type	Measured Value (1/cm ³ /sn)	C/E		Reaction Type	Measured Value (1/cm ³ /sn)	C/E	
			EFF-2	FENDL-1			EFF-2	FENDL-1
0	Fe(n,p)	.22E-4(2.6*)	1.04	1.06	Zr(n,2n)	.20E-3(2.7)	.92	.93
100		.34E-5(2.7)	.99	1.02		.26E-4(2.7)	.91	.92
200		.54E-6(3.0)	1.02	1.04		.41E-5(2.7)	.90	.90
300		.11E-6(3.0)	.92	.94		.70E-6(2.9)	.89	.88
400		.15E-7(3.9)	1.25	1.26		.15E-6(3.6)	.76	.74
500		.35E-8(5.6)	1.04	1.01		.27E-7(4.5)	.79	.74
700		.19E-9(28)	.76	.70		.56E-8(8.9)	.14	.13
0	Al(n, α)	.25E-4(2.8)	.97	.99	Au(n, γ)	.14E-3(3.4)	.64	.55
100		.38E-5(2.8)	.93	.95		.62E-3(3.0)	1.00	.88
200		.63E-6(2.8)	.94	.96		.82E-3(2.8)	1.14	.95
300		.12E-6(3.1)	.86	.88		.74E-3(3.1)	1.28	1.06
400		.22E-7(3.5)	.90	.90		.65E-3(3.3)	1.20	1.03
500		.39E-8(5.9)	1.00	.97		.51E-3(3.2)	1.12	1.01
700		.15E-9 (-)	1.01	.93		.26E-3(3.3)	1.12	1.01

Note: & The same response functions were used in the calculations with isotropic neutron source.

* The numbers in parentheses are relative percent experimental uncertainty.

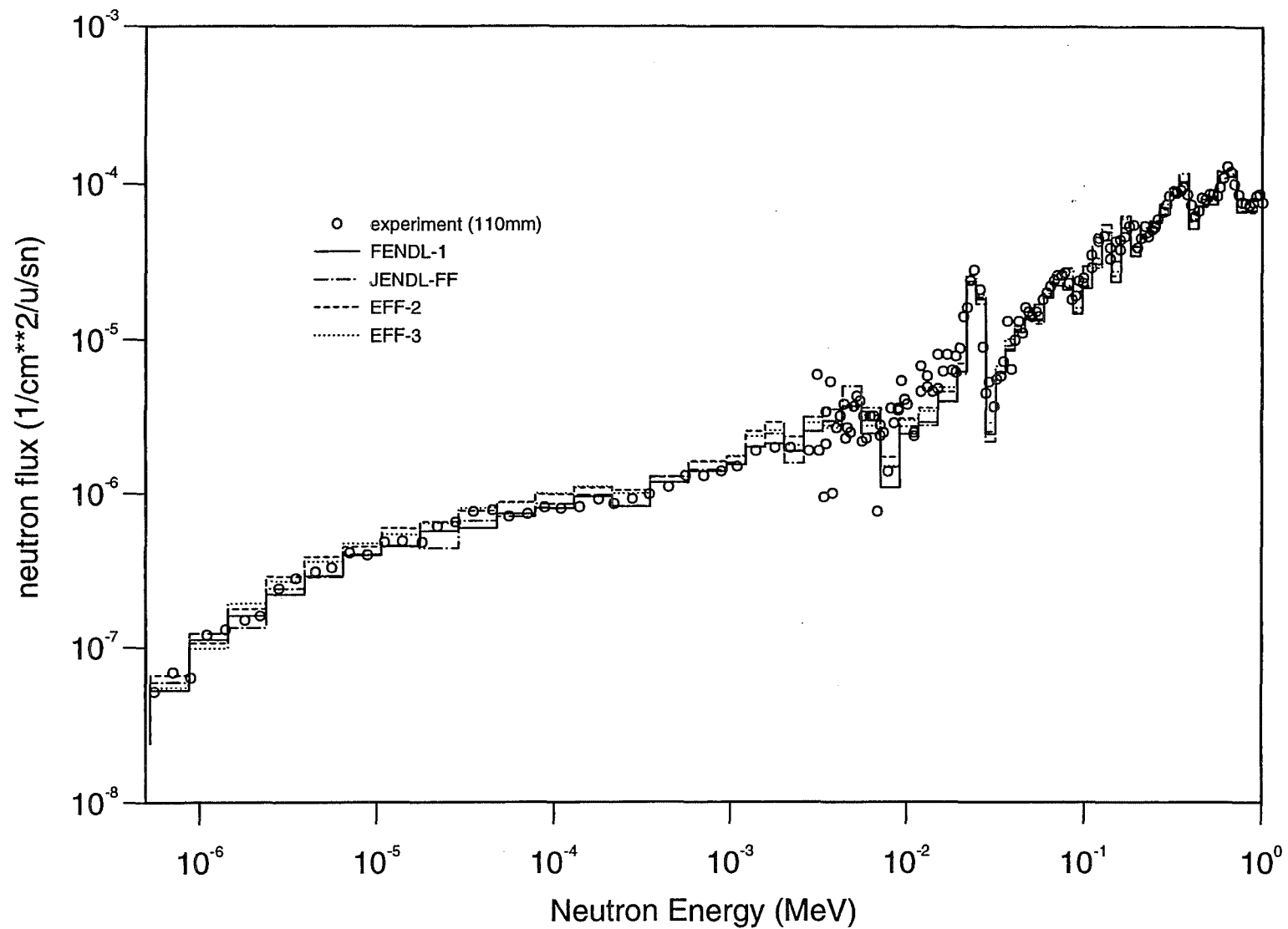


Fig.4.4.1 FNS Iron In-system Experiment Neutron Spectra (110mm)

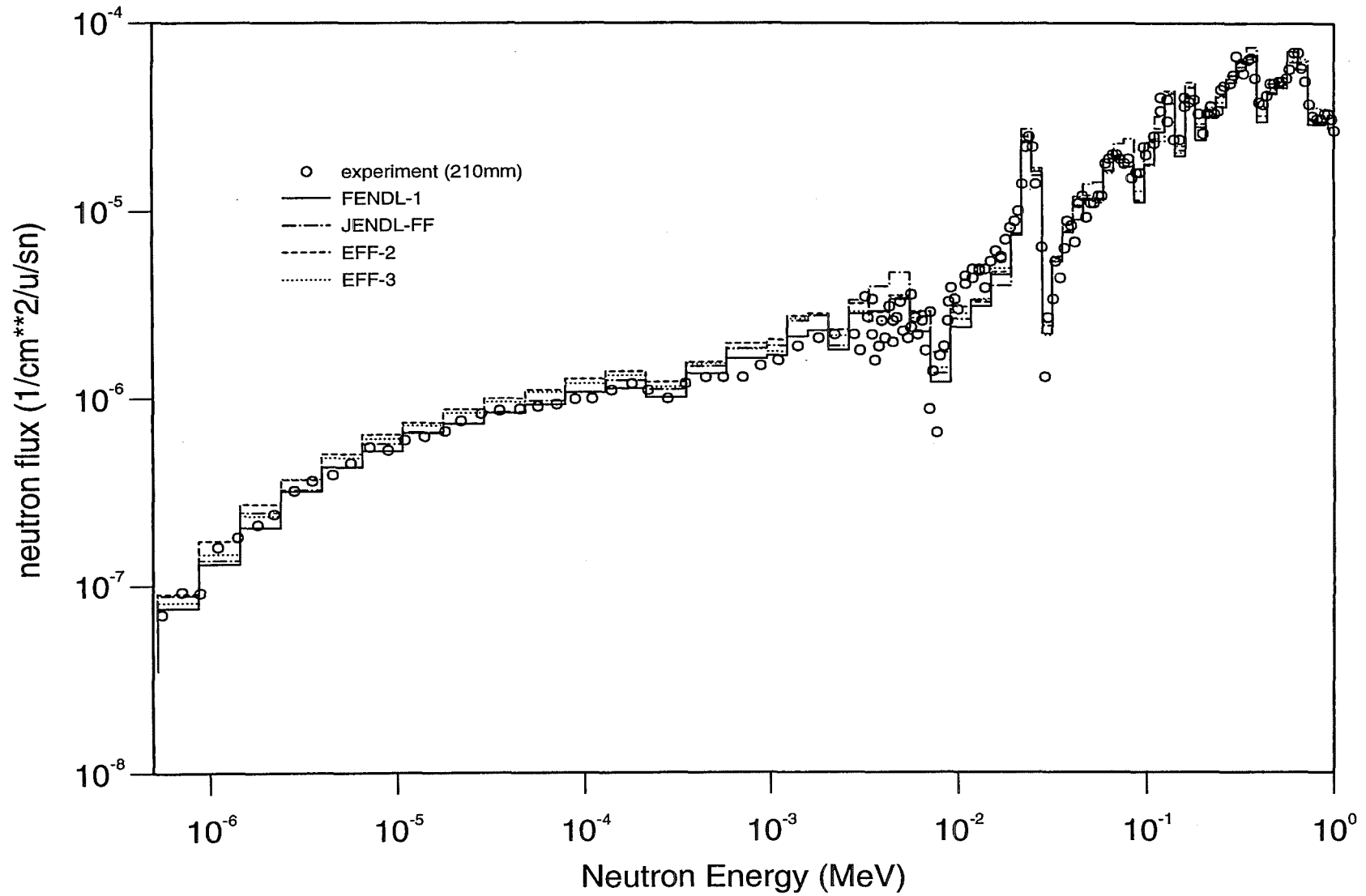


Fig.4.4.2 FNS Iron In-system Experiment Neutron Spectra (210mm)

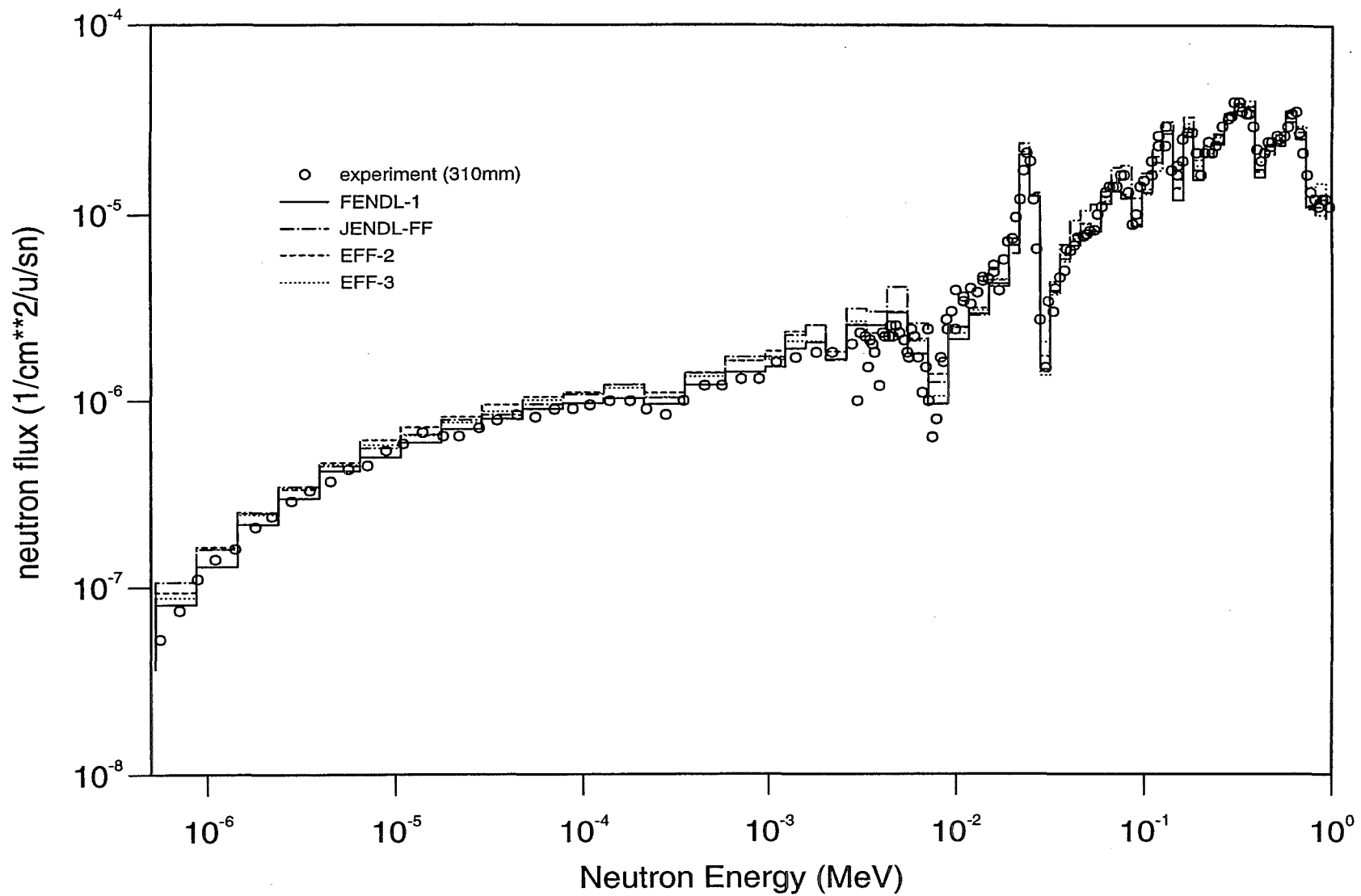


Fig.4.4.3 FNS Iron In-system Experiment Neutron Spectra (310mm)

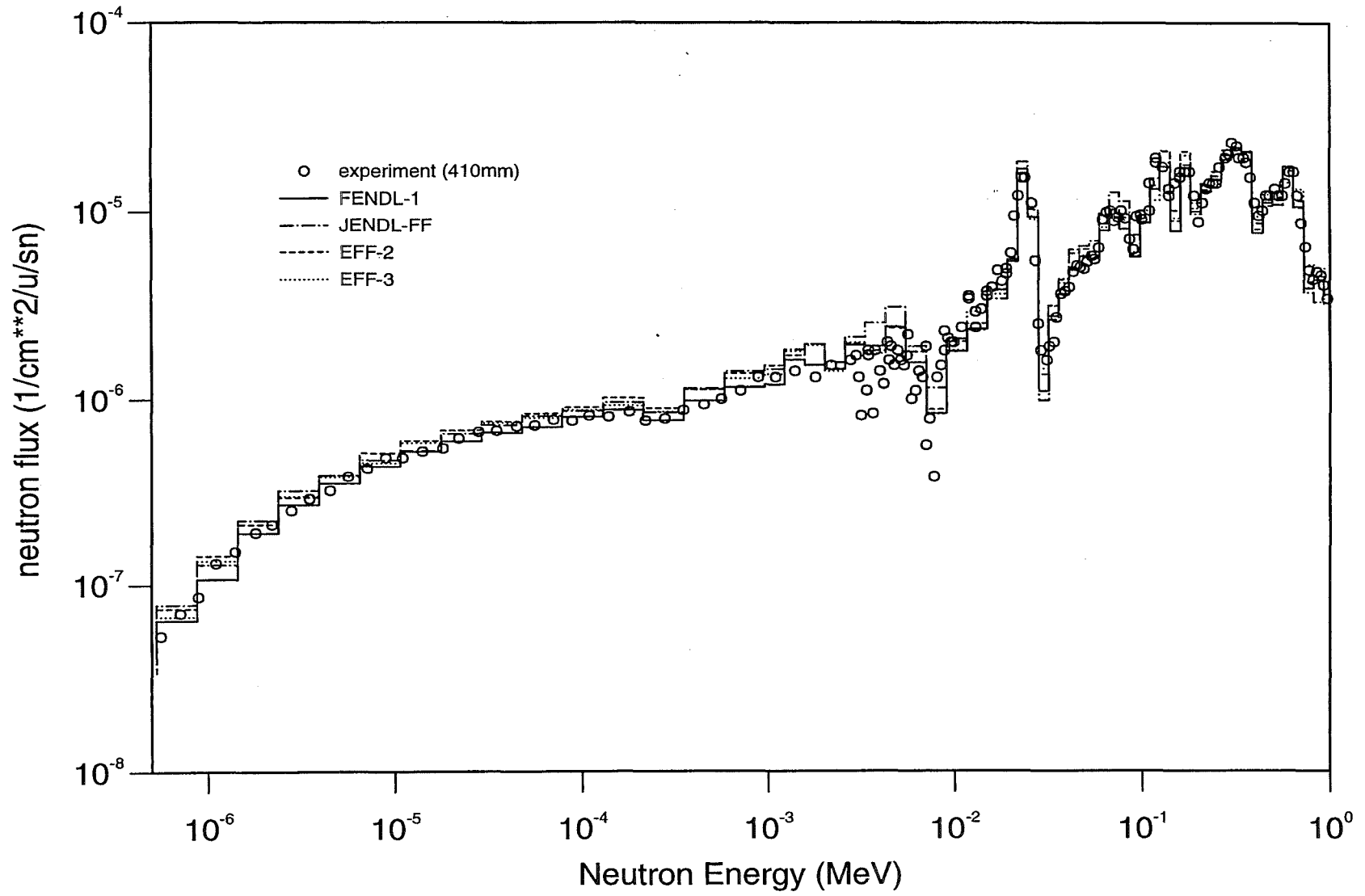


Fig.4.4.4 FNS Iron In-system Experiment Neutron Spectra (410mm)

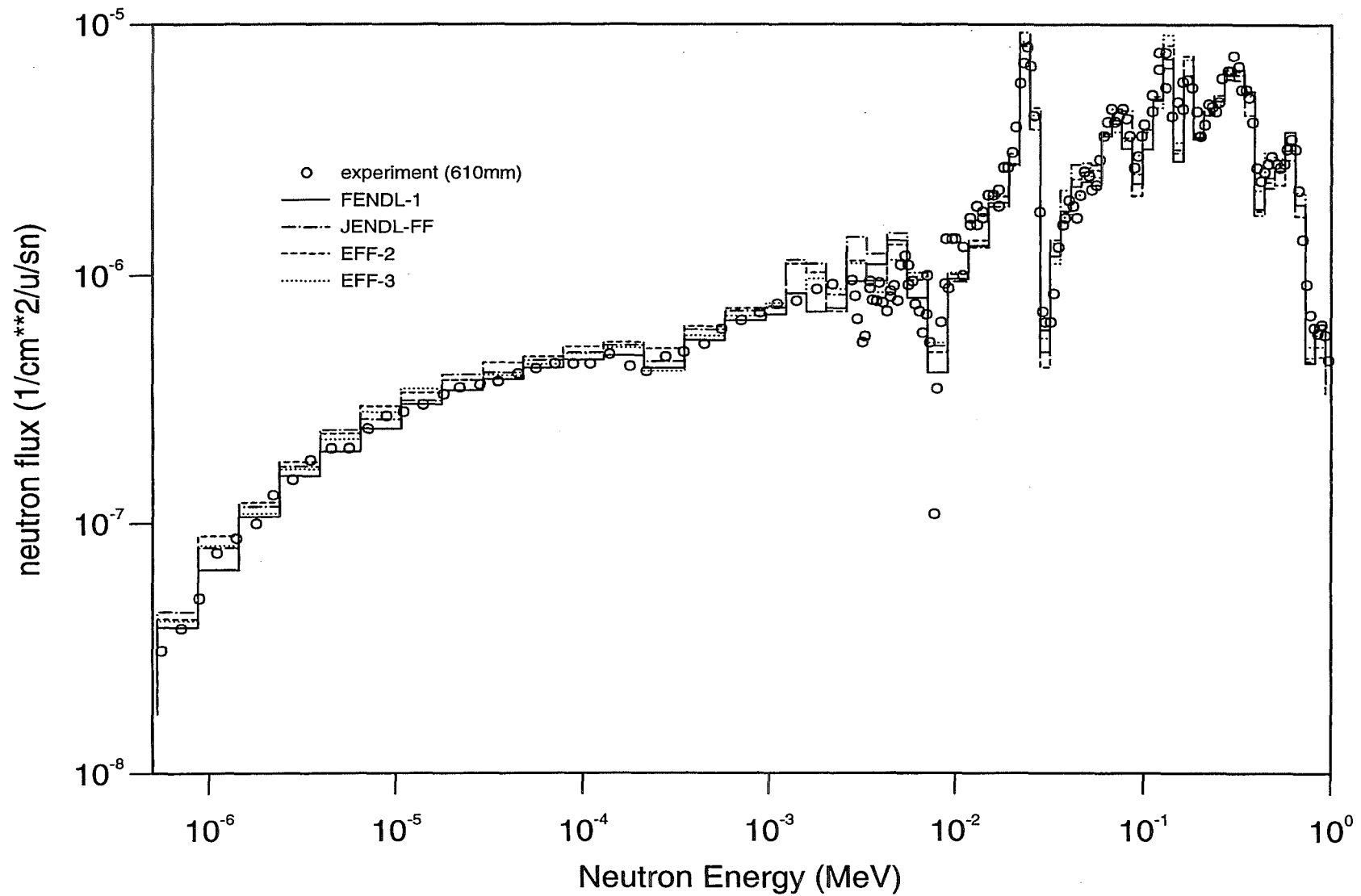


Fig.4.4.5 FNS Iron In-system Experiment Neutron Spectra (610mm)

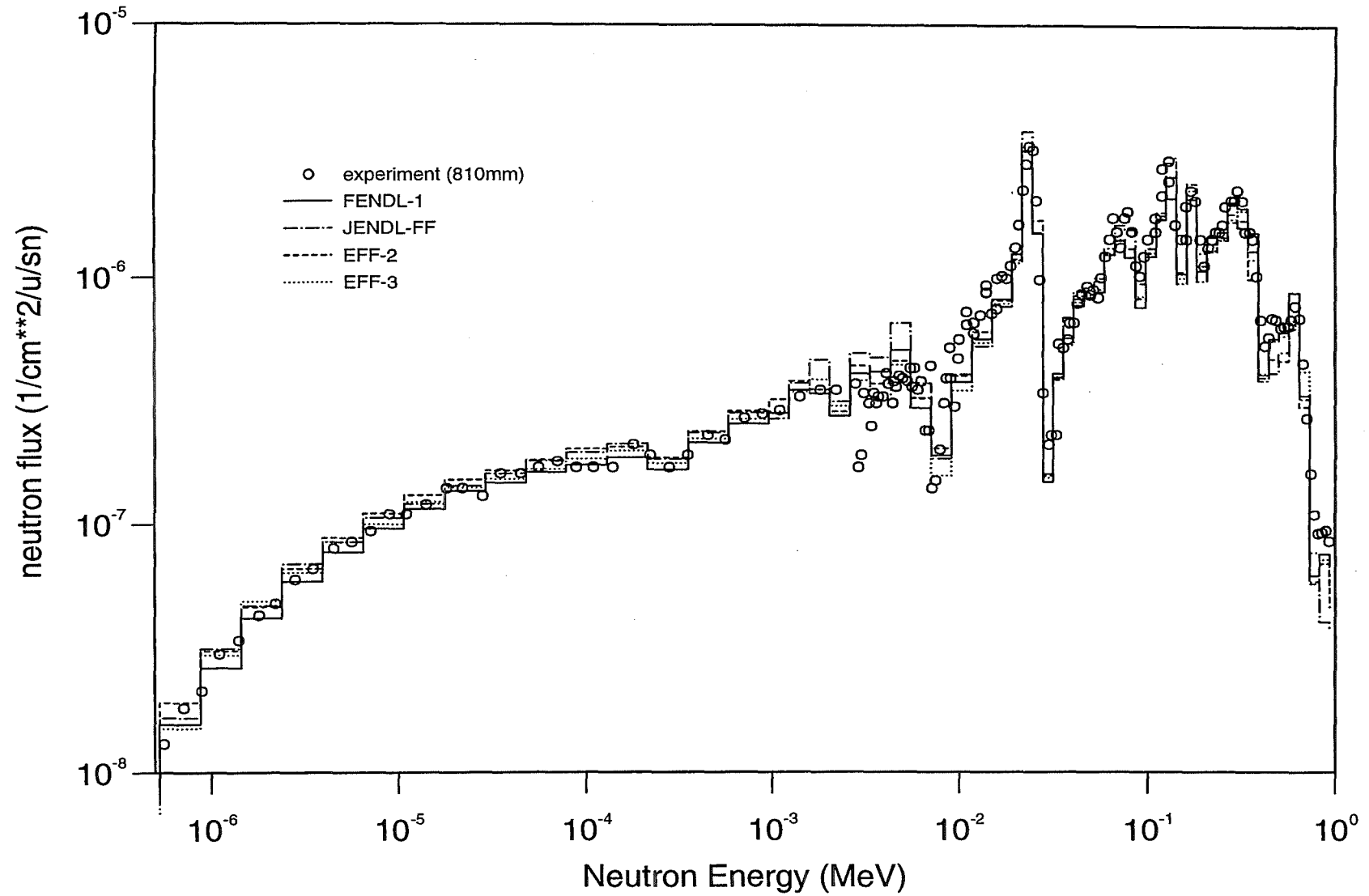


Fig.4.4.6 FNS Iron In-system Experiment Neutron Spectra (810mm)

4.5 FNS(JAERI) Beryllium Slab Time-of-Flight Experiment

The arrangement of this experiment was similar to that of the FNS iron slab experiment with the TOF method. In this work, only the experiment on the 152.4 mm-thick beryllium slab is considered. The systematic error is the same as for the FNS Iron Slab Experiment in section 4.3. The statistical error for the counting rates is listed in Table 4.5.1.

A detailed description of experiment can be found in Ref.[19,29,30].

In the calculation of this experiment, an isotropic angular distribution along with the measured energy spectrum was adopted for the source neutrons.

Similar to the FNS iron slab experiment with the TOF method, the angular flux spectra for the beryllium slab experiment is presented in Fig.4.5.1~Fig.4.5.5 at the five measured angles in comparison with the experimental results. The C/E values of energy integrated angular flux spectra is listed in Table 4.5.1.

Note that the beryllium data of the JENDL-FF working library caused MCNP4A to stop before ever finishing a calculation (this also occurred in the calculations of the KANT- and the OKTAVIAN beryllium shell experiments). This resulted in a very poor statistics for the neutron spectra in some energy ranges, e. g. the 3-10 MeV interval in this experiment.

Table 4.5.1 C/E data for energy integrated angular flux spectra in the FNS TOF-Be-slab experiment

Angle (degree)	Energy Range (MeV)	Experimental Angular Flux (1/src/cm ² /sn)	Experimental Statistic Error (%)	C/E of Neutron Flux		
				FENDL-1	EFF-2	JENDL-FF
0	0.05~1.0	.79-5	5.1	.78	.87	.79
	1.0~5.0	.58-5	3.6	.95	1.38	.96
	5.0~10.0	.29-5	4.2	.97	1.33	1.16
	10.0~20.0	.77-4	0.5	.99	1.13	1.00
	Total	.98-4	1.2	.94	1.09	.94
12.2	0.05~1.0	.64-5	4.7	.98	1.10	1.02
	1.0~5.0	.51-5	3.2	1.02	1.50	1.07
	5.0~10.0	.25-5	3.8	1.05	1.44	1.32
	10.0~20.0	.23-4	0.9	.84	.97	.84
	Total	.37-4	2.0	.90	1.09	.93
24.9	0.05~1.0	.64-5	4.4	.94	1.06	.98
	1.0~5.0	.48-5	3.3	1.00	1.45	1.09
	5.0~10.0	.22-5	4.0	1.07	1.43	1.41
	10.0~20.0	.10-4	1.4	1.04	1.21	1.04
	Total	.24-4	2.9	.98	1.21	1.04
41.8	0.05~1.0	.57-5	4.8	.93	1.06	.99
	1.0~5.0	.43-5	3.5	.96	1.36	1.09
	5.0~10.0	.19-5	4.2	1.00	1.30	1.41
	10.0~20.0	.47-5	2.2	.84	1.01	.83
	Total	.17-4	3.6	.82	1.14	1.01
66.8	0.05~1.0	.44-4	6.3	.86	.99	1.04
	1.0~5.0	.30-5	5.0	.92	1.29	1.04
	5.0~10.0	.13-5	6.8	.92	1.20	1.23
	10.0~20.0	.13-5	6.0	.80	1.00	.74
	Total	.10-4	5.9	.87	1.10	1.01

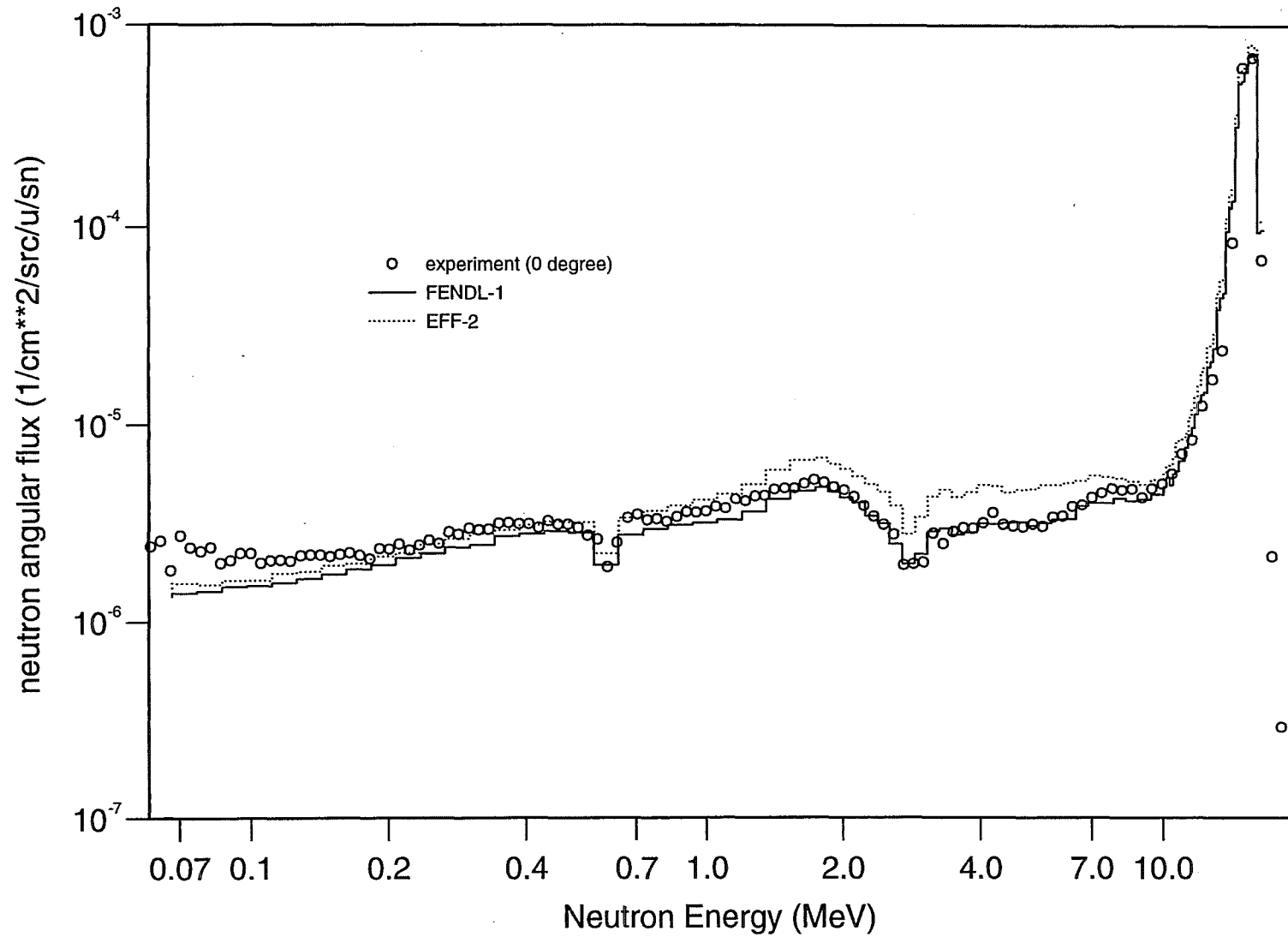
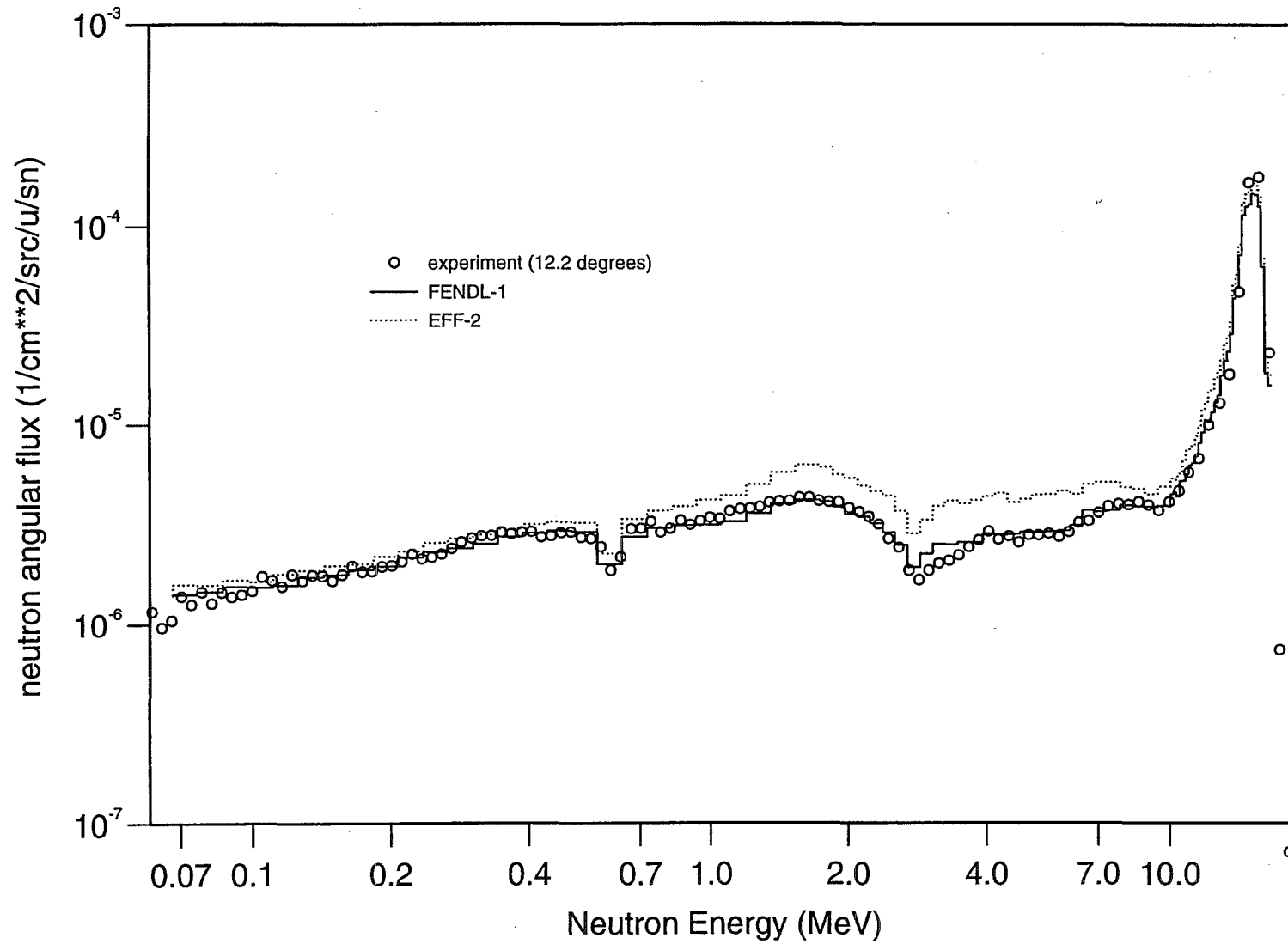


Fig.4.5.1 FNS(TOF) Beryllium Slab Experiment Neutron Spectra (0 deg)



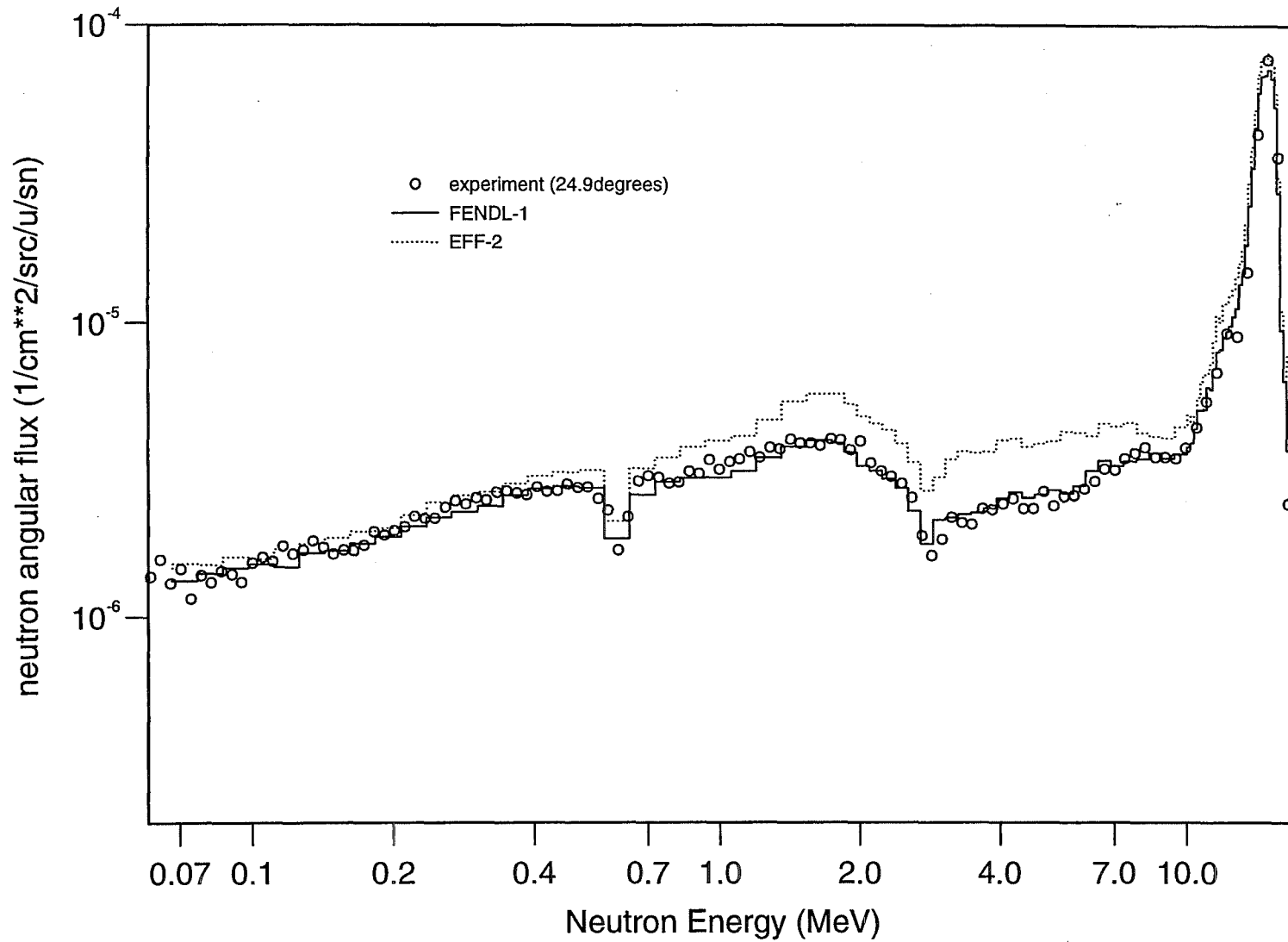


Fig.4.5.3 FNS(TOF) Beryllium Slab Experiment Neutron Spectra (24.9 deg)

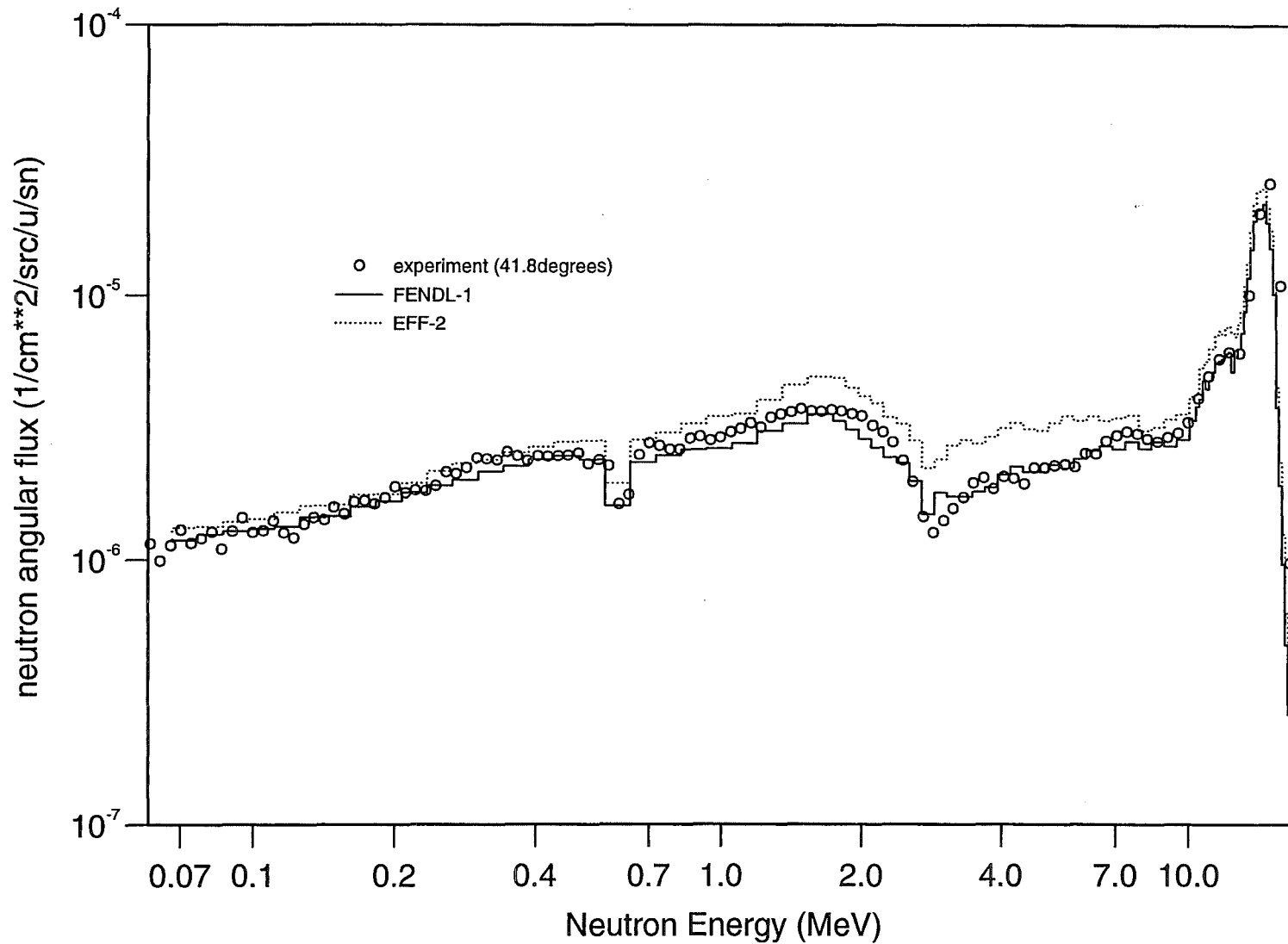


Fig.4.5.4 FNS(TOF) Beryllium Slab Experiment Neutron Spectra (41.8 deg)

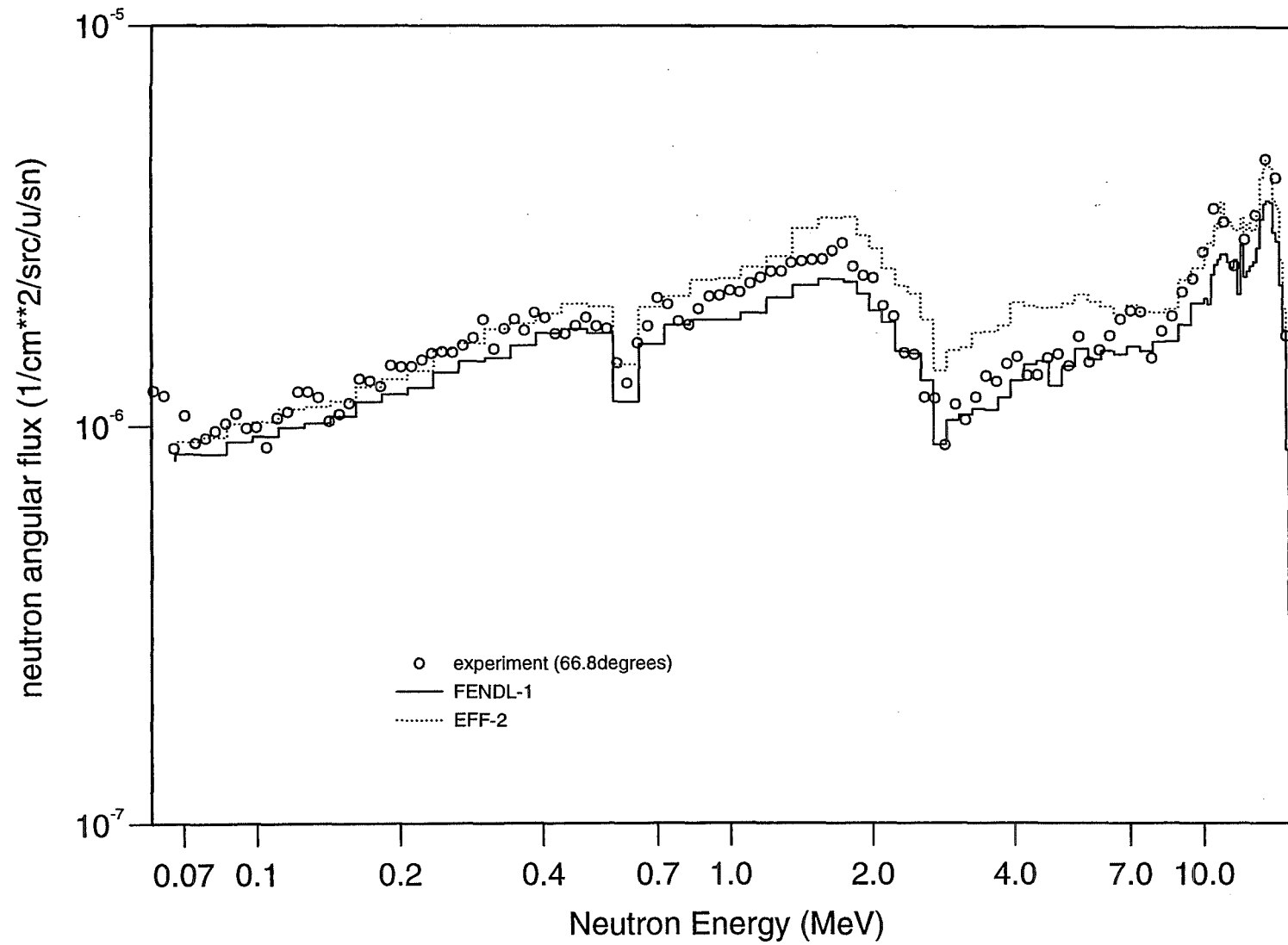


Fig.4.5.5 FNS(TOF) Beryllium Slab Experiment Neutron Spectra (66.8 deg)

4.6 KANT (FZK) Beryllium Spherical Shell Experiment

This is a transmission experiment performed previously at FZK with measurement of the leakage neutron spectrum from 15 MeV down to thermal energy. A detailed description of the experiment can be found in Ref.[22]. In this report we consider only the experiment on the beryllium shell with 17 cm wall thickness with an inner and outer radius of 5 and 22 cm, respectively.

The calculation has been performed using MCMP4A with complete geometry arrangement, and a central neutron point source for D-T neutrons with anisotropic angular distribution was adopted based on Ref.[23].

The calculated and measured neutron leakage spectra of the 17 cm thick beryllium shell is presented in Fig 4.6.1. The C/E values for integrated neutron leakages are given in Table 4.6.1.

Table 4.6.1 C/E data for integrated neutron flux spectra in the KANT Beryllium Shell Experiment

Energy Range (MeV)	Experimental Leakage (1/sn)	C/E		
		EFF-2	FENDL-1	JENDL-FF
0.1~1.0	.270E+00	1.06	.91	.92
1.0~5.0	.264E+00	1.22	.85	.86
5.0~10.0	.955E-01	1.40	1.06	1.09
10.0~20.0	.220E+00	1.39	1.18	1.21
Total	.849E+00	1.23	.98	.99

4.7 OKTAVIAN (Osaka University) Beryllium Spherical Shell Experiment

A beryllium spherical shell experiment with various thicknesses was also conducted at the intense 14 MeV neutron source facility OKTAVIAN at Osaka University, Japan. Neutron leakage spectra were measured applying the TOF technique.

A detailed description of the experiment can be found in Ref.[19].

In this work, the sphere shell with inner radius of 57 mm and outer radius of 173.5 mm has been calculated using MCNP4A and ONEDANT with isotropic point neutron source and the measured neutron energy spectrum. Results are shown in Fig.4.7.1 and Table 4.7.1.

Table 4.7.1 C/E data for integrated neutron flux spectra in the OKTAVIAN beryllium spherical shell experiment

Energy Range (MeV)	Measured Leakage (1/sn)	Experimental Statistical Error (%)	C/E (MCNP+ pointwise data)			C/E (ONEDANT + MG-data)	
			EFF-2	FENDL-1	JENDL-FF	FENDL-1	EFF-2
.003~1.0	.469E+00	5.7	1.06	.98	.98	.98	.82
1.0~5.0	.315E+00	.96	1.13	.83	.85	.83	1.30
5.0~10.0	.143E+00	1.7	1.09	.88	.90	.90	2.09
10.0~20.	.324E+00	1.1	1.34	1.18	1.21	1.17	1.51
Total	.126E+01	2.9	1.15	.98	1.00	.98	1.26

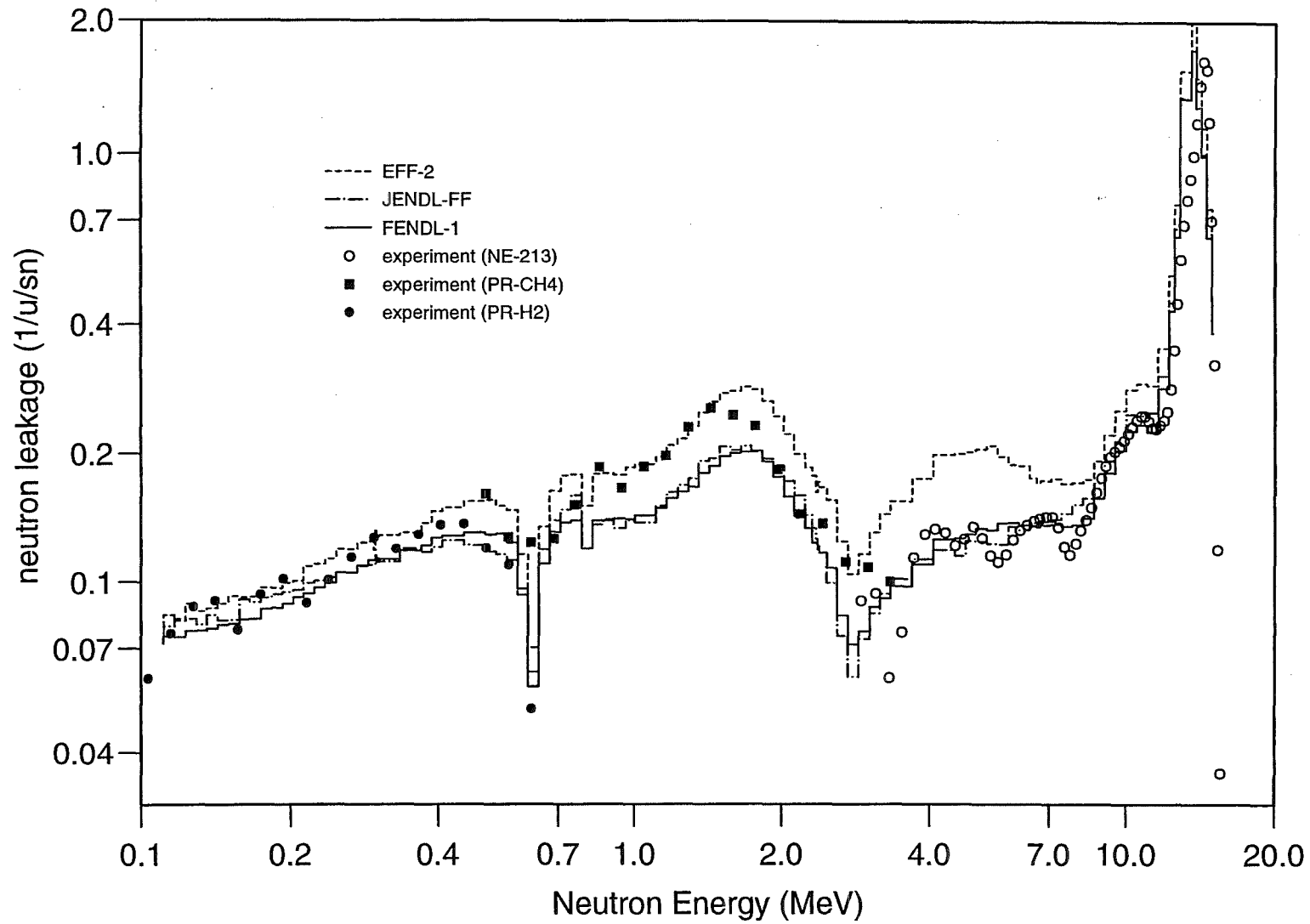


Fig.4.6.1 KANT Beryllium Shell Experiment Neutron Spectra

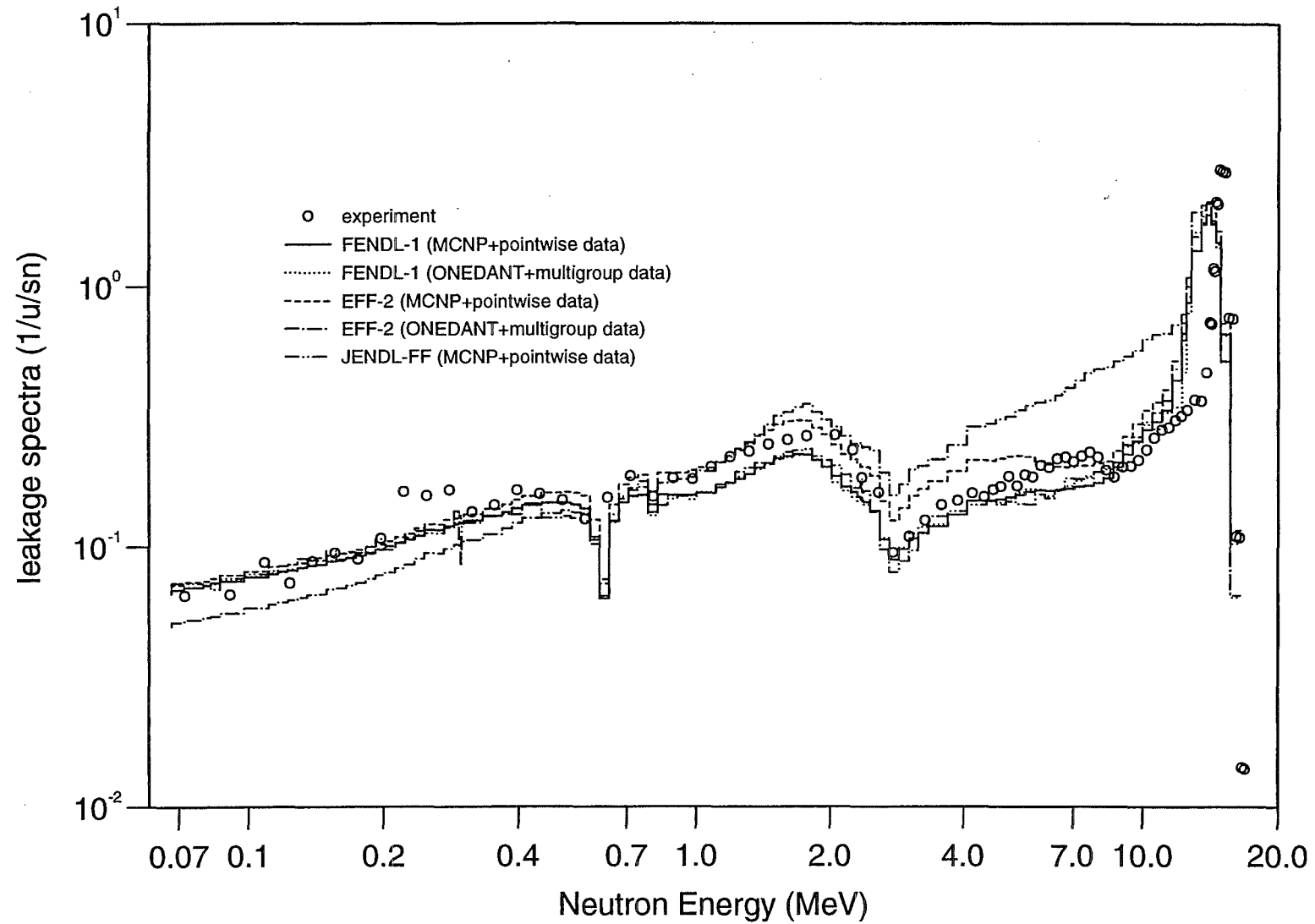


Fig.4.7.1 OKTAVIAN Beryllium Shell Experiment Neutron Spectra

4.8 OKTAVIAN (Osaka University) Sphere Pile TOF Experiments

Sphere pile experiments were performed at the intense 14 MeV neutron source facility OKTAVIAN at Osaka University, Japan, for various materials using the TOF technique. Both the neutron leakage spectra and the source neutron spectrum were measured. The sample piles were made by filling spherical vessels with sample powder or flakes. The characteristic parameters of the sample piles are listed in Table 4.8.1. The experimental uncertainty listed in Table 4.8.1~48.11 included only counting statistical error. The relative error for the measurements with the niobium activation foils was less than 1%, which is not included in the tables.

Table 4.8.1 Characteristic parameters of the sample sphere piles

Pile (element)	Inner diameter (cm)	Apparent density (g/cm ³)	Thickness of pile	
			(cm)	(MFPs)*
Al	40	1.22	9.8	0.5
Si	60	1.29	20.0	1.1
Mo	61	2.15	27.5	1.5
Co	40	1.94	9.8	0.5
Cr	40	3.72	9.8	0.7
Cu	61	6.23	27.5	4.7
Ti	40	1.54	9.8	0.5
Mn	61	4.37	27.5	3.4
Zr	61	2.84	27.5	2.0
Nb	28	4.39	11.2	1.1
W	40	4.43	9.8	0.8

* MFP represents Mean Free Path of neutron in the materials

A detailed description of the experiment can be found in Ref.[19].

In this work, the sphere pile experiments for aluminum, silicon, molybdenum, cobalt, chromium, copper, titanium, manganese, zirconium, niobium, tungsten have been calculated using MCNP4A with continuous energy cross-section data (FENDL-1, EFF-2 and JENDL-FF) and ONEDANT with FENDL-1 and EFF-2 multigroup data. The isotropic angular distribution of source neutrons along with the measured energy spectra and the simplified 1-D geometry model has been adopted in all the calculations.

The calculated and experimental spectra for the shells of Al, Si, Mo, Co, Cr, Cu, Ti, Mn, Zr, Nb, W are presented in Fig. 4.8.1 ~ 4.8.11. The C/E values of integrated neutron leakages are listed in Table 4.8.2 ~ 4.8.12.

Table 4.8.2 C/E data for integrated neutron leakage spectra in the OKTAVIAN Al sphere pile experiment.

Energy Range (MeV)	Measured Leakage (1/sn)	Exp. Uncertainty (%)	C/E (MCNP+ Continuous-Energy Data)			C/E (ONEDANT+ MG-data)	
			FENDL-1	EFF-2	JENDL-FF	FENDL-1	EFF-2
0.1~1.0	.693E-01	1.9	.89	.81	.88	.90	.82
1.0~5.0	.148E+00	3.1	.92	.89	.79	.93	.89
5.0~10.0	.495E-01	1.4	.60	.79	.81	.61	.78
10.0~20.0	.675E+00	3.7	1.10	1.10	1.11	1.09	1.09
Total	.942E+00	3.3	1.03	1.03	1.02	1.02	1.024

Table 4.8.3 C/E data for integrated neutron leakage spectra in the OKTAVIAN Si sphere pile experiment.

Energy Range (MeV)	Measured Leakage (1/sn)	Exp. Uncertainty (%)	C/E (MCNP+Continuous-Energy Data)			C/E (ONEDANT+MG-data)	
			EFF-2	FENDL-1	JENDL-FF	FENDL-1	EFF-2*
0.1~1.0	.930E-01	3.7	.67	1.63	.77	1.66	.67
1.0~5.0	.171E+00	5.0	.79	.69	.87	.69	.77
5.0~10.0	.470E-01	2.1	.79	.71	.78	.71	.78
10.0~20.0	.482E+00	4.6	1.17	.97	1.17	.96	1.16
Total	.793E+00	4.4	1.00	.97	1.04	.97	1.00

* Only Si28 included in the working library

Table 4.8.4 C/E data for integrated neutron leakage spectra in the OKTAVIAN Mo sphere pile experiment.

Energy Range (MeV)	Measured Leakage (1/sn)	Exp. Uncertainty (%)	C/E (MCNP+ Continuous-Energy Data)			C/E (ONEDANT+MG-Data)	
			FENDL-1 FF	EFF-2	JENDL- FF	FENDL-1	EFF-2
0.1~1.0	.516E+00	8.5	.90	.81	.89	.92	.83
1.0~5.0	.287E+00	6.9	.96	1.03	.89	.96	1.04
5.0~10.0	.426E-01	2.1	.60	.63	.83	.60	.63
10.0~20.0	.524E+00	4.7	.97	.97	.93	.95	.96
Total	.137E+01	6.5	.93	.91	.90	.93	.92

Table 4.8.5 C/E data for integrated neutron leakage spectra in the OKTAVIAN Co sphere pile experiment.

Energy Range (MeV)	Measured Leakage (1/sn)	Exp. Uncertainty (%)	C/E (MCNP+ Continuous-Energy Data)			C/E (ONEDANT+MG-Data)	
			EFF-2 FF	FENDL-1	JENDL- FF	FENDL-1	EFF-2
0.1~1.0	.242E+00	4.3	.63	.63	.62	.64	.64
1.0~5.0	.295E+00	6.2	.61	.61	.64	.61	.61
5.0~10.0	.554E-01	2.1	.49	.49	.65	.50	.50
10.0~15.0	.729E+00	5.2	1.02	1.02	1.00	1.01	1.01
Total	.132E+01	5.1	.83	.83	.83	.83	.83

Table 4.8.6 C/E data for integrated neutron leakage spectra in the OKTAVIAN Cr sphere pile experiment.

Energy Range (MeV)	Measured Leakage (1/sn)	Exp. Uncertainty (%)	C/E (MCNP+ Continuous-Energy Data)			C/E (ONEDANT+MG-Data)	
			EFF-2 FF	FENDL-1	JENDL- FF	FENDL-1	EFF-2
0.1~1.0	.211E+00	4.9	1.07	1.07	1.15	1.09	1.07
1.0~5.0	.221E+00	3.2	1.25	1.13	1.11	1.13	1.25
5.0~10.0	.410E-01	1.2	.98	1.14	.96	1.14	.97
10.0~20.0	.549E+00	2.8	.96	.97	.96	.96	.95
Total	.102E+01	3.3	1.05	1.03	1.03	1.03	1.04

Table 4.8.7 C/E data for integrated neutron leakage spectra in the OKTAVIAN Cu sphere pile experiment.

Energy Range (MeV)	Measured Leakage (1/sn)	Exp. Uncertainty (%)	C/E (MCNP+ Continuous-Energy Data)			C/E (ONEDANT+MG-Data)	
			EFF-2 FF	FENDL-1	JENDL- FF	FENDL-1	EFF-2
0.1~1.0	.660E+00	10.2	1.09	1.08	1.04	1.02	1.02
1.0~5.0	.145E+00	4.8	1.06	1.06	.97	1.03	1.03
5.0~10.0	.133E-01	1.2	1.27	1.27	.99	1.22	1.22
10.0~20.0	.794E-01	2.0	.99	.99	1.04	.93	.94
Total	.973E+00	8.4	.99	.99	.95	.94	.94

Table 4.8.8 C/E data for integrated neutron leakage spectra in the OKTAVIAN Ti sphere pile experiment.

Energy Range (MeV)	Measured Leakage (1/sn)	Exp. Uncertainty y (%)	C/E (MCNP+ Continuous-Energy Data)			C/E (ONEDANT+MG-Data)	
			FENDL-1 FF	EFF-2	JENDL- FF	FENDL-1	EFF-2
0.1~1.0	.861E-01	2.2	1.31	1.31	1.38	1.34	not included
1.0~5.0	.152E+00	3.8	1.34	1.34	1.06	1.34	in the
5.0~10.0	.384E-01	1.5	.98	.98	1.00	.98	working
10.0~20.0	.598E+00	4.4	1.19	1.19	1.23	1.10	library
Total	.874E+00	4.0	1.21	1.21	1.20	1.21	

Table 4.8.9 C/E data for integrated neutron leakage spectra in the OKTAVIAN Mn sphere pile experiment.

Energy Range (MeV)	Measured Leakage (1/sn)	Exp. Uncertainty (%)	C/E (MCNP+ Continuous-Energy Data)			C/E (ONEDANT+MG-Data)	
			EFF-2	FENDL-1	JENDL- FF	FENDL-1	EFF-2
0.1~1.0	.661E+00	9.4	1.08	1.08	1.08	1.07	1.07
1.0~5.0	.271E+00	6.5	1.14	1.14	1.13	1.11	1.11
5.0~10.0	.279E-01	1.7	1.00	1.00	1.15	.98	.98
10.0~20.0	.154E+00	2.7	0.94	.094	1.00	.91	.91
Total	.114E+01	7.5	1.07	1.07	1.08	1.06	1.06

Table 4.8.10 C/E data for integrated neutron leakage spectra in the OKTAVIAN Zr sphere pile experiment.

Energy Range (MeV)	Measured Leakage (1/sn)	Exp. Uncertainty (%)	C/E (MCNP+Continuous-Energy Data)			C/E (ONEDANT+MG-Data)	
			EFF-2 FF	FENDL-1	JENDL- FF	FENDL-1	EFF-2
0.1~1.0	.442E+00	7.7	.95	1.07	1.21	1.07	.98
1.0~5.0	.307E+00	8.2	1.58	1.24	1.07	1.25	1.60
5.0~10.0	.333E-01	2.2	1.74	1.20	.98	1.19	1.58
10.0~20.0	.317E+00	4.9	1.19	1.26	1.21	1.24	1.17
Total	.110E+01	6.9	1.22	1.18	1.16	1.17	1.22

Table 4.8.11 C/E data for integrated neutron leakage spectra in the OKTAVIAN Nb sphere pile experiment.

Energy Range (MeV)	Measured Leakage (1/sn)	Exp. Uncertainty (%)	C/E (MCNP+ Continuous-Energy Data)			C/E (ONEDANT+MG-Data)	
			EFF-2 FF	FENDL-1	JENDL- FF	FENDL-1	EFF-2
0.1~1.0	.335E+00	6.1	1.12	1.27	1.37	1.21	1.15
1.0~5.0	.219E+00	3.2	1.47	1.26	1.04	1.18	1.48
5.0~10.0	.355E-01	1.1	1.17	1.09	.94	1.00	1.13
10.0~20.0	.510E+00	2.7	1.05	1.04	1.04	.87	1.04
Total	.110E+01	3.8	1.16	1.15	1.14	1.04	1.16

Table 4.8.12 C/E data for integrated neutron leakage spectra in the OKTAVIAN W sphere pile experiment.

Energy Range (MeV)	Measured Leakage (1/sn)	Exp. Uncertainty (%)	C/E (MCNP+ Continuous-Energy Data)			C/E (ONEDANT+ MG-Data)	
			EFF-2 FF	FENDL-1	JENDL- FF	FENDL-1	EFF-2
0.1~1.0	.360E+00	7.2	.87	.84	.94	.85	.94
1.0~5.0	.241E+00	7.0	.84	.86	.79	.86	1.03
5.0~10.0	.402E-01	2.1	.61	.67	.68	.67	.30
10.0~20.0	.710E+00	6.3	.95	.94	.94	.94	.91
Total	.135E+01	6.6	.89	.90	.90	.89	.92

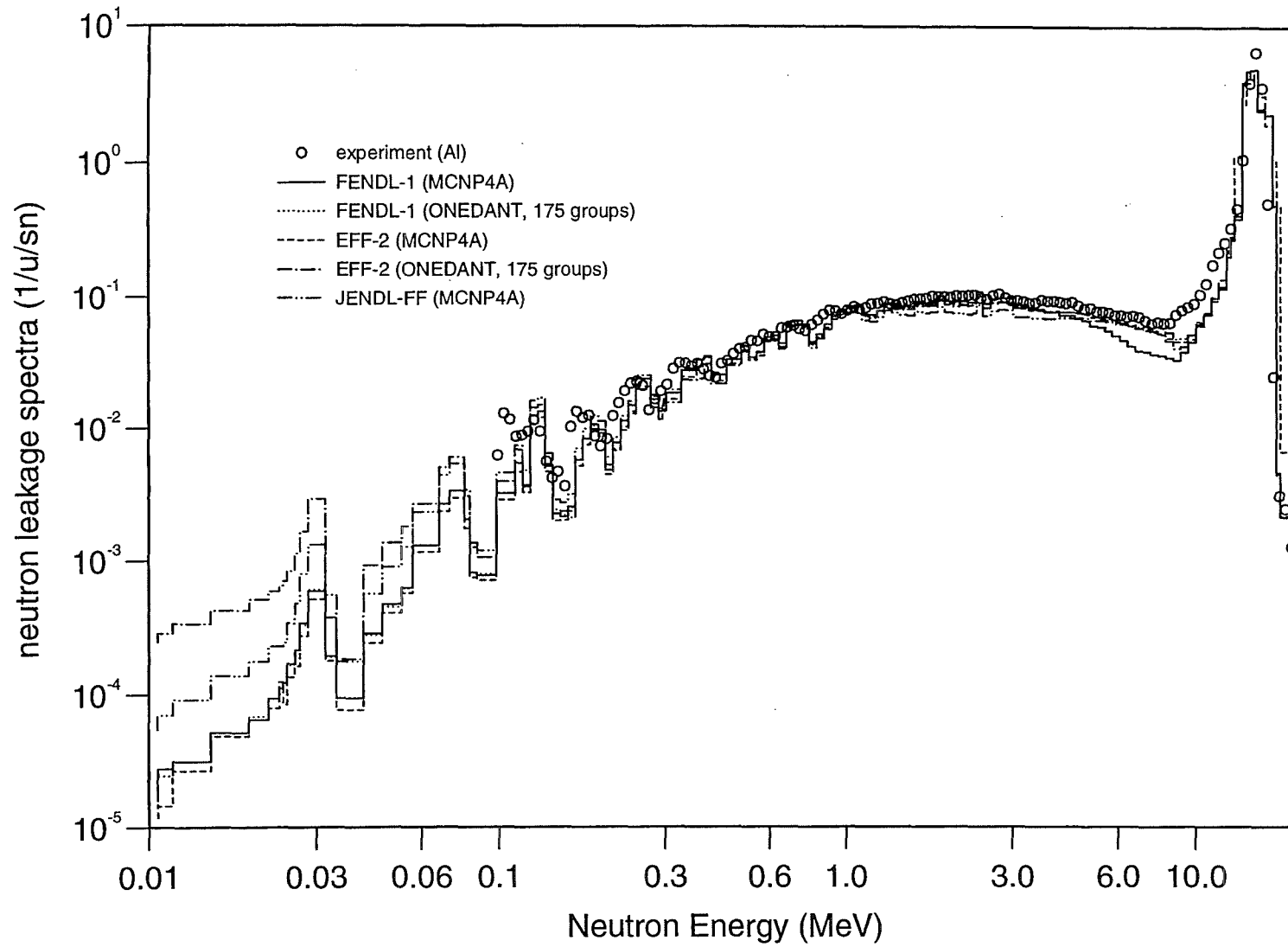


Fig.4.8.1 OKTAVIAN Al Shell Experiment Neutron Spectra

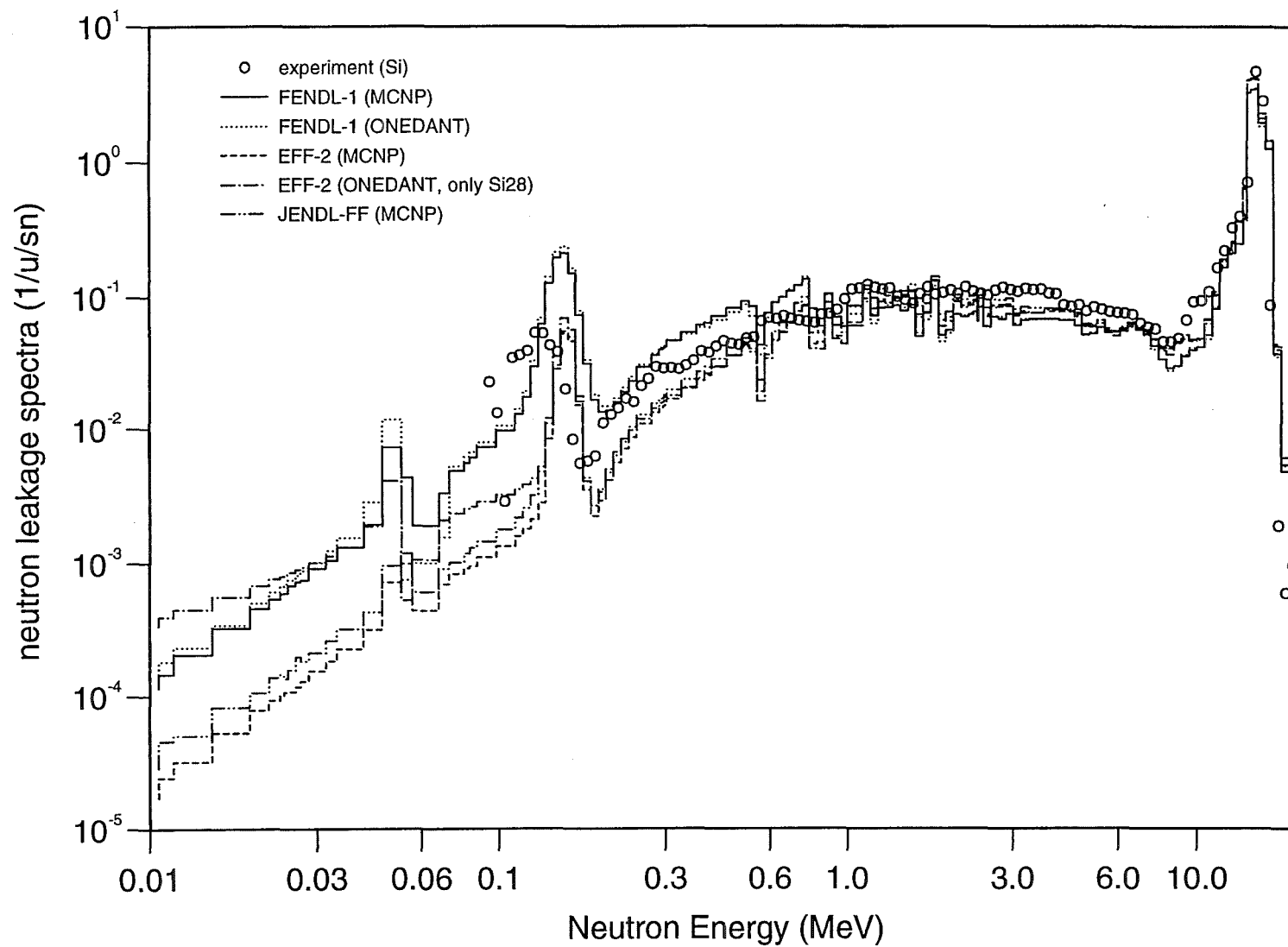


Fig.4.8.2 OKTAVIAN Si Shell Experiment Neutron Spectra

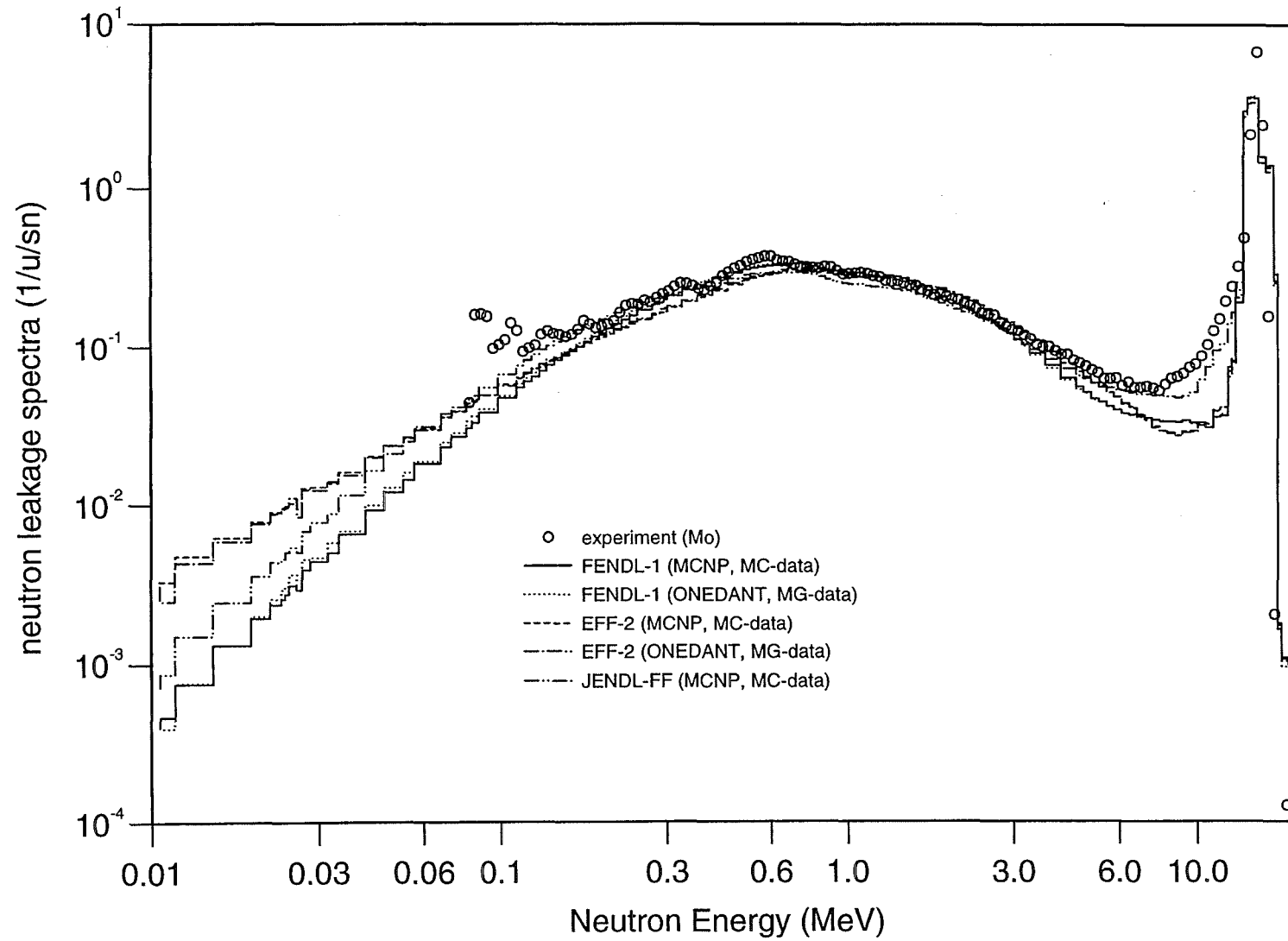


Fig.4.8.3 OKTAVIAN Mo Shell Experiment Neutron Spectra

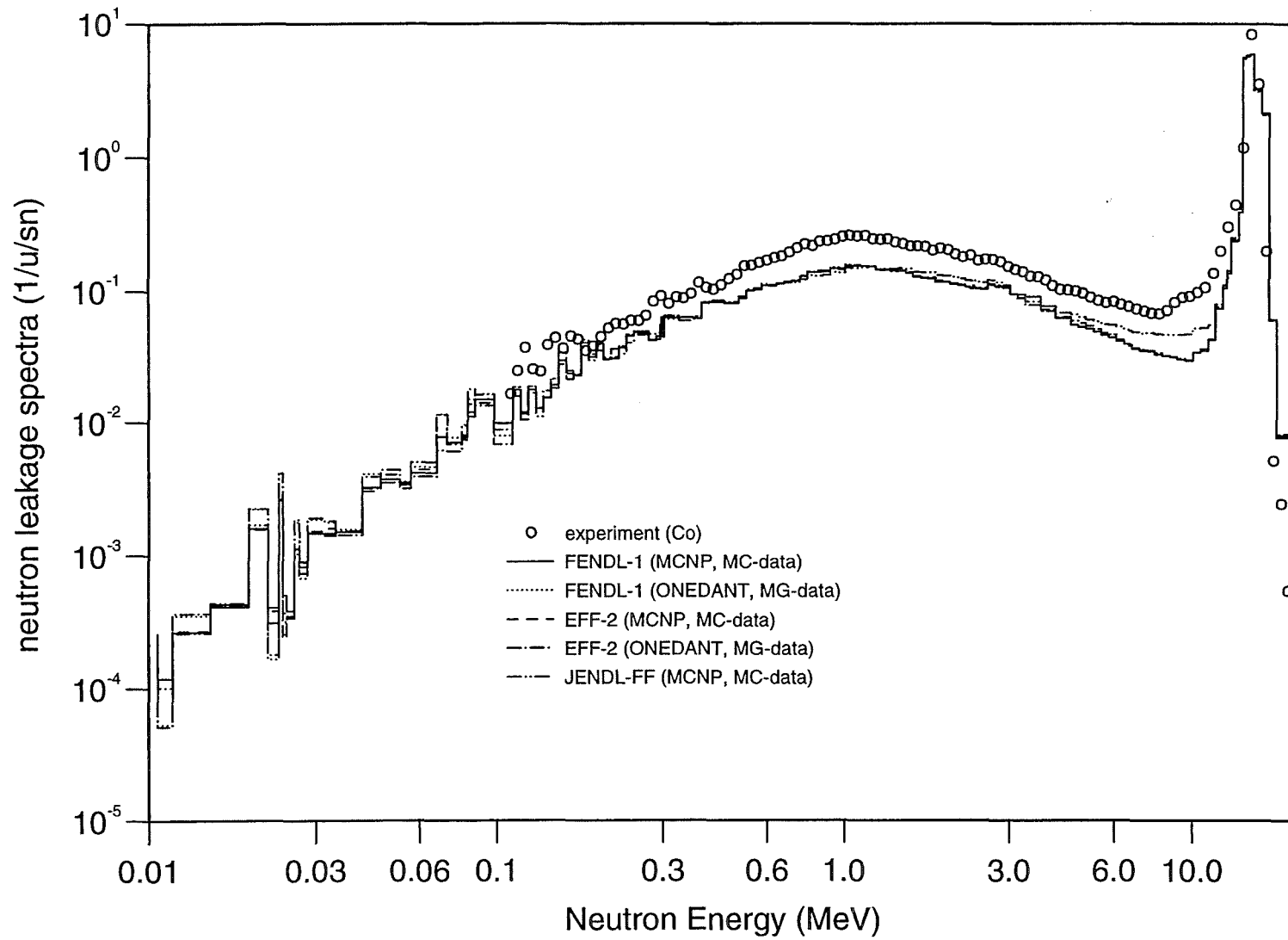


Fig.4.8.4 OKTAVIAN Co Shell Experiment Neutron Spectra

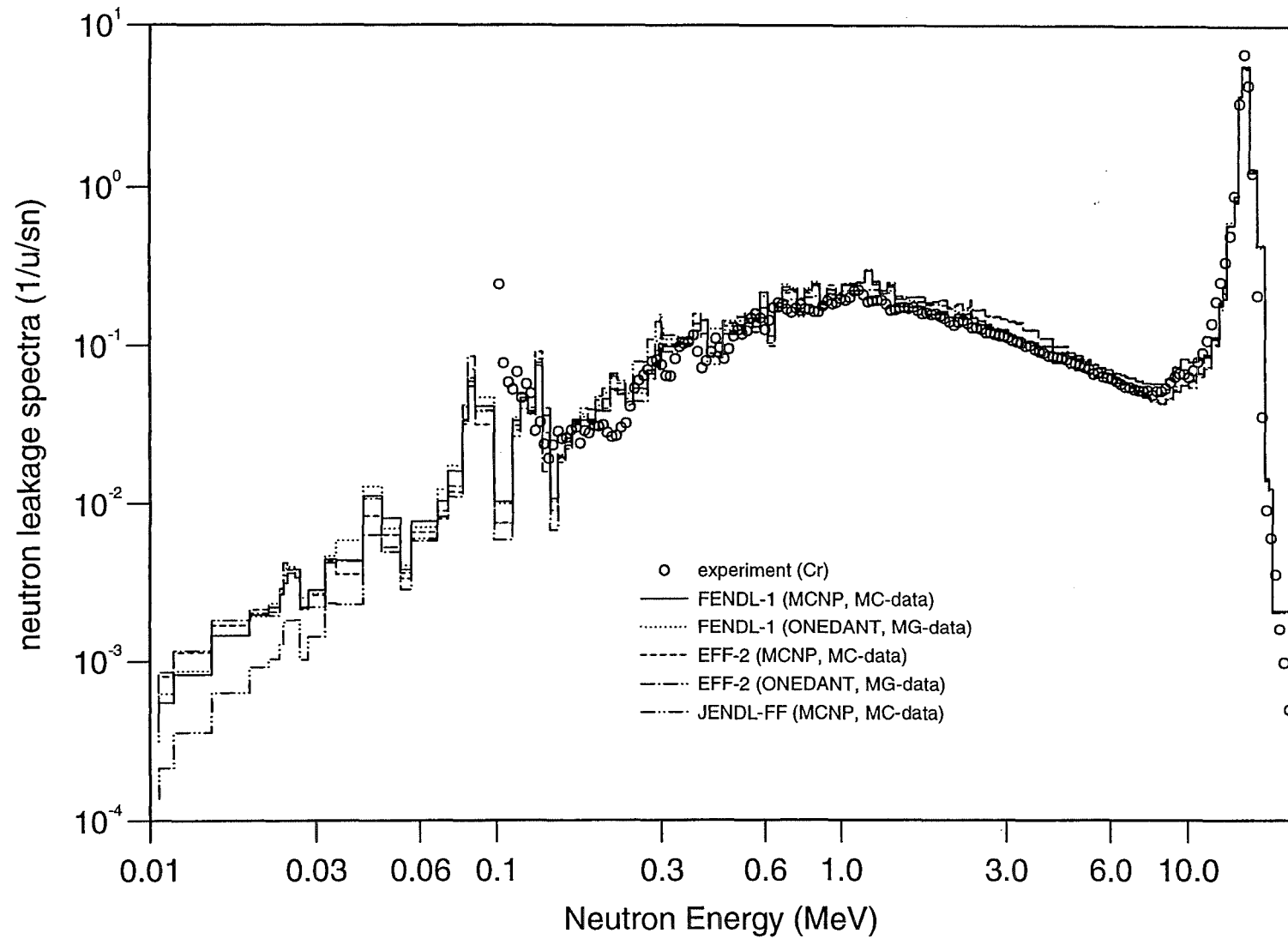


Fig.4.8.5 OKTAVIAN Cr Shell Experiment Neutron Spectra

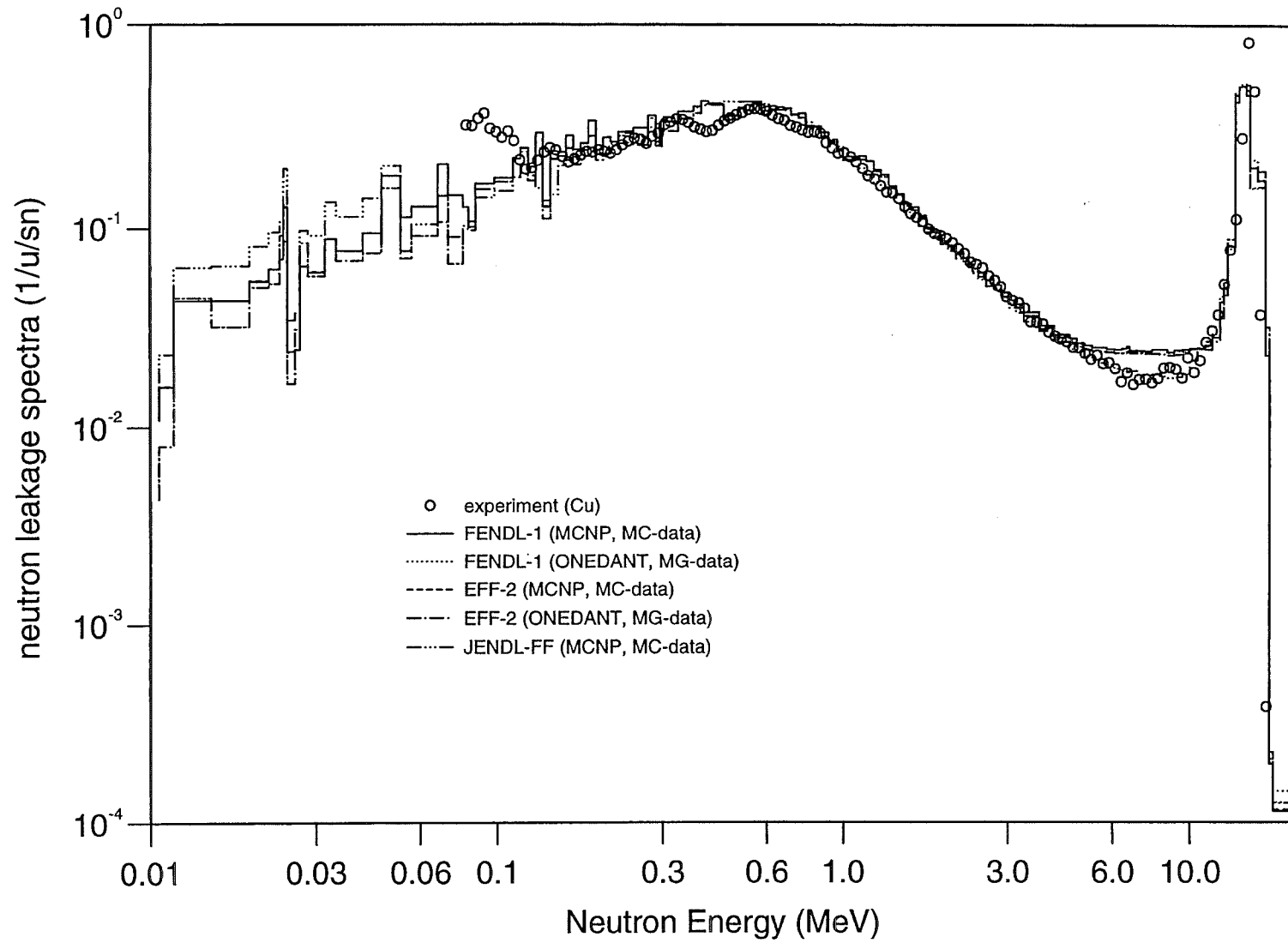


Fig.4.8.6 OKTAVIAN Cu Shell Experiment Neutron Spectra

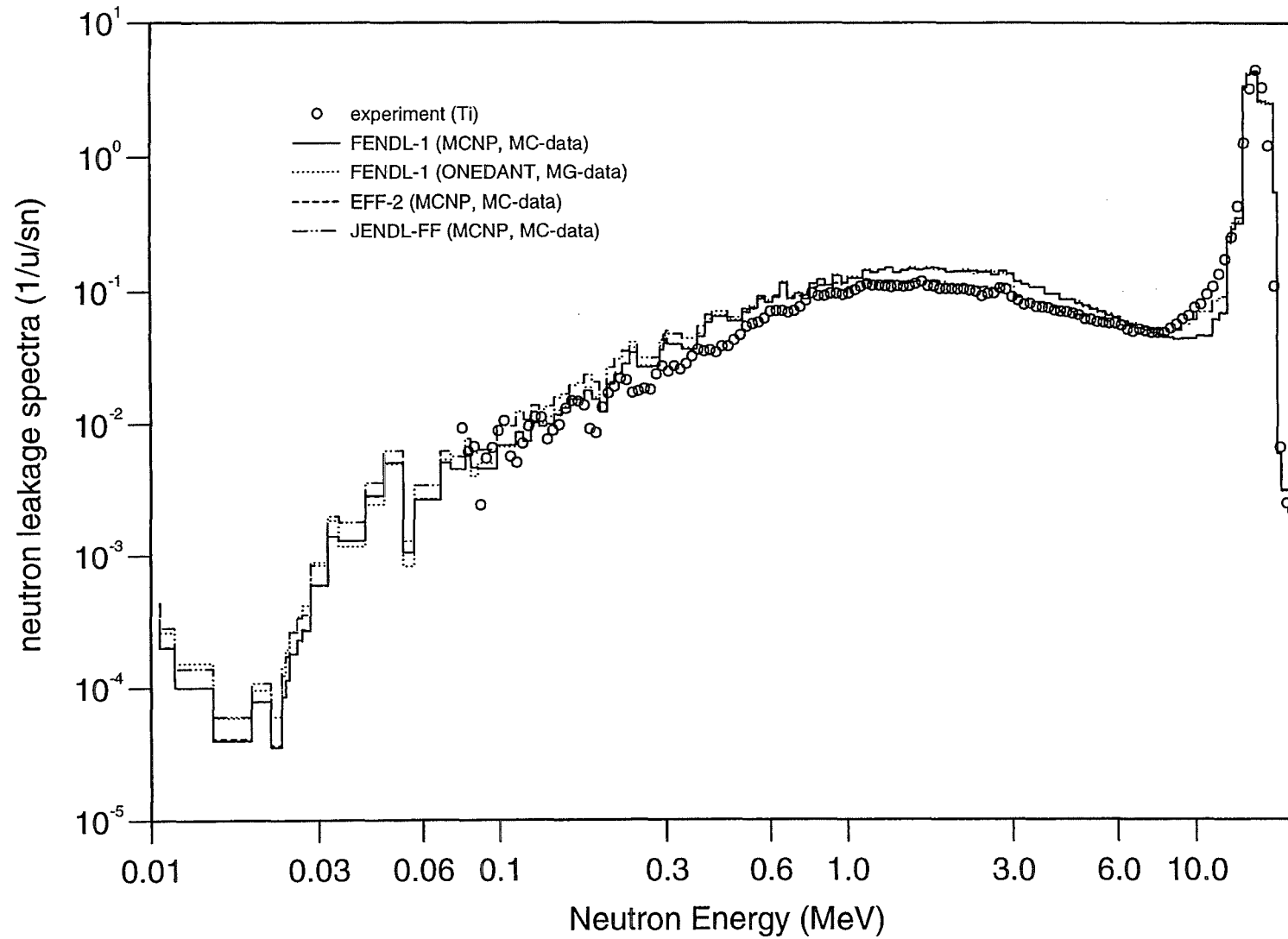


Fig.4.8.7 OKTAVIAN Ti Shell Experiment Neutron Spectra

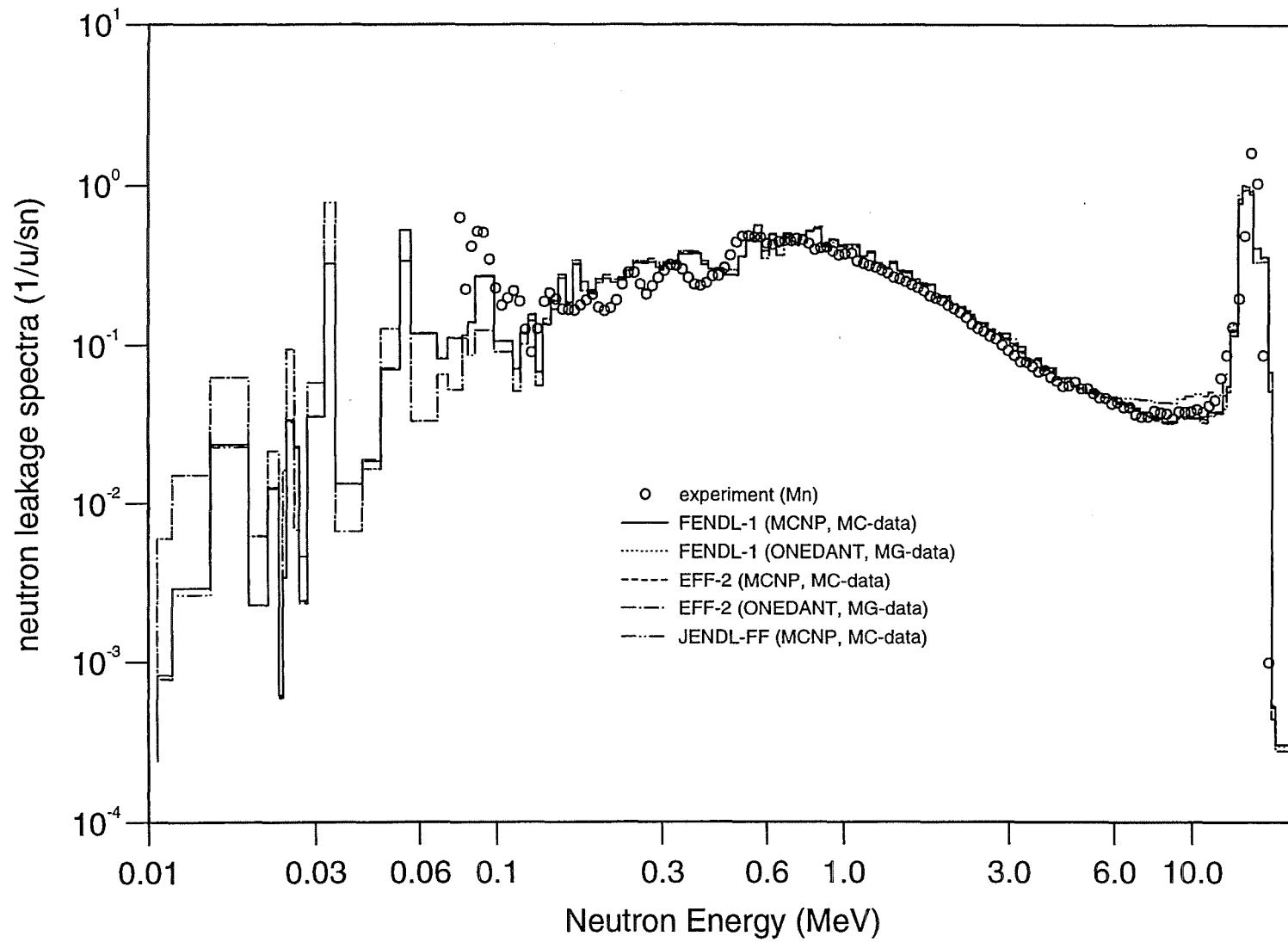


Fig.4.8.8 OKTAVIAN Mn Shell Experiment Neutron Spectra

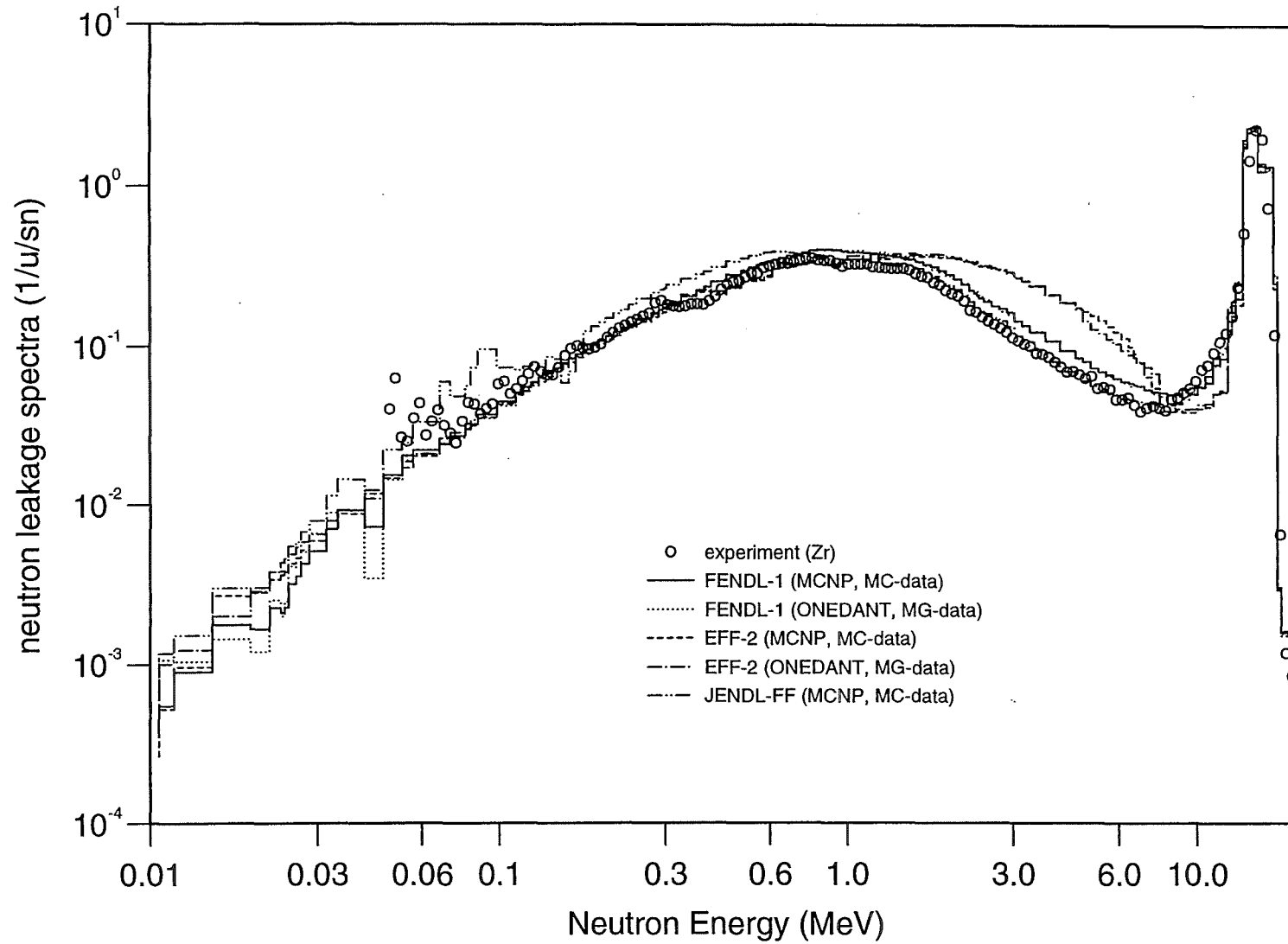


Fig.4.8.9 OKTAVIAN Zr Shell Experiment Neutron Spectra

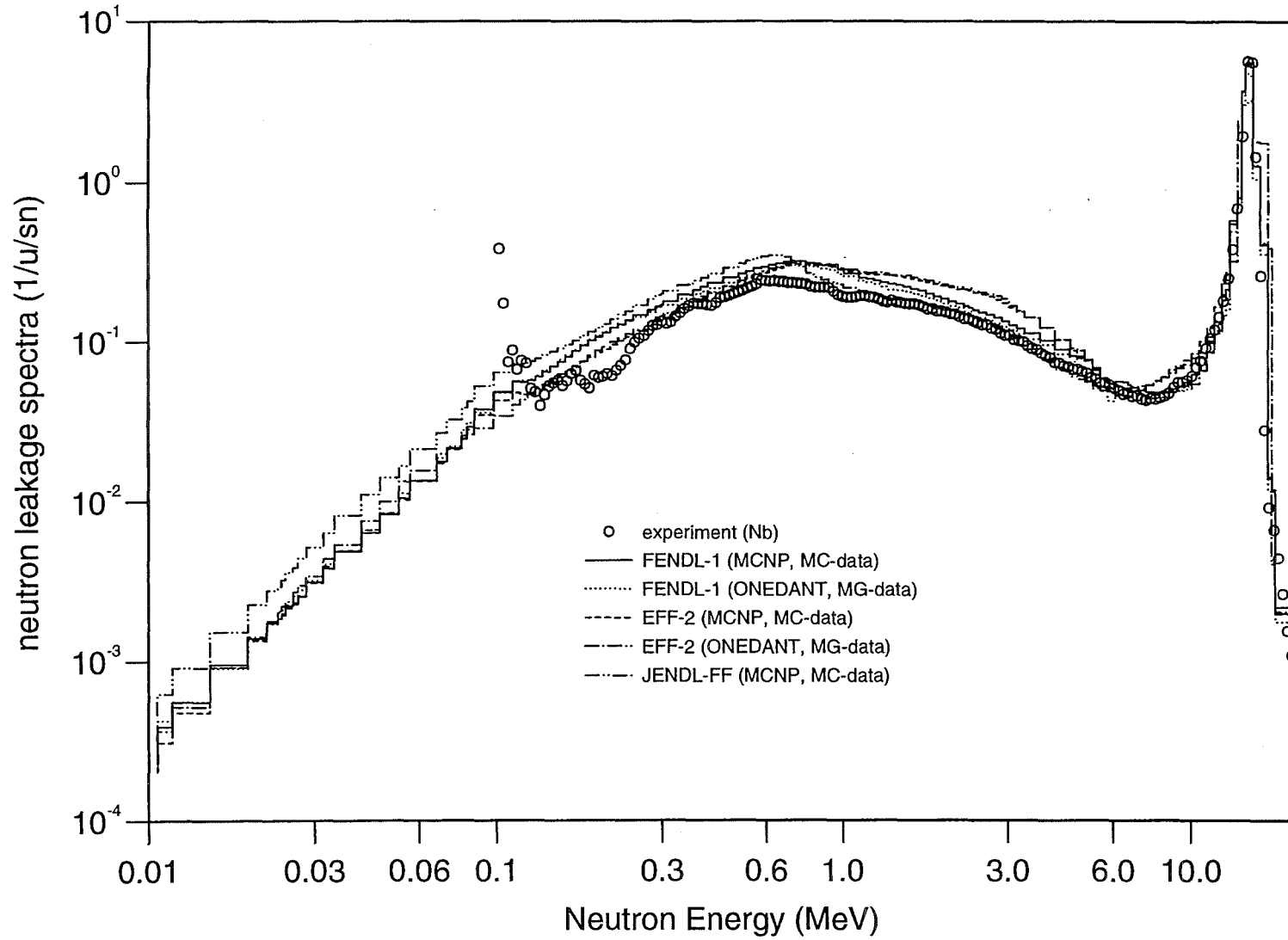


Fig.4.8.10 OKTAVIAN Nb Shell Experiment Neutron Spectra

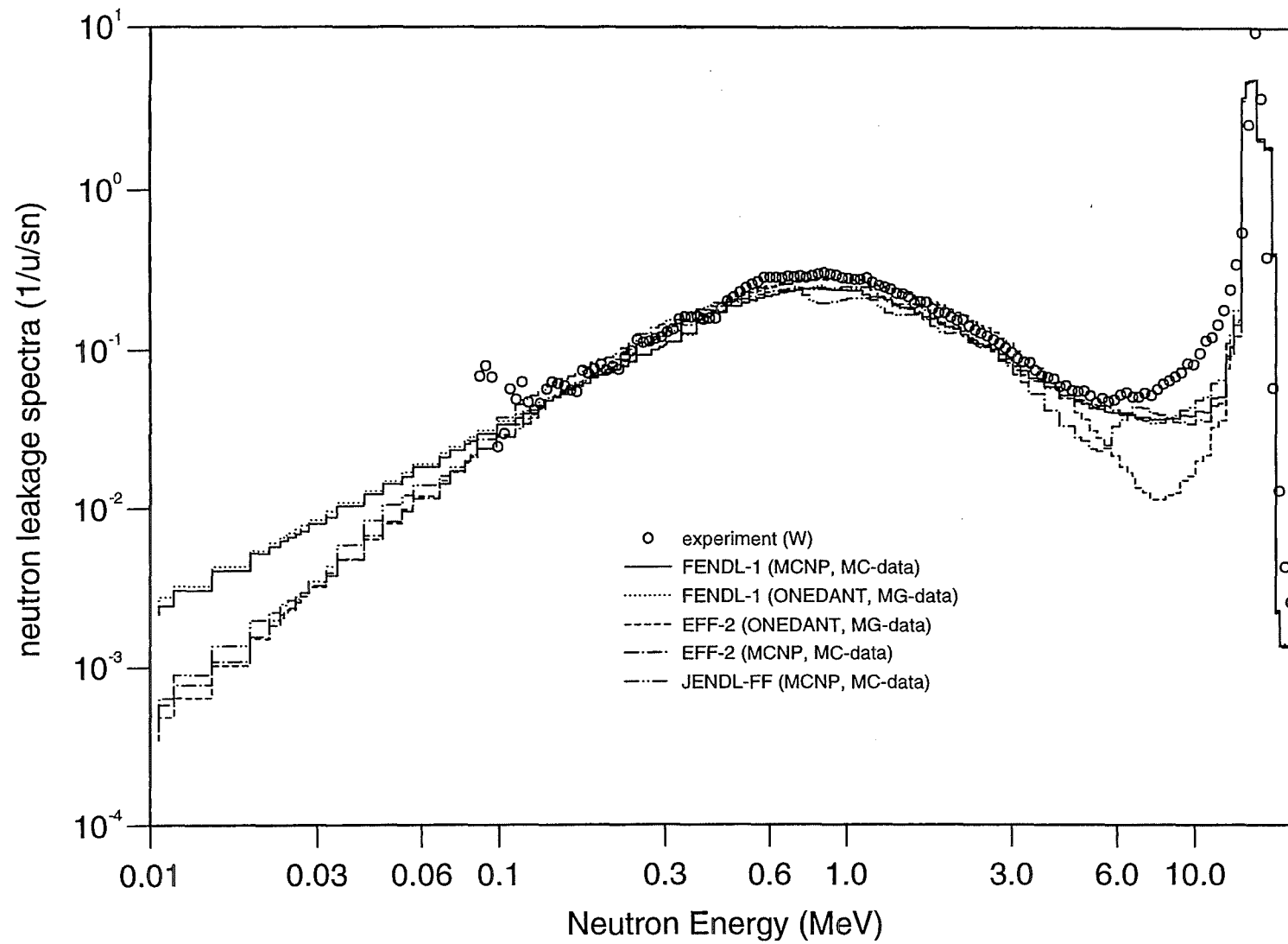


Fig.4.8.11 OKTAVIAN W Shell Experiment Neutron Spectra

4.9 IPPE Vanadium Spherical Shell Experiment

Neutron leakage spectra were measured at the IPPE neutron source facility for two vanadium spherical shells. The inner/outer radii of the two shells amounted to 1.5cm/5cm and 1.5cm/12cm, respectively. The impurities in the shell assembly included 0.2% aluminum, 0.15% iron, 0.2% silicon and 0.07% other elements (C,O,N,H). The total uncertainty of the measured fluences is estimated at about 7%. The details of experiment may be found in Reference[24].

An isotropic neutron source was adopted in the calculation with MCNP4A and EFF-3, FENDL-1 and JENDL-1 ⁵¹V data. For the source energy spectrum the measured distribution in the low energy range was used along with a uniform distribution between 13.36 and 14.89 MeV. A 3-D geometry model was used in the calculation including the deuterium beam duct through the vanadium shell.

The comparison of calculated and measured spectra is presented in Fig.4.9.1, Fig.4.9.2 and Table 4.9.1.

Table 4.9.1 C/E data for integrated neutron leakage spectra in the IPPE V spherical shell experiment.

Thickness of shell (cm)	Energy Range (MeV)	Measured Leakage (1/sn)	C/E (MCNP+ Continuous-Energy Library)		
			EFF-3	FENDL-1	JENDL-FF
3.5 (0.6 MFPS)	0.1~1.0	.123E+00	.997	1.11	1.25
	1.0~5.0	.170E+00	1.14	1.02	1.05
	5.0~10.0	.308E-01	.869	1.06	1.12
	10.0~20.0	.737E+00	.997	.996	.993
	Total	.106E+01	1.02	1.02	1.03
10.5 (1.8 MFPS)	0.1~1.0	.391E+00	1.01	1.06	1.22
	1.0~5.0	.301E+00	1.14	1.04	1.02
	5.0~10.0	.377E-01	.955	1.13	1.25
	10.0~20.0	.381E+00	1.00	1.00	.976
	Total	.111E+01	1.04	1.04	1.08

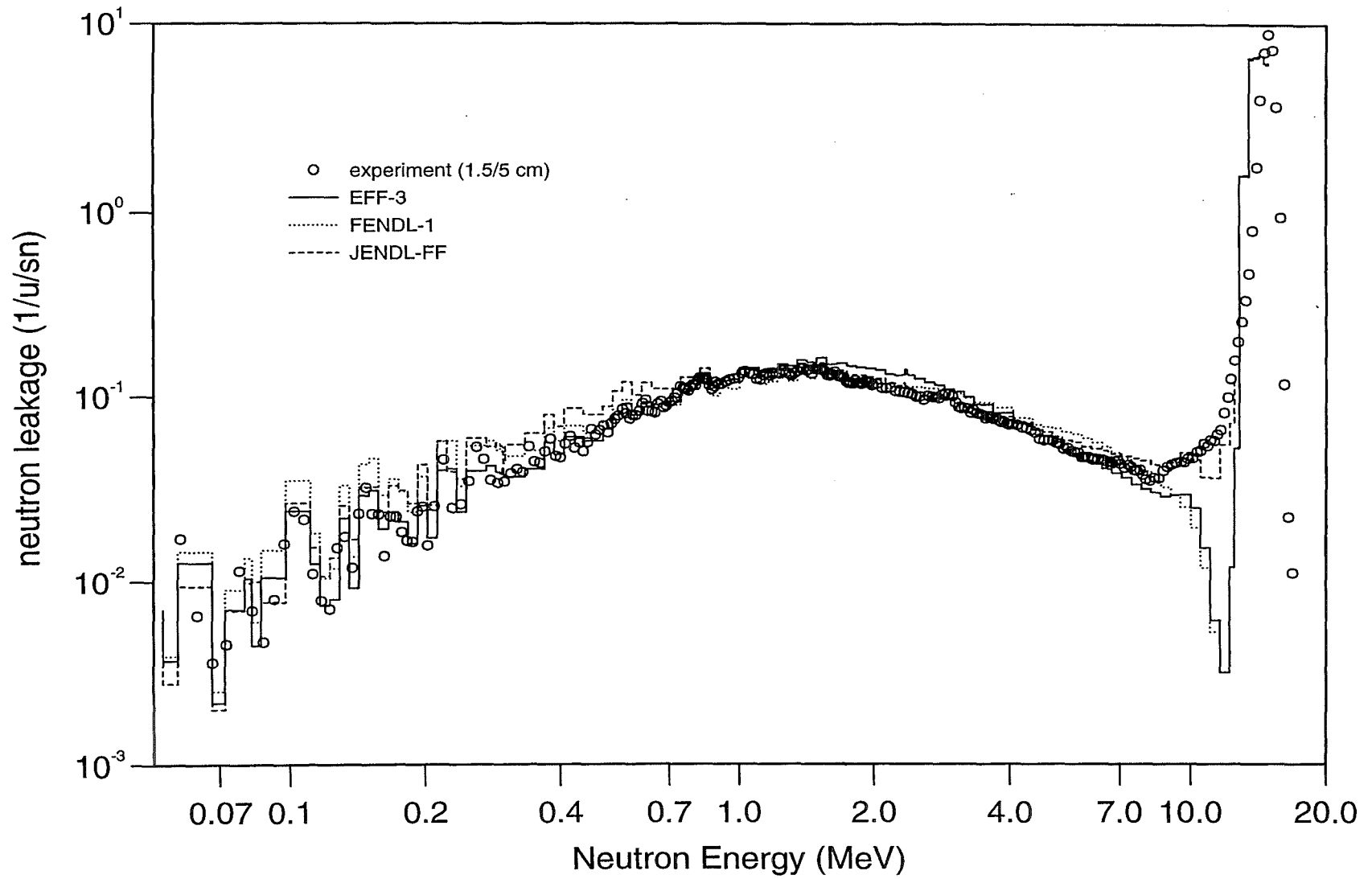


Fig.4.9.1 IPPE Vanadium Shell Experiment Neutron Spectra (3.5cm)

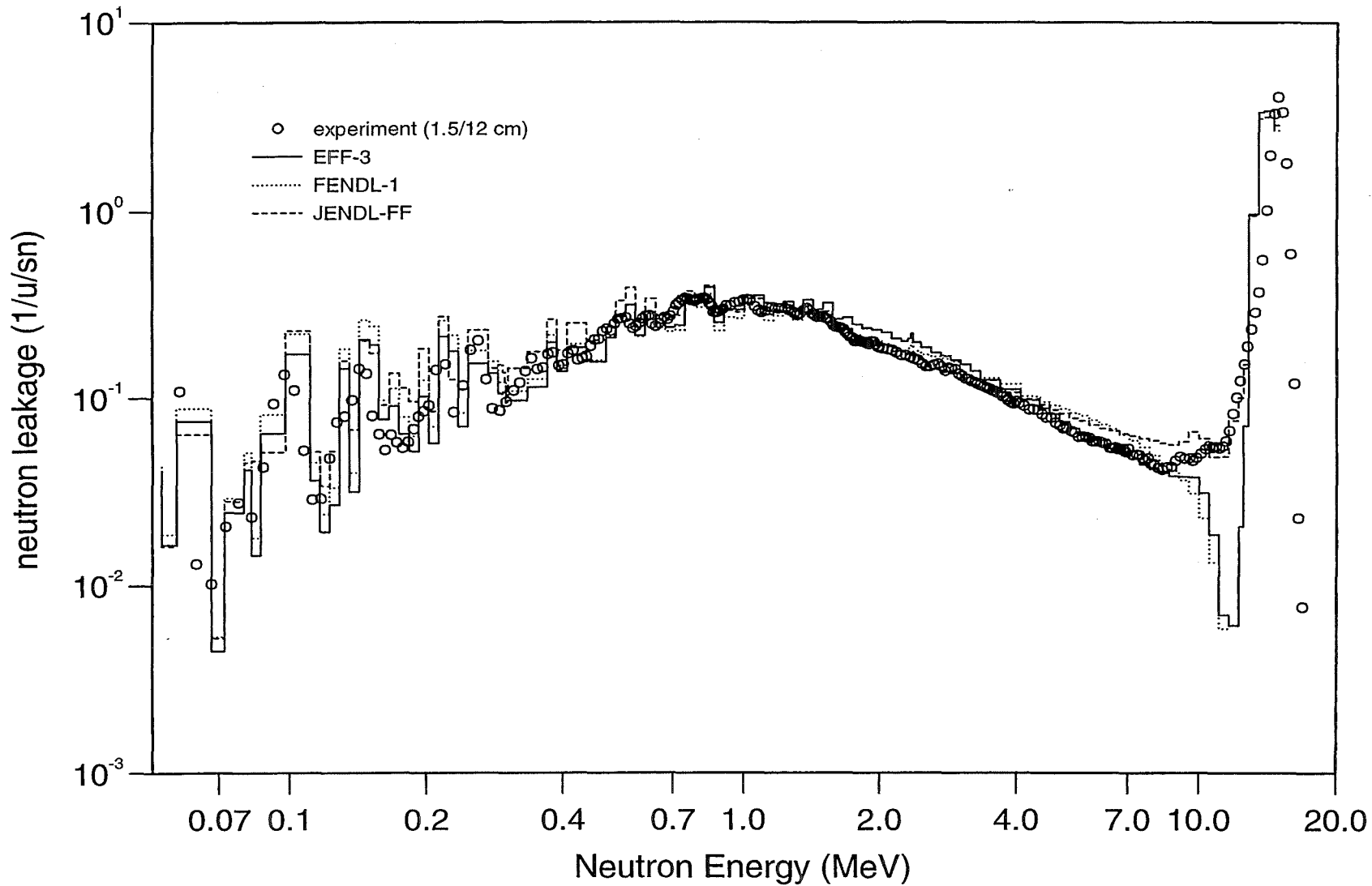


Fig.4.9.2 IPPE Vanadium Shell Experiment Neutron Spectra (10.5cm)

5. Discussion of Results

5.1 Iron

- **Effect of the source neutron anisotropy**

The effect of the anisotropy of the source neutrons was studied for the TUD slab and the IPPE spherical shell experiment. In the TUD experiment, the anisotropy doesn't significantly affect the calculated spectrum due to the fact that the detector was located at an angle of about 75 degrees with respect to the D-beam where the emission probability is close to the average value (see Fig.4.1.1).

Comparing the 3-D MCNP results obtained with FENDL-1 and EFF-2 for the IPPE iron spherical shell experiment (tables 4.2.1 ~ 4.2.3), one can see that the anisotropic neutron source distribution results in only a slight difference in the energy range below 10 MeV and a difference of less than 5% above 10 MeV. This just reflects the differences between the two source neutron spectra themselves, i. e. the uniform spectrum and the one taking into account the anisotropy of source neutrons emitted into the direction of the detector (8 degrees with respect to the D-beam).

- **Source peak energy range (>10 MeV):**

In general, the calculations show an underestimation of the high energy neutron fluxes as measured in the slab experiments. With FENDL-1 and JENDL-FF data this underestimation amounts to up to 20% in the TUD slab experiment and between 5 and 10% in the FNS TOF slab experiment in forward direction. A slightly less underestimation is obtained with EFF-3 and EFF-2 data (tables 4.1.2 and 4.3.1).

In the FNS lab experiment, the underestimation of the high energy flux in forward direction in general corresponds to overestimations at larger angles (see e. g. table 4.3.19) and may be caused by the angular distribution of the elastic scattering. Both EFF-2 and EFF-3 data show an overall better agreement at the measured angles.

In the IPPE shell experiment, no significant differences is obtained for the neutron leakages in the energy range $E \geq 10$ MeV as calculated with the different data files and there is better agreement with the measured spectrum. This is especially true for the thinner shells where the main contribution comes from uncollided source neutrons (for example ~80% for the 2.5cm thick shell). The remaining part of the leakage flux is produced by single-collision neutrons and is not strongly affected by the angular distribution of the emitted neutrons due to the spherical geometry. With thicker shells multiple collisions become more important. For the IPPE spherical shells, this leads to slight differences in the high energy fluxes as calculated with the different data libraries.

- **Energy range 5 to 10 MeV**

For JENDL-FF and EFF-3 data an underestimation is observed by 5 to 15% and 10 to 30%, respectively. This is for both the slab experiments (TUD and FNS slab in forward direction) and the IPPE thin spherical shells and may be traced down to the secondary energy distribution (SED) of the inelastically scattered neutrons. For the thicker IPPE shells and the FNS slab (TOF-experiment) at larger angles, FENDL-1 and EFF-2 overestimate the measured fluxes by 15-40% and 10-30%, respectively. Note that this is not observed in the case of the thinner IPPE shells and both the TUD slab and the FNS slab experiments in forward direction.

The spectrum in the 5 - 10 MeV energy range is mainly populated by 14-MeV neutrons being inelastically scattered into that energy range. Further, it is affected by elastic and inelastic out-scattering reactions from the energy range. Therefore, differences observed in that energy range can be caused by differing elastic and inelastic scattering cross sections in the range 5 - 10 MeV (see Figs 5.1.1 ~ 5.1.3) and by the 14 MeV inelastic scattering cross section and the associated energy-angle distribution. The latter one may explain the underestimation by EFF-3 in the slab experiments and the IPPE thin shell experiment.

- **Energy range 1 to 5 MeV**

In this energy range, fairly good agreement between the measured and calculated values is observed for all of the evaluated data files except for a slight underestimation by JENDL-FF in the TUD-slab experiment and a slight overestimation (5-10%) by both EFF-3 and EFF-2 in the IPPE spherical shell experiment and the FNS slab experiment.

- **Energy range 0.1 to 1 MeV**

In this energy range, there is a slight underestimation of 5 -10% on average with FENDL-1 but a good agreement with other evaluations, especially EFF-3. JENDL-FF gives relatively high calculational values, especially, in the case of the thinner slabs/shells (smaller penetration depth) where there is a larger sensitivity to the secondary energy distribution of the 14 MeV neutrons. As there is, on the other hand, a strong underestimation of the spectrum above 10 MeV with JENDL-FF data, this discrepancy has to be addressed to the SED of the 14 MeV neutrons.

- **Low energy range 1 eV to 0.1 MeV**

Within the given experimental uncertainty there is an overall satisfactory agreement over the whole energy range with the following exceptions (see table 4.41, FNS in-system experiment):

- (1) EFF-2, EFF-3 and JENDL-FF overestimate the measured fluxes below 10 keV systematically by 10 ~ 30% (most seriously for EFF-2) and FENDL-1 overestimates the measured flux in the energy range 1 to 10 keV by 10-30%.

- (2) There is, however, a remarkable systematic overestimation of the measured fluxes in the energy range 1 to 10 keV, in particular at the position of 110 mm depth which is probably due to a large systematic error in the experiment.
- (3) In general, FENDL-1 shows the best agreement with the experimental results in this low energy range.

- **Total energy range for neutrons**

An underestimation by 7 to 10% of the measured total flux ($E > 0.1$ MeV) is obtained for the slab experiments where the measured flux is sensitive to forward-directed scattering. This phenomenon is not observed for the spherical shell experiments where the neutron leakages are insensitive to the secondary angle distributions of elastically and inelastically scattered neutrons. In general, however, there is a trend for underestimating the measured neutron fluxes in the slab experiments. This is also true for the FNS in-system experiment.

- **Comparisons between 1-D and 3-D geometries and between MC- and MG-data**

In tables 4.2.2 and 4.2.3 it is shown that the effect on the total integrated leakage spectra of the D-beam tube penetration in the spherical shells changes from 3% to 8% with varying shell thickness. This is the result of comparing 3d and 1d MCNP-calculations. Almost no difference is found in the high energy range ($E > 10$ MeV) due to the fact that neutron flux in that energy range mainly comes from the direct contribution of the source neutrons. Below 10 MeV the maximum difference amounts to 15% for the 2.5cm- and 10cm thick shells and no more than 2-3% for the 28cm thick shell.

Comparing the results obtained with MCNP, ONEDANT and NGSN, it is found that only slight differences exist between calculations with MG- and MC-data in the energy range above 5 MeV where the MG-data result in slightly smaller fluxes than the MC-data. However, in the energy range below 5 MeV the calculations with MG-data overestimate the results with MC-data by ~10% for the thin shells and underestimate them by ~25% for the thick shells (the energy range 0.3 ~ 2.5 MeV). This is due to the fact that resonance shielding is not properly taken into account with the MG-data.

There is very good agreement between the NGSN and ONEDANT results (tables 4.2.2 - 4.2.3 and figs. 4.2.7 - 4.2.10) even when using very coarse meshes in the NGSN calculation, e. g. only two intervals for the 28cm thick shell.

- **Photon (0.2~10 MeV)**

In the TUD slab experiment, photons originate mainly from neutron inelastic scattering reactions: about 70% of the photons are produced by neutrons in the energy range above 10MeV. Table 4.1.4 shows that the photon flux is overestimated by about 30% with EFF-3 but underestimated by 10 to 20% with the other data files (EFF-2, FENDL-1 and JENDL-FF). As the photon production cross-section itself seems to be well described in the data libraries as compared to experimental value at 14 MeV neutron incidence energy^[25] the observed underestimation by EFF-2, FENDL-1 and JENDL-FF may be explained with the

underestimation of the forward neutron flux. The large overestimation with EFF-3 appears to be the result of a processing error included in the ACE-library that remains to be removed.

5.2 Beryllium

The calculations show that there is a serious and unphysical deficiency with the EFF-2 beryllium data, that is, there is a large overestimation in the energy range above 1.5 MeV. In addition, a big difference exists between the spectra from MG-data and MC-data (see Fig.4.7.1 and Table 4.7.1). Since these results are very different from the results obtained previously with EFF-2 based beryllium data using a different working library^[28], it appears that erroneous data have been introduced into the official EFF-2 ⁹Be data file. It has been clarified meanwhile that this is due to an erroneous representation of the ⁹Be (n,2n) cross-section on the basic EFF-2 data file.

FENDL-1 and JENDL-FF fairly well represent the measured neutron spectra of both the slab and sphere shell experiments, except for a strong overestimation of about 20% around the source energy peak and a 15% underestimation in the energy range 1-5 MeV in the two spherical shell experiments. The latter behaviour is not observed in the slab experiment. In addition, there is also an underestimation at larger angles which is probably due to the secondary angular distribution of the (n,2n) cross section.

For beryllium, there is very good agreement between the results obtained with pointwise (MC) and multigroup (MG) data.

5.3 Aluminum

As shown in Fig. 4.8.1 and Table 4.8.2, the neutron leakage spectrum of the OKTAVIAN aluminum spherical shell experiment can be rather well reproduced with all the data except for an underestimation of 20%~40% in the energy range below the neutron source peak. Note that EFF-2 and JENDL-FF show a better reproduction of the leakage spectrum in the energy range 5 - 10 MeV than FENDL-1 due to a better description of the pre-compound neutron emission.

In addition, the deterministic calculations with FENDL-1 and EFF-2 multigroup data agreed very well with MC-calculations using continuous-energy pointwise data.

5.4 Silicon

As shown in Fig.4.8.2 and Table 4.8.3 for the OKTAVIAN spherical shell experiment, there is a serious discrepancy with the Si data evaluations. FENDL-1 shows an overestimation of about 60% below 1 MeV and an underestimation of 30% in the energy range 1 - 10 MeV. Both EFF-2 and JENDL-FF underestimate the measured neutron leakages by some 20% below the neutron source peak. In general, JENDL-FF agrees relatively better with the experimental leakage spectrum. For silicon, calculations with FENDL-1 MG-data agree well with MC-calculations using pointwise cross-section data.

5.5 Molybdenum

As presented in Fig.4.8.3, the neutron leakage spectrum measured in the OKTAVIAN spherical shell experiment can be well reproduced by all data evaluations except for an underestimation in the energy range 3 - 10 MeV. However, JENDL-FF data show a much better agreement with the measured spectrum in that energy range due an improved neutron emission spectrum. The measured total neutron leakage flux ($E > 0.1$ MeV) is underestimated by about 10% as shown in Table 4.8.4.

There is a good agreement between the results obtained with multigroup (MG) and pointwise (MC) data for molybdenum in the considered energy range.

5.6 Cobalt

Fig.4.8.4 reveals that there is a serious underestimation by about 17% of the leakage spectrum as measured in the OKTAVIAN spherical shell experiment. This is true for all of the applied data evaluation. Note that the shape of the leakage spectrum is nevertheless well reproduced by all of the calculations. Thus there may be a normalization problem in this experiment.

The results of calculations with multigroup data are in good agreement with those of MCNP-calculations with continuous-energy data.

5.7 Chromium

With EFF-2 data, there is an overestimation by more than 20% of the OKTAVIAN spherical shell leakage spectrum in the energy range 1-5 MeV (fig.4.8.5 and table 4.8.6). This implies the need for an improved secondary energy neutron emission spectrum in EFF-2. Results of multigroup data calculations agree very well with MCNP-calculations with continuous-energy data.

5.8 Copper

JENDL-FF data can reproduce very well the measured neutron leakage spectrum of the OKTAVIAN Cu spherical shell experiment (see fig.4.8.6 and table 4.8.7). On the other hand, FENDL-1 and EFF-2, which both make use of the Cu ENDF/B-VI evaluation, give an overestimation of 27% in the energy range 5 - 10 MeV. For copper, there is also a difference by some 5% between the results with MG-data and those with MC-data over the whole considered energy range.

5.9 Titanium

As shown in Fig.4.8.7 and Table 4.8.8, FENDL-1 and EFF-2 data, being again based on the same ENDF/B-VI evaluation, overestimate the measured spectra of the OKTAVIAN Ti spherical shell experiment by more than 20% whereas JENDL-FF shows much better agreement in the energy range of above 1 MeV. For titanium, the results with FENDL-1 multigroup data represent well those obtained with the pointwise data.

5.10 Manganese

As displayed in Fig.4.8.8 and Table 4.8.9, the spectra calculated with FENDL-1 and EFF-2, that both again originate from ENDF/B-VI, are in agreement except for a slight overestimation of about 10% in the energy range below 5 MeV. The results with multigroup data agree with those for the pointwise data within the maximum error of 3 %.

5.11 Zirconium

As shown in Fig.4.8.9 and Table 4.8.10, a serious deficiency (very strong overestimation) is found in the EFF-2 based calculations (for both MC- and MC-data) as compared with the measured spectrum of the OKTAVIAN Zr spherical shell experiment. Furthermore, there is a disagreement by about 10% for the neutron leakages in the energy range 5-10 MeV when comparing EFF-2 based MG- and MC-data calculations. There is, on the other hand, an overall overestimation of some 20% over the whole energy range with FENDL-1. No significant difference is found between the results with FENDL-1 MG-data and MC-data above 0.1 MeV.

In general, JENDL-FF shows the best agreement with the experimental spectrum among the three evaluations, although there is an overestimation by some 15% in the energy above 10 MeV and 1-5 MeV.

5.12 Niobium

The measured leakage spectrum of the OKTAVIAN Nb spherical shell experiment is overestimated by about 15% in total (fig.4.8.10 and table 4.8.11). For EFF-2, originating from ENDF/B-VI, there is an overestimation up to 47% in the energy range of 1 - 5 MeV.

Significant differences in the calculated leakage spectra are observed over the whole energy range when comparing EFF-2 based calculations with MC-data and MG-data. For FENDL-1, there is a large difference of up to 17% between MC-data and MG-data in the energy range above 10 MeV.

5.13 Tungsten

The neutron leakage spectrum measured in the OKTAVIAN W spherical shell experiment is underestimated by more than 10% with all of the three evaluated data (fig. 4.8.11 and table 4.8.12). In particular, there is a strong underestimation for JENDL-FF around 1 MeV and for

EFF-2 in the energy range 2-6 MeV. When comparing EFF-2 based MG- and MC-data calculations one finds a very serious deficiency in the energy range 3 - 10 MeV that has to be attributed to the MG-data.

5.14 Vanadium

In general, the neutron leakage spectra measured in the IPPE vanadium spherical shell experiments can be satisfactorily reproduced with the three different data evaluations (Fig. 4.9.1 - 4.9.2 and table 4.9.1). As compared to the FENDL-1 vanadium data, an improvement is found for the EFF-3 evaluation although there is still a slight overestimation (~10%) in the energy range 1 - 5 MeV. The best agreement with the measured leakage spectra, however, is obtained with JENDL-FF data. This includes the energy range 5-10 MeV where both FENDL-1 and EFF-3 show a clear underestimation of the measured spectra.

6. Summary

A variety of 14 MeV neutron experiments has been analyzed by means of deterministic and Monte Carlo transport calculations with cross-section data from the fusion nuclear data libraries FENDL-1, EFF-2, EFF-3 and JENDL-FF. Transmission experiments on rectangular iron and beryllium slabs, and on spherical iron, beryllium, aluminum, silicon, molybdenum, cobalt, chromium, copper, titanium, manganese, zirconium, niobium, tungsten and vanadium shells with measurements of the neutron leakage spectra were included in the analysis. The main purpose of the analysis was to test the fusion nuclear data libraries against integral 14 MeV neutron benchmark experiments. In addition, the following effects were studied:

- (1) Use of multigroup data in deterministic calculations versus pointwise continuous-energy cross-section data in Monte Carlo (MCNP) - calculations
- (2) Use of different computational codes and methods, in particular the Monte Carlo technique (code MCNP4A) versus deterministic transport procedures (codes ONEDANT, NGSN)
- (3) Simplified versus full geometrical modeling of the experimental configuration
- (4) Angular and energy distribution of the D-T neutron source.

In general, the state-of-the-art fusion nuclear data libraries (FENDL-1, EFF-2, EFF-3, and JENDL-FF) show a high quality level. There is an overall good agreement with integral experiments with a clear superiority, however, of the new EFF and JENDL-FF evaluations over FENDL-1. In addition, there are some remarkable exceptions which are partly due to the evaluated data themselves and partly due to deficiencies in the current working libraries of EFF-2 and JENDL-FF, such as beryllium (EFF-2), silicon (FENDL-1), titanium (EFF-2 and FENDL-1), zirconium (EFF-2/FENDL-1), niobium (EFF-2 and JENDL-FF) and tungsten (EFF-2).

When comparing the results obtained in the high energy range ($E > 0.1$ MeV) with multigroup and continuous energy cross-section data, good agreement was found for most of the analysed elements. Exceptions to this rule were found for beryllium (EFF-2), copper (FENDL-1 and EFF-2), zirconium (EFF-2), niobium (FENDL-1) and tungsten (EFF-2).

The major findings and conclusions of the performed data tests are briefly summarized in Table 6.1. Note that there are listed only the findings and results of the data test analyses, i. e. there is provided the basis for further analyses where there have been observed discrepancies. As a next step, there is required a sensitivity analysis for tracing down the discrepancies to specific cross-section data and, further on, improvements of the corresponding cross section data.

Table 6.1 Summary results of integral data tests for FENDL-1, EFF-2 &-3 and JENDL-FF

Element	Major Findings	Analyzed Integral Experiment
Fe	Underestimation (~10%) of measured total neutron fluxes in slab experiments, agreement in spherical shell experiments. Results with MG- and MC-data agree above 5 MeV, but disagree by 10~25% below 5 MeV. In addition, (1) underestimation of neutron emission cross-section in forward direction and overestimation in backward direction around 14 MeV for all evaluations; EFF-3 shows a slight improvement; (2) Strong underestimation (forward direction) of neutron emission spectra at 5-10 MeV by EFF-3 and JENDL-FF; Overestimation (non-forward direction) by FENDL-1 and JENDL-FF; (3) Need to check photon production data (overestimation by EFF-3 and underestimation in FENDL-1, JENDL-FF and EFF-2).	TUD slab IPPE spherical shell FNS slab TOF & in-system measurements
Be	FENDL-1 and JENDL-FF reproduce well the measured neutron spectra, except ~20% overestimation at 14 MeV and 10~15% underestimation at 1-5 MeV for shell experiments; need to revise SAD of neutron emission in FENDL-1 and JENDL-FF. Unphysical behavior in EFF-2 data, need to check the both the processed EFF-2 MG- and MC-data.	FNS slab KANT spherical shell OKTAVIAN spherical shell
Al	Neutron leakage spectrum underestimated by 40% around 10 MeV with FENDL-1 and by 20% with JENDL-FF and EFF-2. EFF-2 and JENDL-FF show significant improvement in DDX.	OKTAVIAN spherical shell
Si	EFF-2 and JENDL-FF show improvement over FENDL-1, although 20-30% underestimation with EFF-2 and by ~20% with JENDL-FF at 10 MeV. 20~30% underestimation at 1-10 MeV and ~60% overestimation at 0.1-1 MeV with FENDL-1.	OKTAVIAN spherical shell
Mo	Underestimation by ~40% in energy range 3-10 MeV with FENDL-1 and EFF-2. JENDL-FF shows improvement although slight underestimation by 10% over whole energy range.	OKTAVIAN spherical shell
Co	Systematic underestimation by 17% of measured neutron leakage spectra with all evaluations. Need to check the integral experiment.	OKTAVIAN spherical shell
Cr	FENDL-1 and JENDL-FF agree well; overestimation with EFF-2 by 25% at 1-5 MeV.	OKTAVIAN spherical shell
Cu	Overestimation by 27% at 5-10 MeV and difference of ~5% between MC- and MG-data (FENDL-1). JENDL-FF shows significant improvement.	OKTAVIAN spherical shell
Ti	Overall overestimation of ~20% for both evaluations (FENDL-1 and JENDL-FF). Little improvement at 1-5 MeV with JENDL-FF.	OKTAVIAN spherical shell
Mn	All evaluated data agree well; slight overestimation of neutron leakage spectrum at 5-10 MeV by 15% with JENDL-FF.	OKTAVIAN spherical shell
Zr	With FENDL-1 overestimation by ~20% over whole energy range. With EFF-2 serious discrepancy. At 5-10 MeV difference of 10% between EFF-2 MC- and MG-data. Below 1 MeV and around 14 MeV overestimation by ~15% with JENDL-FF.	OKTAVIAN spherical shell
Nb	Below 5 MeV 26% overestimation with FENDL-1; 17% difference between FENDL-1 MC- and MG-data. With EFF-2 overall overestimation by >15%, at 1-5 MeV by 47%. Overestimation by 37% below 1 MeV with JENDL-FF.	OKTAVIAN spherical shell
W	Overall 10% underestimation with all evaluations. Large discrepancy with EFF-2 around 10 MeV; disagreement between EFF-2 MC- and MG-data.	OKTAVIAN spherical shell
V	Overestimation (~10%) below 1 MeV by FENDL-1. With EFF-3 better agreement below 1 MeV, but slight overestimation (~10%) at 1-5 MeV. Overall best agreement with JENDL-FF.	IPPE spherical shells

7. Acknowledgement

This work has been performed in the framework of the Nuclear Fusion Programme of Forschungszentrum Karlsruhe and is supported by the European Union within the European Fusion Technology Programme. Support was granted to the main author (Y. Wu) by the K. C. Wong Foundation of the German DAAD and the Forschungszentrum Karlsruhe.

The authors are grateful to Prof. K. Seidel (Technical University of Dresden, Germany), S. P. Simakov (Institute of Physics and Power Engineering, Russian Federation), Drs. F. Maekawa and Y. Oyama (JAERI, Japan) for providing their experimental data and the helpful communications. Sincere thanks are due to Dr. H. Tsige-Tamirat, D. Leichtle, E. Wiegner, Dr. U. v. Moellendorff and many other colleagues in the Institute of Neutron Physics and Reactor Technology for the assistance and support.

8. References

- [1] J. F. Briesmeister (Ed.), MCNP4A - A General Monte Carlo N-Particle Transport Code, Los Alamos National Laboratory, LA-12626-M, 1993.
- [2] R. Douglas O'Dell, Forrest W. Brinkley, Duane R. Marr. and Raymond E. Alcouffe, Revised User's Manual for ONEDANT: A Code Package for One-Dimensional, Diffusion-Accelerated, Neutral-Particle Transport, Los Alamos National Laboratory, LA-9148-M, UC-705, 1989
- [3] Y.C. Wu, Z.S. Xie, A Discrete Ordinates Nodal Method for One-Dimensional Neutron Transport Numerical Calculation in Curvilinear Geometries, Chinese J. of Nucl. Sci. & Eng., Vol.10, No.1 (1990).
- [4] S. Ganesan and P.K. McLaughlin, FENDL/E Evaluated Nuclear Data Library of Neutron Nuclear Interaction Cross-Sections and Photon Production Cross-Sections and Photon-Atom Interaction Cross-Sections for Fusion Applications, Version 1.0 of May 1994, IAEA-NDS-128 (1995).
- [5] J. Kopecky, H. Gruppelaar, H.A.J. Vanderkamp and D. Nierop, European Fusion File, Vrsion-2, EFF-2, final report on basic data file, ECN-C-92-036, June 1992.
- [6] A.B. Pashchenko, H. Wienke and S. Ganesan, FENDL-/MG-1.0 - Library of multigroup Cross-section in GENDF and MATXS Format for Neutron-Photon Transport Calculations Generated by R.E. MacFarlane by processing FENDL/E-1.0, summary documentation, IAEA-NDS-129, Rev.3, November, 1995.
- [7] L. Petrizzi, V. Rado, Processing EFF-2.4 with ACER of NJOY to Produce a MCNP Working Library, final report on task NDB 1.2, presented at EFF meeting, 10-11 July 1995, Garching.
- [8] R.E. MacFarlane, TRANSX 2: A Code for Interfacing MATXS Cross-Section Libraries to Nuclear Transport Codes, December 16, 1993.
- [9] S. Chiba, B. Yu and T. Fukahori, Evaluation of JENDL Fusion File, JAERI-M-92-027, Japan Atomic Energy Research Institute.
- [10] T.R. Fewell, An Evaluation of the Alpha Counting Technique for Determinig 14-MeV Neutron Yields, Nuclear Instruments and Methods 61 (1968) 61-71.
- [11] J. Benveniste et al., The Problem of Measuring the Absolute Yield of 14-MeV Neutrons by Means of an Alpha Counter, Nuclear Instruments and Methods 7 (1960) 306-314.
- [12] J. Benveniste et al., Information on the Neutrons Produced in the $H^3(d,n)He^4$ Reaction, UCRL-4266 (1954).
- [13] H.V. Argo et al., Phys. Rev.87 (1952) 612.
- [14] W.R. Arnold et al., Phys. Rev. 93 (1954) 483.
- [15] J.P. Conner, T.W. Bonner and J.R. Smith, Phys. Rev.88 (1952) 468.
- [16] E.W. Saker and J.D.L.H. Wood, Calculated Neutron Yield from Titanium-Tritium Targets under Deuteron Bombardment, SERL no.M.61 (1958).
- [17] H. Freiesleben et. al., Shield Penetration Experiments, TUD-IKTP/95-01 (Jan. 1995).
- [18] B. V. Devkin et. al, Unpublished Report, November 1995.
- [19] Collection of Experimental Data for Fusion Neutronics Benchmark, JAERI-M-94-014, Japanese Atomic Energy Research Institute (Feb. 1994).
- [20] F. Maekawa and Y. Oyama, Measurement of Neutron Energy Spectrum below 10 KeV in an Iron Shield Bombarded by D-T Neutrons and Benchmark Test of Evaluated Nuclear Data from 14 MeV to 1 eV, Nucl. Sci. & Eng. 125 (1997), 205-217.

- [21] C. Konno et. al, Measurement and Analysis of Low Energy Neutron Spectrum in a Large Cylindrical Iron Assembly Bombarded by D-T Neutrons, *Fusion Eng. Des.*, 18, 297 (1991).
- [22] U. v. Möllendorff et al., et al., Measurements of 14-MeV Neutron Multiplication in Spherical Beryllium Shells, *Fusion Eng. and Design* 28 (1995), 737-744
- [23] Report LA-12212 (November 1991).
- [24] U. v. Möllendorff, B.V. Devkin, U. Fischer, B.I. Fursov et al., A 14-MeV Neutron Transmission Experiment on Vanadium, presented at the 19th Symposium on Fusion Technology, September 16-20, 1996, Lisboa, Portugal.
- [25] S. Hlavac, P. Oblozinsky, γ -ray production cross sections and γ -ray multiplicities from Fe and Ni bombarded with 14.6 MeV neutrons, Report INDC/CSR-5/GI, IAEA Vienna, 1983.
- [26] U. Fischer, Y. Wu, Final Analyses of the Spectrum Measurements at the FNG Bulk Shield Experiment Using FENDL-1, Eff-2, -3 and JENDL-FF Data, ITER Task T218 Final Review Meeting, Garching, Germany, February 26-28, 1997.
- [27] H. Freiesleben, W. Hansen, D. Richter, K. Seidel et al., Measurement and Analysis of Spectral Neutron and Photon Fluxes in an ITER Shield Mockup, presented at the 19th Symposium on Fusion Technology, September 16-20, 1996, Lisboa, Portugal.
- [28] U. Fischer, E. Wiegner, FENDL data testing for beryllium, lead, iron and copper, *Fusion Engineering and Design* 28 (1995) 437-445.
- [29] Y. Oyama and H. Maekawa, Measurement and Analysis of an Angular Neutron Flux on a Beryllium Slab Irradiated with Deuterium-Tritium Neutrons, *Nucl. Sci. & Eng.*, 97,220-234 (1987).
- [30] Oyama, Y. Yamaguchi and H. Maekawa, Experiment Results of Angular Neutron Spectra Leaking from Slab of Fusion Reactor Candidate Materials (I), JAERI-M 90-092 (1990).